TU Vienna

Master Thesis

Performance evaluation of grid-connected PV Battery Energy Storage Systems for residential applications

---

A thesis submitted in fulfilment of the requirements
for the degree of Master of Science supervised by

Univ.-Prof. Dr.-Ing. Wolfgang GAWLIK
Dipl.-Ing. Franz ZEILINGER

Johannes KATHAN MSc (Austrian Institute of Technology)

at the

Institute of Energy Systems and Electrical Drives
Technical University of Vienna

by

Christian MESSNER
Student ID: 0814086

January 15, 2016

Declaration of Authorship

I, Christian MESSNER, declare that this thesis titled, 'Performance evaluation of grid-connected PV Battery Energy Storage Systems for residential applications' and the work presented in it are my own. I confirm that:

- This work was done wholly or mainly while in candidature for a research degree at this University.

- Where any part of this thesis has previously been submitted for a degree or any other qualification at this University or any other institution, this has been clearly stated.

- Where I have consulted the published work of others, this is always clearly attributed.

- Where I have quoted from the work of others, the source is always given. With the exception of such quotations, this thesis is entirely my own work.

- I have acknowledged all main sources of help.

- Where the thesis is based on work done by myself jointly with others, I have made clear exactly what was done by others and what I have contributed myself.

Abstract

Institute of Energy Systems and Electrical Drives

Technical University of Vienna

Master of Science

Performance evaluation of grid-connected PV Battery Energy Storage Systems for residential applications

by Christian MESSNER

Increased interest in local use of generated energy from Photovoltaics (PV) is seen in the residential field. Decreasing PV feed-in tariffs and system costs with simultaneous rising electricity prices, provide best conditions for profitability of grid-connected PV Battery Energy Storage Systems (PV-BESS). Such a system consists basically of PV modules, a PV inverter, battery and charge controller. An energy management system controls the battery discharge power in a way, that grid imported energy for coverage of the local electricity demand is reduced by stored PV energy.

A variety of manufactures and products of PV-BESS are available at the current market situation. The user has the choice between different system configurations (AC coupled or DC coupled, modular construction or all-in-one system, single or three phase, lead-acid or lithium-ion battery). The system size, considering PV generator peak power and battery capacity determines the effectiveness in increasing local consumed PV energy. The optimal size is related to individual PV generation and electricity demand patterns.

Due to missing standards for PV-BESS, the evaluation of efficiency and effectiveness is not easy feasible. The comparison between systems is complicated due to the high amount of system configurations, system size and individual PV and load profiles. The aim of this work is to develop an index portfolio, determined with test methods in a laboratory environment, for a comprehensive evaluation of overall PV-BESS performance. PV-BESS manufacturers profit from differentiation of high quality products from low performing competitors and gain insights about deficits and optimization possibilities of its product. The provided evaluation methods shall serve as basis for further standardization processes and finally allow the user to select the most appropriate product and provide a guaranteed performance in the specific application of PV-BESS.

Kurzfassung

Ein steigendes Interesse an der Nutzung lokal erzeugter Photovoltaik (PV) Energie zur Deckung des Eigenbedarfs ist ersichtlich. Sinkende Einspeisetarife und Systemkosten, bei gleichzeitig steigenden Strompreisen bieten gute Voraussetzungen für Rentabilität und Einsatz eines netzgekoppelten PV-Batterie-Energiespeicher-Systems. Ein solches besteht grundsätzlich aus PV-Modulen, einem PV-Wechselrichter, Batterie und Laderegler. Ein Energiemanagementsystem steuert die Batterieentladung so, dass der Netzbezug zur Deckung des lokalen Elektrizitätverbrauch durch gespeicherte PV Energie verringert wird.

Eine Vielzahl an Herstellern bietet mittlerweile PV-Batterie-Energiespeicher-Systeme an, mit denen die Erhöhung des Eigenverbrauchs und Senkung der Elektrizitätskosten erreicht werden soll. Der Anwender hat dabei die Auswahl zwischen verschiedenen Systemkonfigurationen (AC oder DC-gekoppelt, modulare Bauwiese oder All-In-One, Ein oder Drei-Phasig, Blei oder Lithium-Ionen Batterie). Desweiteren bestimmt die maximale Leistung des PV-Generators und die Batteriekapazität maßgebend den Grad der Direktnutzung und Eigendeckung. Die Systemgröße muss dabei auch im Kontext des Einstrahlungs- und Lastprofils des jeweiligen Anwenders gesehen werden.

Die Bewertung solcher Systeme hinsichtlich Effizienz und Effektivität ist aufgrund fehlender Standards auf Gesamtsystemebene derzeit nur schwer möglich. Die Vergleichbarkeit ist durch die Anzahl an Systemkonfigurationen, Systemgröße und individuellen Eingangsprofilen erschwert. Ziel dieser Arbeit ist es ein Kennzahlportfolio zu entwickeln, welches eine umfassende Bewertung von PV-Batterie-Energiespeicher-Systemen, im Rahmen von Labortests ermöglicht. Dadurch soll der Hersteller sein Produkt besser vermarkten können und Schwächen bzw. Optimierungsmöglichkeiten aufgezeigt werden. Die Performance verschiedener Systeme wird für den Anwender besser vergleichbar und er kann auf ein qualitativ getestetes, funktionierendes System vertrauen.

Acknowledgements

First, I would like to thank Professor Dr.-Ing. Wolfgang Gawlik for granting me this thesis topic. I want to thank my supervisor Dipl.-Ing. Franz Zeilinger for the time and effort he spent helping me.

I would also like to thank my supervisor at the Austrian Institute of Technology (AIT) Johannes Kathan for his motivation and excellent support. His inputs and patience have been very valuable for this work. I'd like to thank all my colleagues from the AIT for the very pleasant working atmosphere, great collaboration and help.

This thesis is dedicated to my friends and family for their help, love and encouragement in my life.

Contents

List of Figures

List of Tables

Acronyms

ACU	Air Conditioning Unit
AGM	Absorbed Glass Mat
BCC	Battery Charge Controller
BCE	Battery Coulombic Efficiency
BEE	Battery Energy Efficiency
BESS	Battery Energy Storage Systems
BMS	Battery Management System
BOL	Beginning of Life
BSS	Battery Support System
BVE	Battery Voltaic Efficiency
C-Si	Crystalline Silicon Solar Cell
CC-CV	Constant Current / Constant Voltage Charge
CCV	Closed Circuit Voltage
CEC	California Energy Commission
CPLD	Complex Programmable Logic Device
DAQ	Data Acquisition System
DERri	Distributed Energy Research Infrastructure
DLMS	Device Language Message Specification
DMD	Direct Matched Demand
DOD	Depth of Discharge
DR	Demand Response
DSP	Digital Signal Processor
DU	Direct Use
EMS	Energy Management System
EOC	End of Charge
EOCV	End of Charge Voltage
EOD	End of Discharge
EODV	End of Discharge Voltage

EOL	End of Life
FIT	Feed-In Tariff
FSB	Full Sized Battery
HP	Heat Pump
HVB-BESS	High Voltage Battery Energy Storage System
I/V	Current/Voltage Characteristic
ICT	Information and Communication Technology
IEC	International Electrotechnical Commission
LCO	Lithium Cobalt Oxide $LiCoO_2$
LFP	Lithium Iron Phosphate $LiFePO_4$
LMO	Lithium Manganese Oxide $LiMn_2O_4$
LTO	Lithium Titanate $Li_4Ti_5O_{12}$
LVB-BESS	Low Voltage Battery Energy Storage System
MPP	Maximum Power Point
MPPT	Maximum Power Point Tracking
MSE	Mean Signed Error
NCA	Lithium Nickel Cobalt $LiNiCoAlO_2$
NCM	Lithium Nickel Manganese Cobalt $LiNiMnCoO_2$
NCP	Neutral Point Clamp
NICC	Non Isolated Charge Controller
OBIS	Object Identification System
OCV	Open Circuit Voltage
P&O	Perturb & Observe
PCB	Printed Circuit Board

PCC   Point of Common Coupling

PCS   Power Conversion System

POC   Point of Connection

POC-GRID   Point of Connection - Utility Grid

PV   Photovoltaics

PV-BESS   PV Battery Energy Storage Systems

PWM   Pulse-width modulation

RES   Renewable Energy Source

ROI   Return of Investment

RTE   Round Trip Efficiency

SC   Self Coverage

SLA   Sealed Lead-Acid

SML   Smart Meter Language

SOC   State of Charge

SOE   State of Energy

SOH   State of Health

TC   Total Coverage

TF   Thin-Film Solar Cell

VRLA   Valve-Regulated Lead-Acid

ZVS   Zero Voltage Switching

List of symbols

Battery parameters

C_{NET}	Ah	Battery net capacity, expressed in ampere-hours (Ah)
C_{NOM}	Ah	Battery nominal capacity, expressed in ampere-hours (Ah)
DOD_{NET}	%	Maximum Depth of Discharge for obtaining the defined net capacity
E_{NET}	kWh	Battery net capacity, expressed in kilo-watt-hours (kWh)
Q_c	Ah	Charge capacity (Ampere-hours)
Q_d	Ah	Discharge capacity
R_{BAT}	Ω	Internal battery (cell) resistance

Current

I_{BAT}	A	Battery DC current
I_c	A	Charge current
I_d	A	Discharge current
$I_{DC,i}$	A	Sampled value of the inverters input current at t_i
$I_{DC,max}$	A	Maximum DC input current PV inverter
I_{MPP}	A	Output current of a PV generator at the Maximum Power Point for given irradiation and temperature
I_{SC}	V	Short circuit current of a PV generator / PV cells

Efficiency

η_{AVG}	%	Average efficiency of instantaneous power efficiency samples
$\eta_{AC/DC}$	%	AC/DC Rectifier efficiency
η_C	%	Battery Coulomb efficiency
$\eta_{Charge,BAT\&PCS}$	%	Hypothetical calculated charge efficiency, including battery one way efficiency as square root of Round Trip Efficiency

$\eta_\text{ChargeController}$	%	Charge Controller efficiency - Efficiency varies between AC and DC coupled system
η_CONV	%	PV Inverter conversion efficiency according EN50530
C_rf	%	Charge return factor. The number of Ah returned of the battery during the charge cycle divided by the number of Ah delivered by the battery during discharge. Inverse of coulomb efficiency
$\eta_\text{DC/AC}$	%	DC/AC inverter efficiency
$\eta_\text{DC/AC/DC}$	%	DC/AC followed by AC/DC energy conversion efficiency
$\eta_\text{DC-Input}$	%	PV inverter input stage efficiency
$\eta_\text{Discharge,BAT\&PCS}$	%	Hypothetical calculated discharge efficiency, including battery one way efficiency as square root of Round Trip Efficiency
$\eta_\text{Discharge}$	%	Overall discharge efficiency to the AC link as function of AC output power and battery voltage
η_E	%	Battery Energy efficiency
$\eta_\text{Feed-In}$	%	Feed-In efficiency, MPPT, conversion or overall efficiency as function of DC input power and voltage
$\eta_\text{Feed-In,conv}$	%	One Way Feed-In Conversion Efficiency (excluding MPP tracking)
$\eta_\text{Feed-In,t,dyn}$	%	Overall One Way PV Feed-In Efficiency during a dynamic PV generation input sequence
$\eta_\text{Feed−In,t,static}$	%	Overall One Way Feed-In Efficiency evaluated at steady state operation
η_MPPT	%	Maximum Power Point Tracking efficiency (tracking error)
η_MPPT	%	MPPT/tracking error efficiency
$\eta_\text{MPPT,dyn}$	%	Dynamic MPPT efficiency

$\eta_{\text{MPPT,stat}}$	%	Static MPPT efficiency
$\eta_{\text{PCS,t,dyn}}$	%	Overall PCS efficiency during a dynamic PV generation input sequence
$\eta_{\text{PCS,t,static}}$	%	Overall PCS efficiency evaluated at steady state operation
η_{P}	%	Instantaneous efficiency $\eta(ti)$
$\eta_{\text{PCS,conv}}$	%	Power Conversion Sytem Efficiency (excluding MPP tracking). Evaluated as instantaneous value or for a specific measurement time period
$\eta_{\text{PV-BESS}}$	%	System efficiency, evaluated during an application related test sequence
$\eta_{\text{RTE,PV-BESS}}$	%	Round Trip Efficiency PV-BESS, considering PCS and battery losses
$\eta_{\text{RTE,PV-BESS,conv}}$	%	Round Trip Efficiency PCS losses
$\eta_{\text{PV-Charge}}$	%	Average PV charge efficiency evaluated for several battery voltage/SOC ranges as function of power
$\eta_{\text{PV-Charge,conv}}$	%	PV charge conversion efficiency (excluding MPP tracking) as function of DC input power, PV generator and battery voltage
$\eta_{\text{PV-Charge}}$	%	Overall PV charge efficiency as function of DC input power, PV generator and battery voltage
$\eta_{\text{PV-Charge,t,dyn}}$	%	Overall One Way PV Charge Efficiency during a dynamic PV generation input sequence
$\eta_{\text{PV-Charge,t,stat}}$	%	Overall One Way PV Charge Efficiency evaluated at steady state operation
$\eta_{\text{RTE,Bat}}$	%	Round Trip Efficiency battery (DC) only
$\eta_{\text{RTE,PCS}}$	%	Round Trip Efficiency PCS only
η_{t}	%	PV Inverter Overall efficiency according EN50530, including MPP and conversion losses

η_{V}	%	Battery Voltage efficiency

Energy Distribution

$E_{\mathrm{Grid}\leftarrow\mathrm{PV}}$	kWh	Grid exported power from PV generation within a specified time period. Energy is determined at the Sink: Grid
$E_{\mathrm{Load}\leftarrow\mathrm{Battery}}$	kWh	Electricity demand covered by battery discharged energy within a specified time period: Energy is determined at the Sink: Load
$E_{\mathrm{Load}\leftarrow\mathrm{Bat},i}$	kWh	Electricity demand covered by battery discharged energy within a specified time period: Energy is determined at the Source: Load
$E_{\mathrm{Load}\leftarrow\mathrm{Grid}}$	kWh	Energy demand covered from grid imported energy within a specified time period. Energy is determined at the Sink: Grid
$E_{\mathrm{Load}\leftarrow\mathrm{PV}}$	kWh	Direct Matched Demand, PV energy consumed from the load, within a specified time period. Energy is determined at the Sink: Load
$E_{\mathrm{PV}\rightarrow\mathrm{Battery}}$	kWh	PV generated energy used for charging the battery, within a specified time period. Energy is determined at the Source: PV Generator
$E_{\mathrm{PV}\rightarrow\mathrm{Bat},i}$	kWh	PV generated energy used for charging the battery, within two subsequent measurement cycles. Energy is determined at the Source: PV Generator
$E_{\mathrm{PV}\rightarrow\mathrm{Load}}$	kWh	PV generated energy used for load coverage within a specified time period. Energy is determined at the Source: PV Generator
$E_{\mathrm{PV}\rightarrow\mathrm{Grid}}$	kWh	PV generated energy exported into the utility grid within a specified time period. Energy is determined at the Source: PV Generator

Energy

$E_{\text{aux,charge}}$	kWh	Energy Charged
$E_{\text{aux,discharge}}$	kWh	Energy Discharged
E_{In}	kWh	Energy Input (generic) within a specified time period
E_{Out}	kWh	Energy Output (generic) within a specified time period
E_{charged}	kWh	Energy charged
$E_{\text{discharged}}$	kWh	Energy discharged
$E_{\text{Grid,export}}$	kWh	Energy exported into the utility grid in a specified time period
$E_{\text{Grid,import}}$	kWh	Energy imported from the utility grid in a specified time period
$E_{\text{Input},i}$	kWh	BESS Input/Charged Energy within a specified the time period
E_{Load}	kWh	Energy consumed by electrical loads in a single family household or emulated load in the laboratory, in a specified time period
$E_{\text{Output},i}$	kWh	BESS Output/Discharged Energy within a specified the time period
E_{PV}	kWh	Generated PV energy (MPPT of DC power)
$E_{\text{PVS,DC}}$	kWh	Generated DC energy from the PV simulator for a specified time period
L_{E}	kW h	Instantaneous energy loss in a specified time period

Measurement Points

MP_{BAT}		Measurement Point (V/I) battery DC terminal
MP_{BESS}		Measurement Point (V/I) battery converter/inverter connected to the AC-Link (AC coupled system)
$\text{MP}_{\text{DCL-Bat}}$	W	Charge Controller connected to the DC-link of a PV inverter
MP_{GRID}		Measurement Point (V/I) at POC-GRID

MP_{LOAD}		Measurement Point (V/I) for the electrical load (Measured or calculated by use of the nodal rule)
MP_{PVS}		Measurement Point (V/I) PV simulator DC output power

Power Distribution

$P_{Bat \to Grid}$	W	Battery discharged power, exported into the utility grid. Determined at the power source: Battery
$P_{Bat \to Load}$	W	Battery discharged power used for load coverage. Determined at the power source: Battery
$P_{Bat \leftarrow Grid}$	W	Battery DC charge power, imported from the utility grid. Determined at the power sink: Battery
$P_{Grid \to Bat}$	W	Grid imported power used for charging the battery. Determined at the power source: Grid
$P_{Grid \leftarrow Bat}$	W	Grid exported power from battery discharge. Determined at the power sink: Grid
$P_{Grid \to Load}$	W	Grid import used for load coverage. Determined at the power source: Grid
$P_{Load \leftarrow Grid}$	W	Load power covered from grid imported power. Determined at the power sink: Load
$P_{Load \leftarrow Bat}$	W	Load covered by batter discharge power. Determined at the power sink: Load
$P_{Load \leftarrow PV}$	W	Load covered from PV generated power. Determined at the power sink: Load
$P_{Bat \leftarrow PV}$	W	Battery DC charge power from PV generation. Determined at the power sink: Battery
$P_{PV \to Bat}$	W	PV generated power used for charging the battery and coverage of charge losses. Determined at the power source: PV generator

$P_{\mathrm{Grid}\leftarrow\mathrm{PV}}$	W	Grid exported, PV generated power. Determined at the power sink: Grid
$P_{\mathrm{PV}\rightarrow\mathrm{Grid}}$	W	PV power comprising for grid exported power and feed-in losses. Determined at the power source: PV generator
$P_{\mathrm{PV}\rightarrow\mathrm{Load}}$	W	PV power used for load coverage. Determined at the power source: PV generator

Power

$P_{\mathrm{DC,r}}$	W	Rated input power PV Inverter
L_{P}	W	Instantaneous power loss
$P_{\mathrm{AC,r}}$	W	Rated AC output power PV Inverter
P_{BAT}	W	Active battery DC power
$P_{\mathrm{Bat,charge},i}$	W	Sampled value of active battery DC charge power at t_i
$P_{\mathrm{Bat,discharge},i}$	W	Sampled value of active battery DC discharge power at t_i
P_{BESS}	W	Power at the AC terminals of an AC-coupled battery system
$P_{\mathrm{DCL\text{-}Bat}}$	W	Power of the charge controller, measured at the DC-link of the inverter
P_{Grid}	W	Active import or export power
$P_{\mathrm{Grid,import},i}$	W	Sampled value of grid import power at t_i
$P_{\mathrm{Grid,export},i}$	W	Sampled value of grid export power at t_i
P_{In}	W	Instantaneous input power
$P_{\mathrm{In},i}$	W	Sampled value of specified input power at t_i
P_{Inv}	W	PV Inverter (AC-coupled) or PV-BESS (DC-coupled) AC power
$P_{\mathrm{INV,AC},i}$	W	Sampled value of the PV Inverter AC output power at t_i
P_{Load}	W	Load power
P_{Load}	W	Power consumed by the load (load in the laboratory emulated demand of electrical household appliances

$P_{\text{Load},i}$	W	Sampled value of the load power at t_i
$P_{\text{Load(max.discharge)}}$	W	Maximum power, the load can be supplied entirely from battery discharge power and no additional grid import power is required
P_{loss}	W	Not direct usable power after a power conversion process
$P_{\text{PVS,MPP(max,charge)}}$	W	Maximum power of the PV simulator, where entirely power can be charged into the battery and is not additionally fed in
$P_{\text{PVS,MPP,x-cycle}}$	W	PV simulator MPP power used to charge the battery during the RTE test routine for cycle x
$P_{\text{Out},i}$	W	Sampled value of specified output power at t_i
P_{Out}	W	Instantaneous output power
$P_{\text{POC-AC,export},i}$	W	Sampled value of PV-BESS AC output power determined at the connection to the AC link at t_i
$P_{\text{POC-AC,import},i}$	W	Sampled value of PV-BESS AC input power determined at the connection to the AC link at t_i
P_{PV}	W	PV Generator output power
$P_{\text{PV,MPP}}$	W	PV generator output at Maximum Power Point, for given irradiation and temperature
$P_{\text{PVS,DC},i}$	W	Sampled value of the PV Simulator DC output power at t_i
$P_{\text{PVS,DC},i}$	W	Sampled value of the PV simulator DC output current at t_i
$P_{\text{PVS,MPP},j}$	W	MPP power provided by the PV Simulator within the time period T_j
$P_{\text{PVS,MPP}}$	W	MPP power provided by the PV simulator
$P_{\text{AC},i}$	W	Sampled value of the inverters output power $V_{AC\text{-}RMS,i} \cdot I_{AC\text{-}RMS,i}$

Step Response

$2 \cdot \Delta v_s$		Specified tolerance limit
u		Input variable
U_0		Initial value of the input variable
U_s		Step height of the input variable
v		Output variable
V_0		Steady-state value before application of the step
V_∞		Steady-state value after application of the step
V_m		Overshoot - maximum transient deviation from the final steady-state value

Time

ΔT_i	s	Period between two subsequent measurement samples $(T_{i+1} - T_i)$
T_c	s	Required time for a full battery charge at specified discharge power and temperature
T_d	s	Required time for a full battery discharge at specified discharge power and temperature
T_j	s	Period in which MPP power $P_{\mathrm{PVS,MPP},j}$ is provided
T_M	s	Measurement period, used for the analysis
T_S	s	Settling time
T_SR	s	Step response time
T_t	s	Dead or Delay time

Voltage

$V_\mathrm{DC,r}$	V	Rated DC input voltage PV Inverter
V_BAT	V	Battery DC voltage
V_c	V	Charge voltage (Average or instantaneous at a specified SOC/OCV)
V_d	V	Discharge voltage (Average or instantaneous at a specified SOC/OCV)
$V_{\mathrm{DC},i}$	V	Sampled value of the inverters DC input voltage at t_i

$V_{\text{DC,max}}$	V	Maximum DC input voltage PV Inverter according EN-50530
$V_{\text{DC,min}}$	V	Minimum DC input voltage PV Inverter
V_{EOC}	V	End of charge Voltage
V_{EOD}	V	End of Discharge Voltage
V_{MPP}	V	Output voltage of a PV generator at the Maximum Power Point for given irradiation and temperature
$V_{\text{MPP,max}}$	V	Minimum DC input voltage MPP tracking of PV Inverter is activated
$V_{\text{MPP,min}}$	V	Minimum DC input voltage MPP tracking of PV Inverter is activated
V_{OC}	V	Open Circuit Voltage of a PV generator / PV cells

Chapter 1

Introduction

1.1 Motivation and Background

Due to global warming and the requirement to meet national and worldwide climate stabilization targets, an increased need for integration of Renewable Energy Sources (RESs) in the electricity network is seen [8]. The European Commisson postulates within the EU 2020 climate & energy package [9] the fulfillment of a 20% change for following targets until the year 2020:

- Reduction of greenhouse gas emissions (from 1990 level)
- Energy generation from RES (which is double to the 2010 level)
- Improvements in energy efficiency

The development and integration of photovoltaic systems in the electricity grid was accelerated by financial subsidy schemes, as feed-in tariffs for customers and sinking PV system prices. In Europe installed PV capacity increased from 1.3 GW in the year 2004, to approximately 81.5 GW in 2013. [10] The average system price for roof-mounted PV systems installed in Germany decreased from 5000 €/kWpeak in the year 2006 to 1300 €/kWpeak in 2015 [11]. PV generated energy can be used directly for coverage of local electricity or it is fed into the utility grid and paid according the applied Feed-In Tariff (FIT). Direct use of PV energy reduces the amount of imported and exported grid energy. The price of imported energy from the utility grid is higher as the renumeration of exported energy. Therefore the overall electricity costs are decreased. The field of application which profits from local used PV energy is basically the residential sector, small business enterprise, agriculture and industry. As PV generated electricity is intermittent and cannot be used during the night the share

of direct used PV energy and the reduction of electricity costs is limited. The profitability of PV systems decreases with declining FITs, as result local consumption of generated PV energy is beneficial. A reduction of imported energy from the utility grid is favorable, because of increasing electricity costs. The average electricity costs for single family households in Germany, increased from 0.195 in the year 2006 to 0.288 €/kWh[12] in 2015. The average feed-in tariff for PV energy in Germany for 2006 was approx. 0.5€/kWh[13] and at the end of 2015 between 0.085 and 0.123 €/kWh given by contract for 20 years [11]. Considering these aspects an increase of local use of PV energy is attractive. This can be done by using a Battery Energy Storage Systems (BESS), which stores PV energy at the day and supplies the electrical demand when no PV energy is available. The profitability of a PV-BESS depends basically on electricity costs, feed-in tariffs and system prices. PV-BESS use a lead-acid or lithium-ion based battery. Recent studies show, that newly installed systems mainly uses lithium-ion technology and that battery and overall system prices are decreasing. [14]. The described aspects make PV-BESS progressively attractive for the residential field. This can be further observed at the current market situation, were a variety of PV-BESS manufacturers (>30) offer their products. The systems are usually designed and dimensioned for single family households [15]. Apartment houses require higher battery capacity, power and special utilization/billing concepts [16]. This thesis focuses primarily on PV-BESS used in single family households with the specific application of increasing the local consumption of PV energy.

1.2 Problem Description

Several risks are identified for PV-BESS concerning safety, reliability and performance. The primary aim shall be the realization of the Return of Investment (ROI), which is related to the effectiveness the PV-BESS is able to decrease overall electricity costs. The effectiveness depends primarily on the system size, considering PV input peak power, battery capacity and charge/discharge power limitations. Thereby the optimal sizing is related to the individual profiles of PV irradiation and electricity demand of the household. Assuming an optimal sized system, effectiveness is decreased with energy conversion losses for feed-in, charging and discharging the battery. The performance of the control system determines the speed and accuracy the electrical loads in the household are supplied with battery discharge power. No standard procedures are available for evaluating the overall performance, considering the

described aspects. The development of standardized test procedures is seen important for the following reasons:

Market needs:

- Criteria to select the most appropriate product
- Guaranteed performance of the PV-BESS in an application environment
- Validated data sheet information the customer can rely upon

Industry needs:

- Differentiation of high quality products from low performing competitors
- Standardized procedures for product comparison
- Insight about deficits and optimization possibilities of the system

A lack in standardization for PV-BESS is observed. Standards exist basically for single components as PV inverter, battery or charge controller but not for the complete system. An evaluation of the complete system is necessary, because of the interaction between components. Developed laboratory test procedures shall be performed at the full integrated system as it is installed at the customer site (household). Not all PV-BESS provide interfaces for direct setting of charge/discharge power levels. The battery power during laboratory tests is controlled basically by the same inputs as in the field. This is PV generation, emulated by a PV simulator and the demand of electrical appliances in a household, emulated by controllable loads in the laboratory. PV-BESS are available at different system sizes. This makes a comparison with one characteristic index impossible. One system might work better for a specific user and worse for an other. Depending on the specific construction type (modular, full integrated) and electrical topology (AC coupled, DC coupled) the accessibility to measurement points may be restricted. Table 1.1 gives a first overview about the options for system configurations, which results in a large number of possible system states as combination of power distribution and SOC.

TABLE 1.1: PV-BESS configuration possibilities and dependent operation variables

System configuration	Operation
Topology (AC,DC)	SOC
Battery Technology (Lithium-ion, lead acid)	Temperature
Phases (Single, three phase)	Charge / discharge power
Battery capacity / nominal voltage level	Feed In Power (Local use)
Power limitations: feed-in/charge/discharge	
Control / charge algorithm	

It is seen that information about energy efficiency is sometimes provided by PV-BESS manufacturers. The applied procedures are mostly performed with individual power settings and not necessarily described. It does not allow a comparison between systems nor it gives insight about efficiency in the application. For instance the often stated maximum efficiency can differ widely form efficiency during partial load operation.

1.3 Objectives and Hypotheses

This thesis focuses on performance evaluation of PV-BESS. The objective is to develop proposals for possible standardized test procedures with the purpose of a better comparison of PV-BESS and a validated data-sheet the customer can relay on. It shall provide information that the system operates at a minimum quality and meets the requirement of the specific application aims. The basic aim of the PV-BESS is defined herein as the reduction of grid imported energy to zero by discharging the stored PV energy within its power limits to supply the electrical demand in the household. The PV-BESS shall store PV energy in the battery if a surplus is available (PV power > electrical demand) within its SOC and power limits.

It is seen that PV-BESS may provide operation at different charging strategies. The charging strategy can deviate if a price signal is considered and feed-in is prioritized. The market incentive program (2013-2015) for PV-BESS from the German Federal Government and state-owned KfW banging group requires the limitation of maximum feed-in power to 60% of the PV generator peak power [17]. Smart charge algorithms use weather forecasts to charge the battery when curtailment occurs. The developed test procedures shall be performed with a PV-BESS configured for the standard/basic operation mode, without concerns to extended charging schemes or ancillary services.

The test procedures are performed in laboratory environment using a PV simulator for emulation of a PV generator and electrical loads which emulate the demand of electrical household appliances. The time effort shall be kept less as possible and automatic test procedures are preferably used to limit the testing costs for the manufacturer. The aim of this work is not to express the overall performance by using one characteristic index but moreover a portfolio of test procedures, providing performance indices as single numbers or as graphical representation. The performance of the PV-BESS is divided into:

- Energy Conversion Efficiency
- Effectiveness to meet the application aims of grid connected PV-BESS
- Performance of the control system

The developed procedures and test portfolio shall serve as basis performance evaluation and can be extended in further developments for variations of the specific application aim or ancillary services. Despite the customer needs the PV-BESS manufacturer shall obtain more detailed information about the test progress (voltages, currents, etc.) for better knowledge and optimization possibilities of the system or single components.

The thesis is structured that in Section 2 comprehensive knowledge about PV-BESS is given. It describes single components and interaction between them. The third chapter reveals the basic methodology, related to performance testing. Chapter 4 describes a proposal for a test portfolio, developed test procedures and examples of test results.

1.4 Basic Overview

A basic overview about the application and operation principle of grid connected, PV battery energy storage systems will be given. Based on Figure 1.1 a PV system is described first, without concerns to the battery system. Section 1.4 explains the additional components and added value of a BESS in detail.
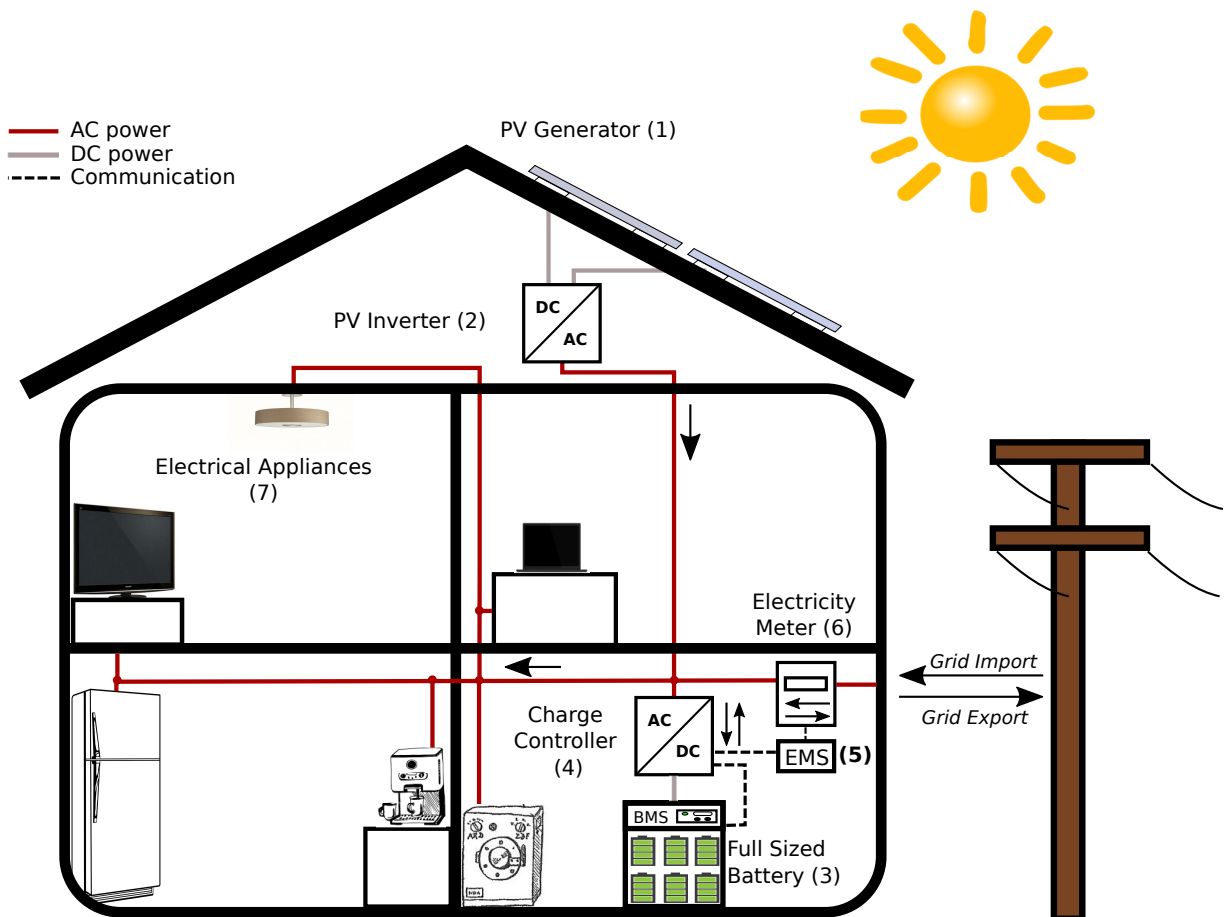
FIGURE 1.1: PV system (1,2) with extension of a battery system (3,4,5). The grid imported/exported energy is measured by the energy meter (6). The household consists of several electrical appliances as television, fridge, lighting etc.(7).

PV System

The concept of a PV system for use in private households is shown in Figure 1.1. The household consists on the on hand of electric consumers, as oven, washing machine or television and at the other hand of a PV generator. A PV inverter converts the produced DC power of the PV generator into AC power. The system boundary is set by the point of connection between residential customer and the utility grid. The generated PV power is either used for demand coverage of electrical appliances - Direct Matched Demand (DMD) or exported into the utility grid (feed-in). Figure 1.2 shows the power distribution for three days with low, medium and high PV irradiation and measured electrical demand of a four-person household. The PV generator is sized to 3.2 kW peak .
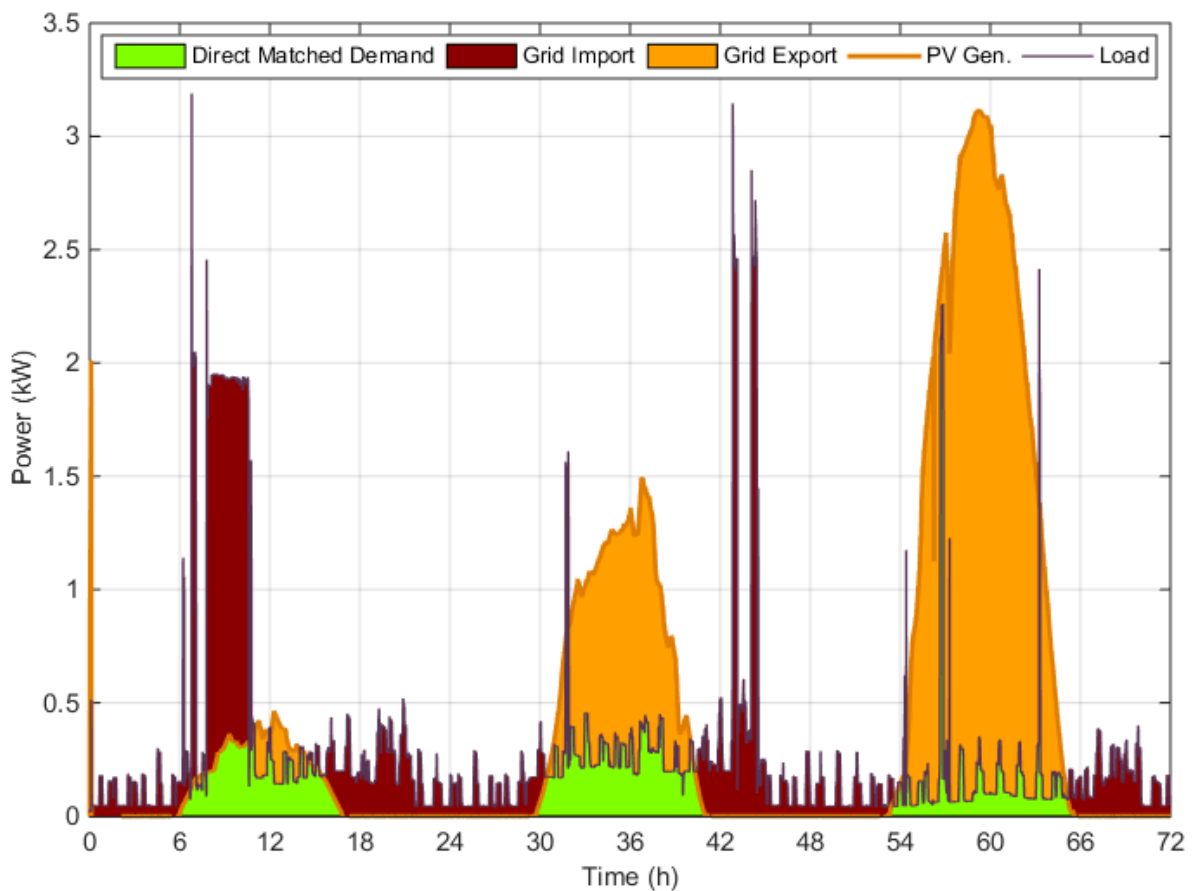
FIGURE 1.2: Example for concurrency between PV generation and demand. The illustration does not include losses of the PV inverter. PV irradiation data from upper Austria, month March (Source:SoDa [18]), load profile from ADRES dataset[19].

The DMD is determined by the concurrency between PV generation and electrical demand. If the generated PV power is less than the electrical demand additional power is imported

from the utility grid. This is always the case from sunset to sunrise. The nightly electricity consumption may consist of electrical appliances as lighting, television, fridge, standby consumption and eventually auxiliary heating.

The effectiveness in using PV power locally, instead of exporting into the grid is expressed as Direct Use (DU) or self-consumption ratio (Equation 1.2). The ability to cover the electrical demand with local PV generated power, instead of grid imported power, is expressed as Self Coverage (SC) or self-Sufficiency ratio (Equation 1.3). In addition the relation between total generated PV energy and demand is given in Equation 1.1. DU and SC are in principle determinable for a single instant of time but are usually given for a specific time period, i.e. one year.

Total coverage

Is defined as ratio between total PV generation and demand for a certain period of time. It does not considers concurrency between generation and demand. [20]

$$\text{Total Coverage (TC)} = \frac{\text{total generation}}{\text{total demand}} \cdot 100 \tag{1.1}$$

Direct use (Self-consumption)

Is defined as ratio between direct matched demand of electrical appliances in the household and total PV generation. It considers the concurrency between demand and PV generation. [20]. DU includes usually losses of the PV inverter.

$$\text{DU} = \frac{\text{direct matched demand} + \text{PV inverter losses}}{\text{total generation}} \cdot 100 \tag{1.2}$$

Self-coverage (Self-sufficiency)

Is defined as ratio between direct matched and total demand, considering the concurrency between demand and PV generation. It represents the part of the electrical demand, which is immediately matched by PV generated power. [20]

$$\text{SC} = \frac{\text{direct matched demand}}{\text{total demand}} \cdot 100 \tag{1.3}$$

For the shown sequence in Figure 1.2 a direct use of 21% and self-coverage of 34% is achieved. In general average values are within 25 to 40% per year [21] for single family households and an appropriate dimensioned PV system (Peak power of the PV generator). The upper limit

of SC is given by times with no solar irradiation (night). DU decreases with more installed PV peak power, as more power is fed into the grid and SC increases due to higher achievable concurrency between generation and demand.

direct use and self-coverage are further affected by the seasonal characteristic of PV irradiation and demand. Irradiation is low in winter and has highest values in summer. The seasonal progress of electrical demand in single family households, behaves usually inversely to the generation. It decreases in summer and increases in winter (Figure 1.3). User behavior, electrical appliances and specific building equipment influence the ability to match the PV generation. A day-active household will achieve higher concurrency between generation and demand as a night-active household. An air condition system increases daily demand in summer, whereas a heating pump increases the demand in winter.[8]
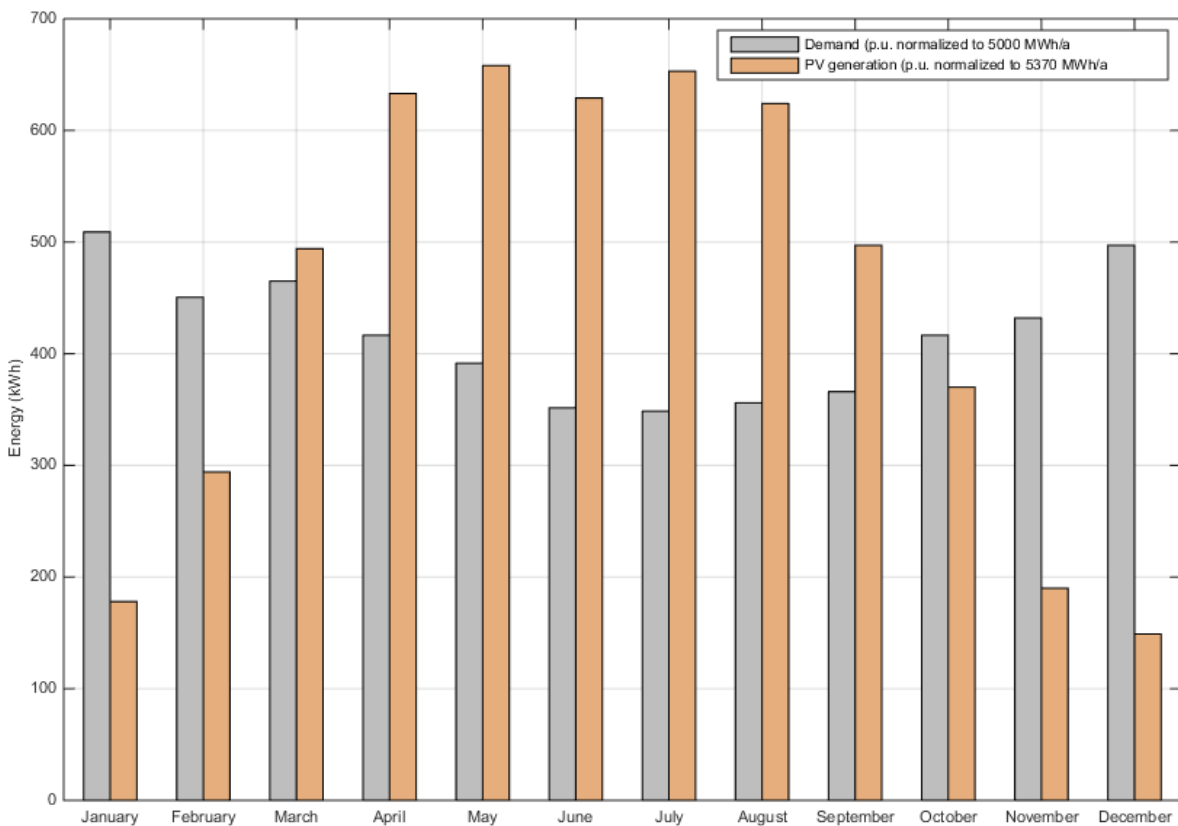
FIGURE 1.3: Typical PV generation and demand during the year (Location Vienna - PV-peak power: 5 kWp, Orientation: South, Inclination: 35°| Annual PV generation 5370 kWh | Annual Demand 5000 kWh) [22],[23]

Increased shares of direct use and self-coverage are generally achievable by demand side management, which shifts the electrical demand into times with PV generation. As result the concurrency between total generation and demand is increased. This method is limited

to times when PV generation is available. The entire electrical demand outside this times (e.g. nightly demand) will not be covered and energy must be imported from the utility grid. The following options are available.

- Change of specific user behaviour
- Demand Response (DR) (demand controlled by an energy management system)
- Domestic Hot Water

Alternatively an Energy Storage System (ESS) can be used. The generated PV energy is stored and usable for later demand coverage, when generation is not sufficiently available. The storage system is not restricted to BESS, for instance conversion in hydrogen and vice versa could be an alternative. This work focuses only on PV battery energy storage systems, which provide the most developed option to fit the application for increasing direct use an self-coverage in the residential field.

PV Battery Energy Storage System

A grid connected PV-BESS offers a good opportunity to supply the demand with electricity when not sufficient PV generation is available. The use of a BESS in combination with a PV system is well studied, it provides high achievable shares in direct use and self-coverage. [8],[24],[20]. The amount of imported electricity from the utility grid is reduced by discharging the stored PV energy, in order to supply electrical loads. The overall electricity costs of the residential customer are lowered. The second effect is the reduction of exported (fed-in) electrical energy into the grid by charging the battery. Figure 1.4 gives a first insight about the energy use within a PV and PV-BESS respectively. It illustrates simplified the increase of DU and SC by charging and discharging the battery.

PV System

PV generation   Electrical demand

Grid
Export

Direct Matched
Demand

Grid
Import

PV Battery System

Grid
Export

Direct Matched
Demand

Grid
Import

Storage
Charge

Storage
Discharge

PV Generation

**Grid
Export**

Direct Use

Electrical Demand

**Grid
Import**
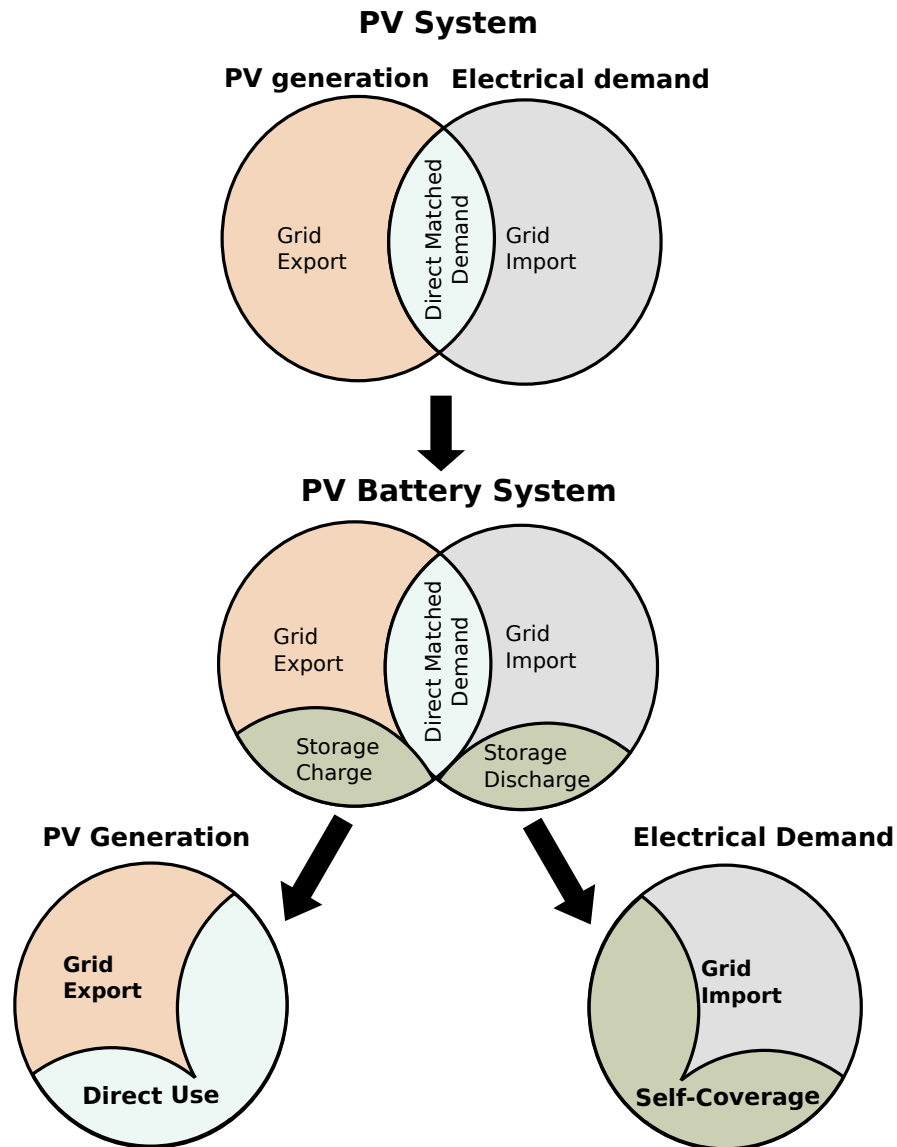
Self-Coverage

FIGURE 1.4: Simplified energy distribution within a PV-BESS (Increase of direct use and self-coverage)

The main components are described for the illustrated system in Figure 1.1. The corresponding component list is found in Table 1.2. The illustrated topology connects the battery over an inverter to the AC link (AC coupled system). Another topology is the DC coupled system, which is described later in detail. The main components and functions are in principle the same for both topologies. The core of the BESS is the battery (3) and charge controller (4). In order to charge or discharge the battery, a bidirectional battery inverter is used. PV inverter and battery inverter build up the whole Power Conversion System (PCS). The Energy Management System (EMS) (6) controls the charge/discharge in order to maximize DU and

SC. It is connected to the battery inverter and the electricity meter (6), which measures the power at the Point of Connection - Utility Grid (POC-GRID).

A surplus of generated PV power is exported into the utility grid. As grid export is registered by the EMS, the battery shall start charging the surplus within its power and state of charge limits. If the EMS registers imported energy from the utility grid the battery is discharged for coverage of the electrical demand. This results in a decreased electricity consumption from the utility grid. During these operations the battery state is permanently monitored by a Battery Management System (BMS). A division of the PV-BESS is done into three main subsystems in Figure 1.5.

TABLE 1.2: Basic components of the PV-BESS, illustrated in 1.1

Index	Component	Description
1	PV generator	DC power generation from solar irradiation
2	PV inverter	DC/AC conversion of PV power
3	Battery	Electrochemical storage
4	Charge controller	Bidirectional battery inverter
5	EMS	Charge/Discharge decisions
6	Electricity (power/energy) meter	Measurement grid power. Input sensor EMS
7	AC powered electrical appliances	Electrical demand
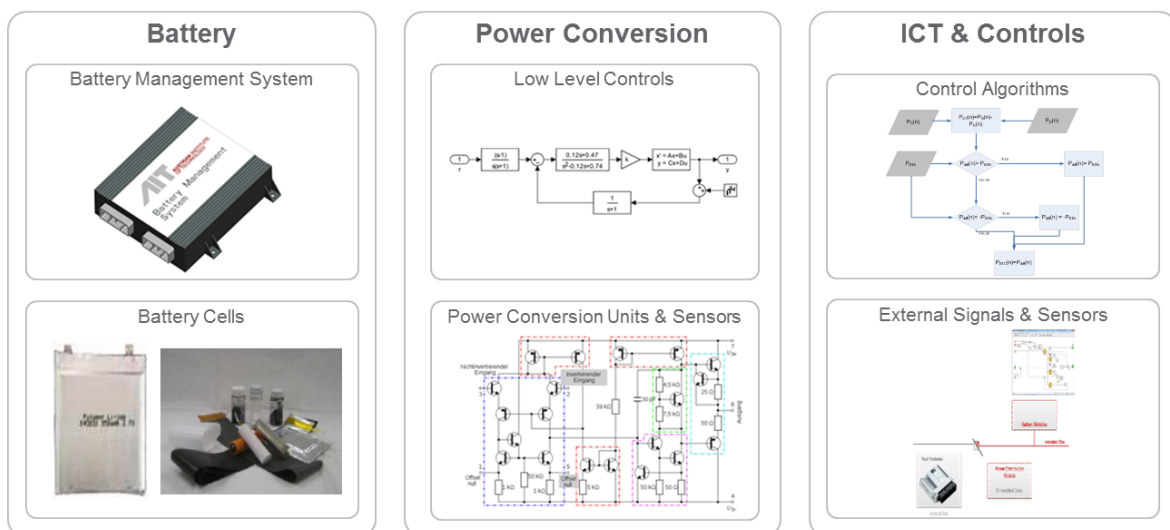
FIGURE 1.5: Subsystems within a PV-BESS

The PCS consists basically of power electronics and eventually transformers for charging the battery and feed-in. A low level control system regulates the currents, to operate at the requested power from a high-level control system.

- DC/DC converter (step-up/step-down converters)
- DC/AC converter (inverter)
- AC/DC converter (rectifier)
- AC/AC converter (high or low frequency transformers)

The Information and Communication Technology (ICT) system represents high level controls (EMS) and communication between components or subsystems. The battery consists of single cells connected in series and/or parallel, which are assembled to standardized, interchangeable battery modules. The BMS protects the battery from overcharge or deep discharge and may control single cells individually for cell equalization.

A grid connected PV-BESS is characterized by the following specifications:

- **Electrical connection scheme**
  — Topology (AC or DC coupled system)
  — Phases (single phase or three phase system)
- **PV Input/AC Output power**
  — Maximum PV input power
  — Maximum output power (PV + battery discharge)
- **Battery Characteristics**
  — Battery chemistry (lead-acid/lithium-ion)
  — Low/high voltage battery system
  — Maximum charge/discharge power
- **Construction Type**
  — All-In-One
  — Modular

Two basic construction designs are available, the All-In-One and modular system design. The All-In-One system comprises PV inverter, charge controller and battery in one single housing. The modular design allows extended configuration possibilities. For instance the choice of PV inverter, battery converter and battery is not limited to one manufacturer. In addition the battery system provides modularity, if it allows the use of a variable amount of single, standardized battery modules.

Based on the electrical connection scheme, PV-BESS are available in two main variations. DC or AC coupled. They are distinguished by the Point of Connection (POC) of the battery. The DC coupled system connects the battery directly to the DC link. The AC coupled system connects the battery to the AC link over a bidirectional inverter unit. As result a prior DC/AC followed by a AC/DC conversion is required for charging.

DC coupled

The advantage of this topology is that no prior DC/AC conversion is required for charging the battery. The DC/AC converter is usually used for PV feed-in and battery discharge to the AC link or both. The DC coupled system is subdivided into DC hybrid and DC generator coupled system:

The **DC hybrid coupled system** is illustrated in Figure 1.6. The battery is connected over a bidirectional charge controller to the DC link (intermediate circuit) of the PV inverter. The PV generator is frequently connected over a DC/DC boost converter to the intermediate circuit. The DC voltage of the PV generator is adjusted by a control system for Maximum Power Point Tracking (MPPT) and the DC link voltage of the inverter is kept at a constant level (360 V to 480 V) for single phase [25] and a voltage >560 V for three phase systems.

A step-down DC/DC converter is used for charging the battery. Discharging the battery to the AC link is done by a step-up DC/DC converter and the DC/AC inverter stage . The DC/DC converters may include HF transformer for galvanic isolation purpose.

The **DC generator coupled system** connects the battery over a bidirectional charge controller directly to the output of a PV generator and to the DC input of a PV inverter (Figure 1.7). The system is basically retrofittable, as a commercial available PV inverter is used. If the BESS and PV inverter is not provided from the same manufacturer, compatibility conflicts may be an issue. The main challenge is the MPPT (Section 2.2.1). It is performed by the PV inverter or/and charge controller respectively. Incompatibilities of these devices may lead to instabilities of the MPPT and increased energy losses. In order to cover the nightly electrical demand the BESS is discharged over the PV inverter. Therefore it must maintain a convenient DC input voltage, ideally it emulates the I/V characteristic (Section 2.2.1) of a PV module. A PV inverter in standby mode needs some time to start up, this could be problematic if the BESS has to supply loads with a dynamic on/off characteristic. For instance the demand of a fridge during the night has such a cyclic pattern. The BESS

can try to keep the inverter 'woken up' by discharging and therefore injecting low power into the PV inverter, but this may effect the overall efficiency of the system because of increased standby consumption.
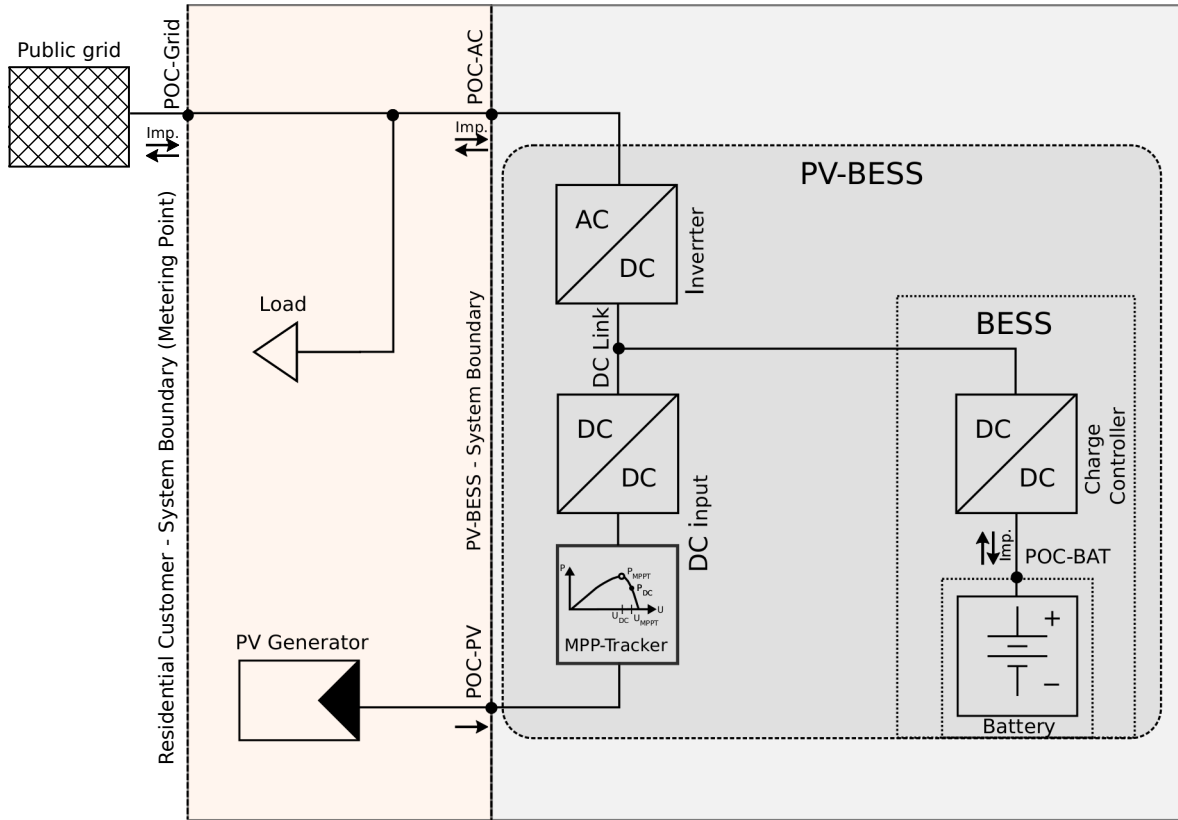
FIGURE 1.6: DC hybrid coupled system
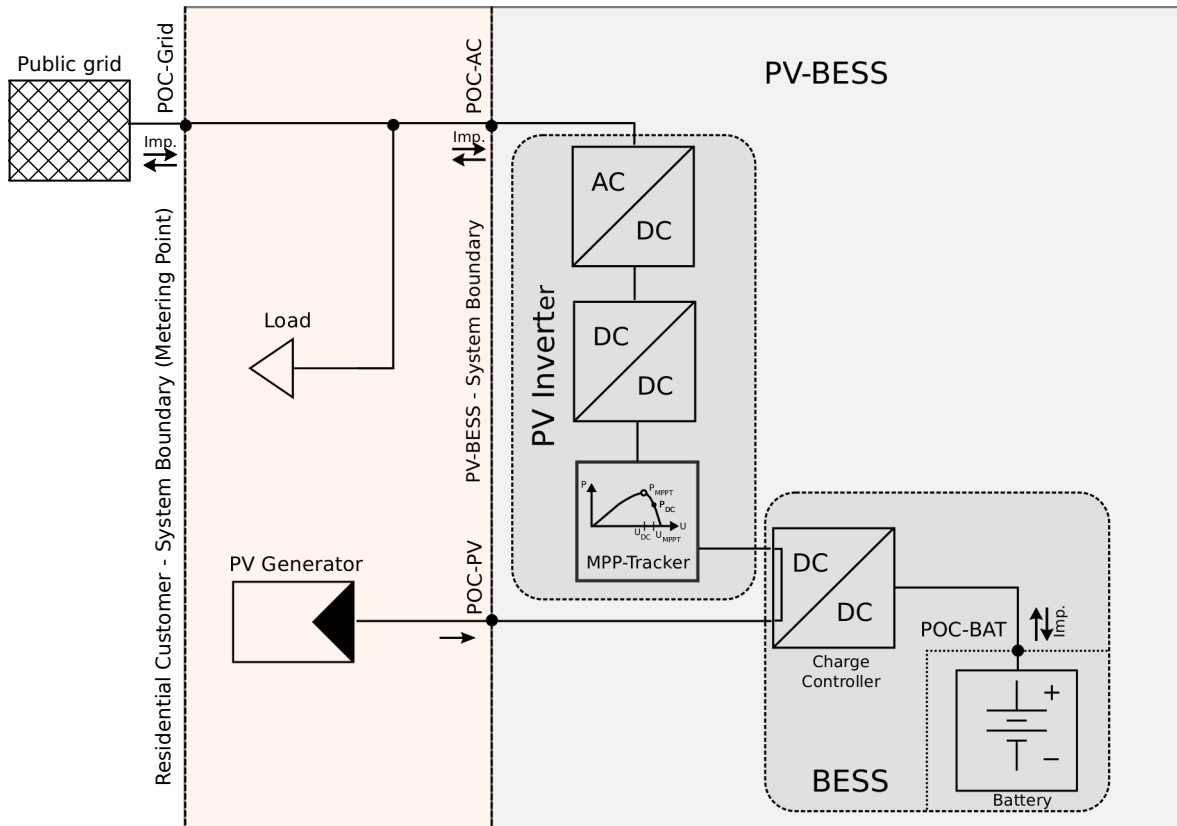
FIGURE 1.7: DC generator coupled system

AC coupled system

The AC coupled system offers flexibility, as it is retrofittable to existing PV system instal-
lations. Charging the battery from PV requires two energy conversion steps, which is a
disadvantage against the DC coupled system. The system consists of two AC/DC converters
(bridges), whereas the DC coupled system usually uses only one. The battery is connected
over a bidirectional charge controller and inverter to the AC link. The PV generator is con-
nected over a standard PV inverter to the AC link. (Figure 1.8) The voltage of the utility
grid 230 V (Europe) is transformed to the battery voltage, usually 48-60V for LVB-BESS.
Therefore a DC/DC converter or LF transformer is used. Figure 1.9 shows a commonly used
single stage topology using a 50/60 Hz transformer. The battery is connected to the inverter
stage and no DC/DC converter is used.
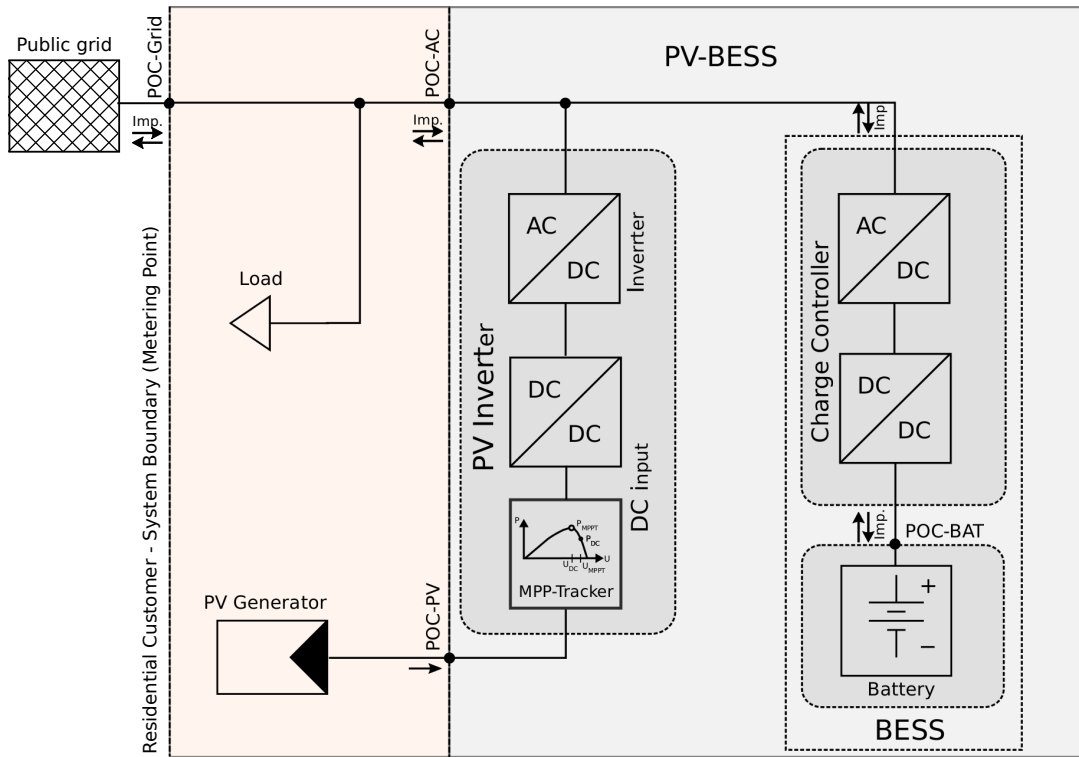
FIGURE 1.8: AC coupled system using a DC/DC converter for voltage adaptation
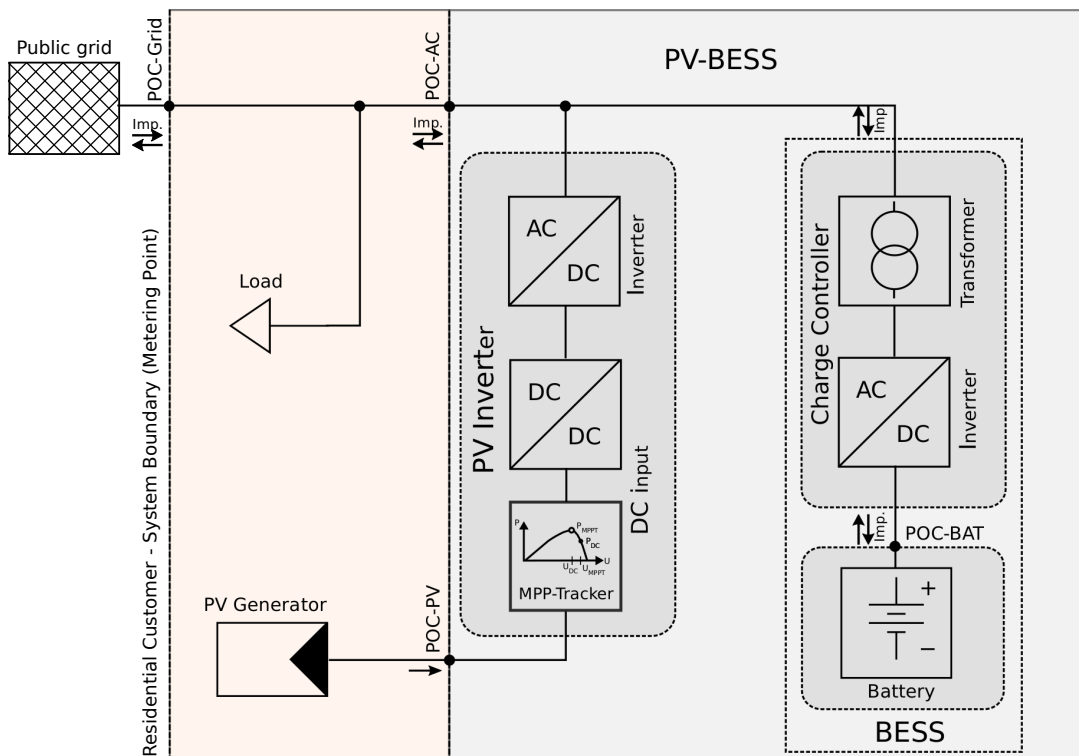
FIGURE 1.9: AC coupled system, single stage topology using a LF transformer for voltage adaptation

Phases / Battery voltage

Further specifications of a PV-BESS are given by the amount of phases and the battery voltage. Three phase inverters require a higher DC link voltage and therefore usually a High Voltage Battery Energy Storage System (HVB-BESS) is used. The battery voltage of these systems is given between 120 V to 400 V. The energy loss of the charge controller is decreased due to a lower transformation ratio. At the other complexity and standby losses may increase because off additional equipment due to stricter safety requirements.. Single phase systems usually use LVB-BESS in the range of 48 V to 60 V, because of the lower DC link voltage, less safety requirements and decreased overall costs.

Summary

Figure 1.10 gives an overview of a few commercial available systems, categorized by electrical connection scheme and construction type.

DC-coupled- Single or three phase System			AC-coupled Single or three phase System	
DC-Generator	**DC-Hybrid**			
• DC- charge unit connected to PV-String, and PV-Inverter	• Battery connected to the DC-Link of a conventional PV-Inverter		• Bidirectional Battery Inverter charge unit	
Modular	**Full integrated** • Integrated Battery • Integrated EMS	Modular • External Battery • Integrated EMS	Modular • External Battery • External EMS • External PV-Inverter	Modular • Integrated Battery Modules (Extendable) • External EMS • Integrated EMS • External PV- Inverter
Ökosolar Power Storage	Sunny Boy Smart Energy (1-ph)	FroniusSymoHybrid (3ph)	SMA – Sunny Island (1ph)	Varta Enigon (3ph)
Sia ProLine	SAMSUNG-ESS (1ph)	NEDAP–Powerrouter (1ph)	Studer-Xtender (1ph)	

FIGURE 1.10: System variety, demonstrated for a few commercial available PV-BESS (Sources of pictures can be found in Appendix C)

An evaluation program for installed PV-BESS in Germany was done by ISEA-RTWH-Aachen. Figure 1.11 shows the market share of different system types. Related to all registered systems between 2013 and 2015 the lead-acid technology still has a high share, but the trend goes definitely to lithium batteries. In the year 2013 70% of installed systems based on lead-acid technology, in the first quarter of 2015 about 70% of installed systems based on lithium-ion technology [14].
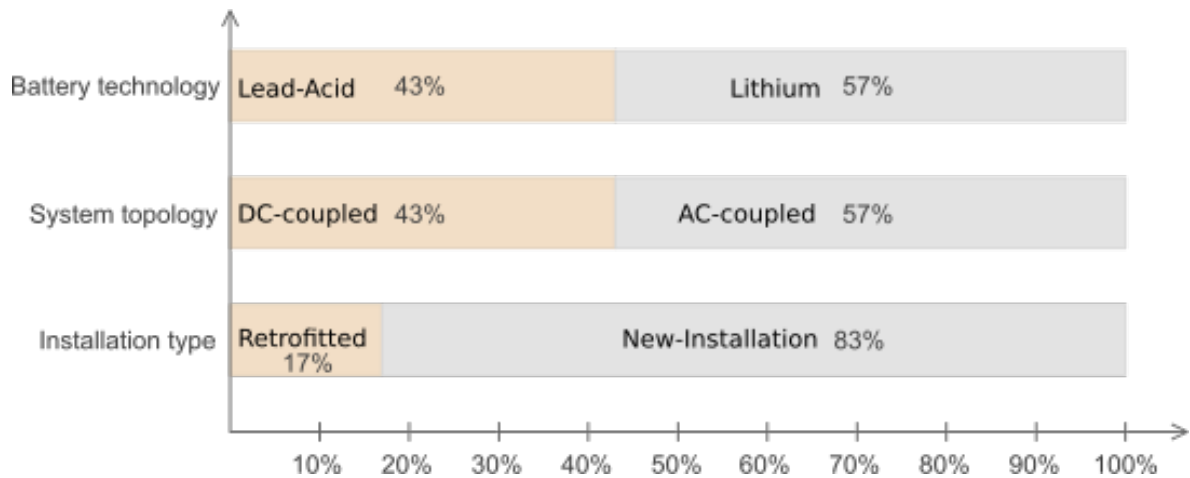
FIGURE 1.11: Segmentation of installed PV-BESS in Germany, related to total amount of registered systems, within the evaluation storage monitoring program of the RTWH-Aachen. [14].

Chapter 2

Technical Background

A comprehensive understanding about the energy distribution of a PV-BESS and detailed description of single components and functions is given within this chapter.

2.1 Application - Residential PV Storage Systems

The application aim of PV storage systems for residential use (home storage systems), is a reduction of electricity costs by increasing the share of direct use and self-coverage. At the End of Life (EOL) of the PV-BESS, the savings shall increase the overall PV-BESS costs for profitability. The characteristic effectiveness indexes DU and SC are determined usually for long term observations within a simulation approach or field measurements. In general energy conversion losses are simplified or not considered in PV-BESS simulation models. The model of the ICT and control system usually does not consider limited dynamics or communication latencies between components. These simplifications are acceptable for generic profitability analyses [26] or optimization of the PV-BESS sizing (battery capacity, PV generator peak power etc.) [27]. Effectiveness and efficiency evaluation in laboratory environment must consider all aspects, which requires knowledge of used energy transfer paths within a PV-BESS. These are illustrated in Figure 2.1.
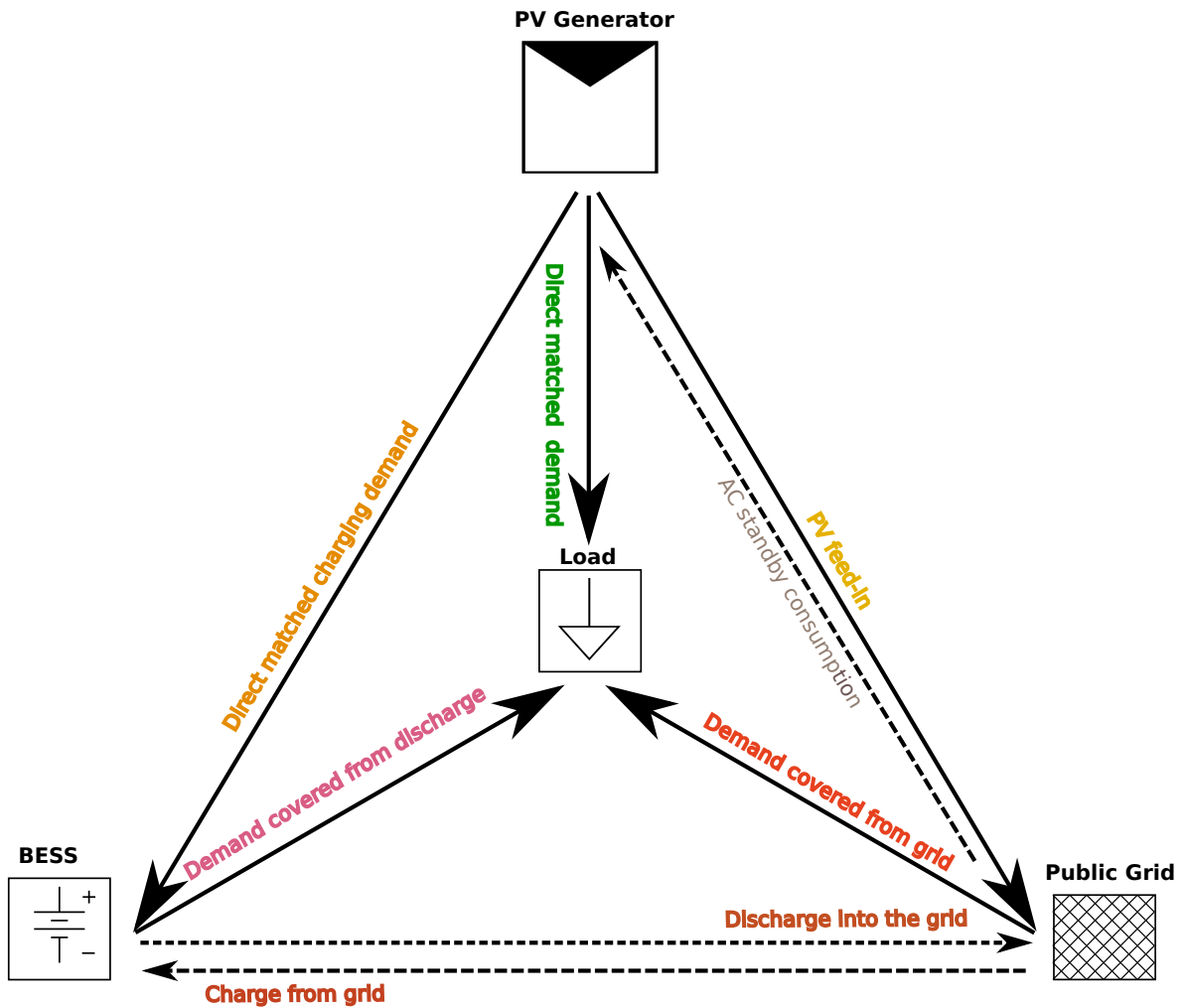
FIGURE 2.1: Energy transfer paths within grid-connected PV battery energy storage systems

A division into energy sources and sinks is done. Table 2.1 shows the corresponding allocation. PV generator and load (electricity demand) evoke basically unidirectional energy flow. Energy transfer from the grid to the PV generator results from standby consumption from the PV inverter during the night and is usually very low.

TABLE 2.1: Energy sources and sinks in a grid-connected PV battery system

	Energy Source	Energy Sink
PV Generator	PV generation	PV inverter AC standby consumption
BESS	Discharge	Regular Charge + AC standby consumption
Public Grid	Grid import	Grid export
Load	-	Electrical household appliances

In an ideal system, with the only purpose of increasing the degree of direct use and self-coverage, no energy is charged from the grid nor discharged into the grid. In a real PV-BESS this is usually not the case, for the following reasons:

- Three Phase Compensation (Section 2.4)

- Limited dynamic of the control system (Section 3.4)

- Emergency grid charge (avoids deep-discharge of battery cells)

- Provision of ancillary grid support services as P(f), Q(U) [28]

- Consideration of additional control inputs, as e.g. a price signal

The corresponding energy transfer paths are illustrated in Figure 2.2 for an AC coupled and in Figure 2.3 for the DC hybrid coupled system. The electrical demand is defined as 'Load' in the subsequent symbol convention.
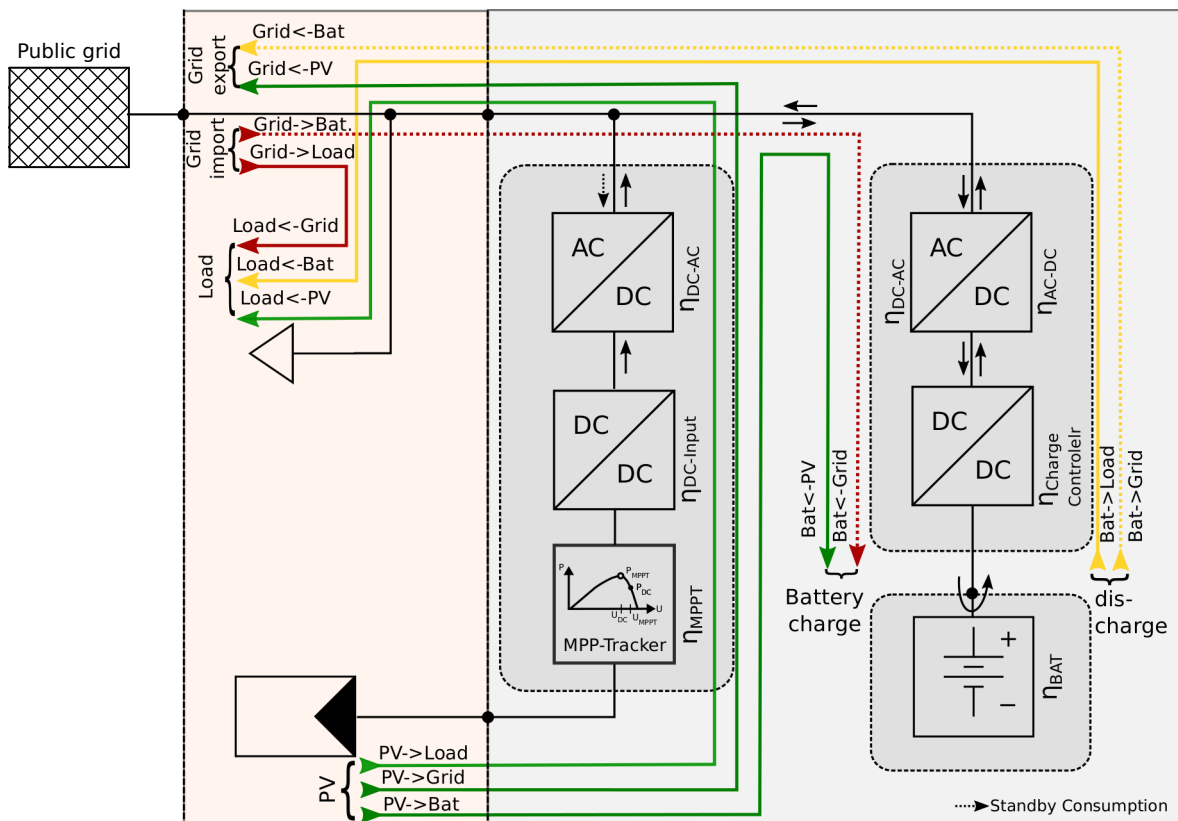
FIGURE 2.2: Power distribution in an AC coupled system
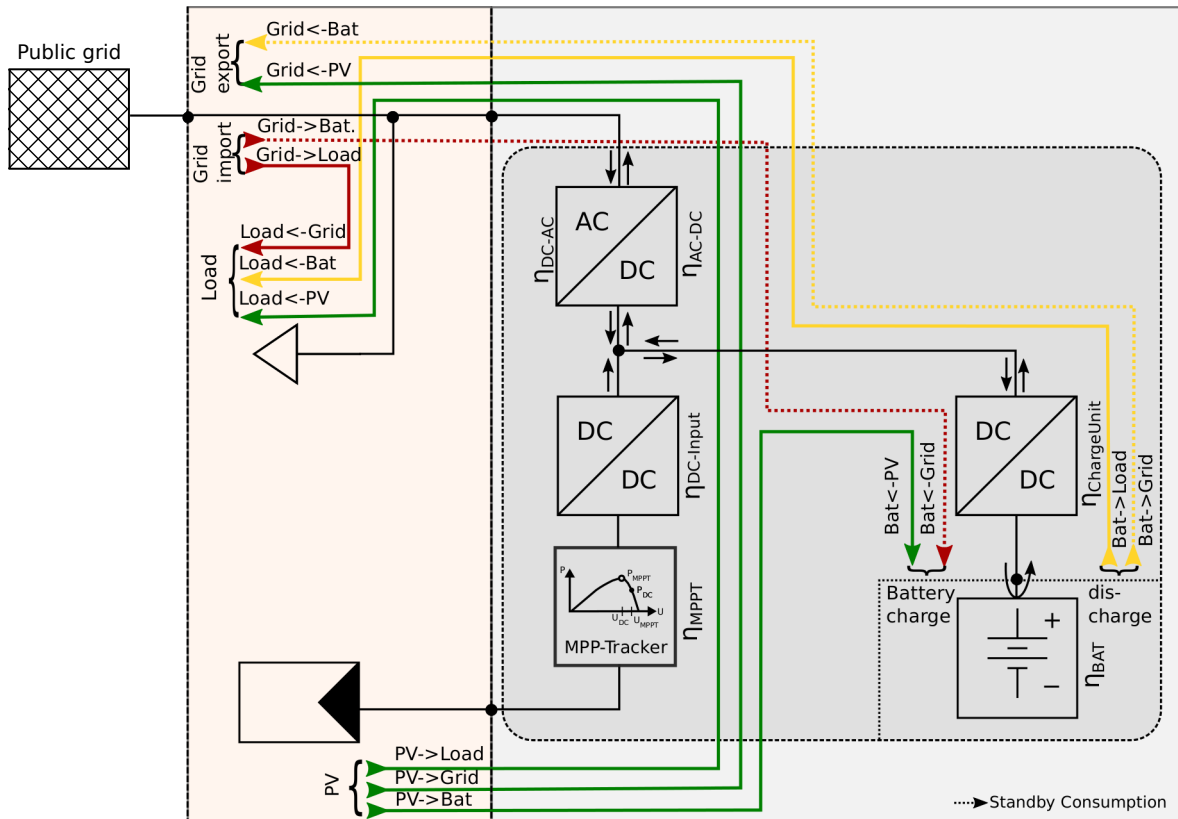
FIGURE 2.3: Power distribution in an DC hybrid coupled system

The power distribution is given for the AC and DC coupled system in Table 2.2. The symbol convention is designed to describe the power at source or sink as follows:

- $P_{\text{Source}} \rightarrow P_{\text{Sink}}$ Power is assigned at the source
- $P_{\text{Sink}} \leftarrow P_{\text{Source}}$ Power is assigned at the sink

The main difference between both systems (AC, DC) is the energy transfer path for charging the battery from PV power (PV to Battery).

TABLE 2.2: Power Distribution PV-BESS

	P_{SOURCE}	$\rightarrow$ **Efficiency(η)/Losses(L)** $\rightarrow$	P_{SINK}
PV to Grid	$P_{\text{PV}\rightarrow\text{Grid}}$	$\eta_{\text{MPPT}} \cdot \eta_{\text{DC-Input}} \cdot \eta_{\text{DC/AC}}$	$P_{\text{Grid}\leftarrow\text{PV}}$
PV to Load	$P_{\text{PV}\rightarrow\text{Load}}$	$\eta_{\text{MPPT}} \cdot \eta_{\text{DC-Input}} \cdot \eta_{\text{DC/AC}}$	$P_{\text{Load}\leftarrow\text{PV}}$
PV to Bat. (DC)	$P_{\text{PV}\rightarrow\text{Bat}}$	$\eta_{\text{MPPT}} \cdot \eta_{\text{DC-Input}} \cdot \eta_{\text{ChargeController}}$	$P_{\text{Bat}\leftarrow\text{PV}}$
PV to Bat. (AC)	$P_{\text{PV}\rightarrow\text{Bat}}$	$\eta_{\text{MPPT}} \cdot \eta_{\text{DC-Input}} \cdot \eta_{\text{DC/AC/DC}} \cdot \eta_{\text{ChargeController}}$	$P_{\text{Bat}\leftarrow\text{PV}}$
Battery to Load	$P_{\text{Bat}\rightarrow\text{Load}}$	$\eta_{\text{ChargeController}} \cdot \eta_{\text{DC/AC}}$	$P_{\text{Load}\leftarrow\text{Bat}}$
Battery to Grid	$P_{\text{Bat}\rightarrow\text{Grid}}$	$\eta_{\text{ChargeController}} \cdot \eta_{\text{DC/AC}}$	$P_{\text{Grid}\leftarrow\text{Bat}}$
Grid to Load	$P_{\text{Grid}\rightarrow\text{Load}}$	/	$P_{\text{Load}\leftarrow\text{Grid}}$
Grid to Battery	$P_{\text{Grid}\rightarrow\text{Bat}}$	$\eta_{\text{AC/DC}} \cdot \eta_{\text{ChargeController}}$	$P_{\text{Bat}\leftarrow\text{Grid}}$

The share of local or direct used PV energy is calculated for a PV-BESS according Equation 2.1. Charging the battery and charge/feed-in losses increase the DU and reduce exported energy into the grid.

$$\text{DU} = \frac{\text{direct matched demand} + \text{Battery Charge} + \text{Losses}}{\text{Total Generation}} \cdot 100 \tag{2.1}$$

$$\text{DU} = \frac{E_{\text{PV}\rightarrow\text{Load}} + E_{\text{PV}\rightarrow\text{Battery}}}{E_{\text{PV}}} \cdot 100 = \frac{E_{\text{PV}\rightarrow\text{Load}} + E_{\text{PV}\rightarrow\text{Battery}}}{E_{\text{PV}\rightarrow\text{Load}} + E_{\text{PV}\rightarrow\text{Battery}} + E_{\text{PV}\rightarrow\text{Grid}}} \cdot 100$$

Alternatively the exported energy into the utility grid can be taken for the calculation (Equation 2.1)

$$\text{DU} = \frac{E_{\text{PV}} - E_{\text{Grid}\leftarrow\text{PV}}}{E_{\text{PV}}} \cdot 100 \tag{2.2}$$

The degree of self-coverage is calculated according Equation 2.3.

$$\text{SC} = \frac{\text{direct matched demand} + \text{Demand Supplied From Battery Discharge}}{\text{Total Demand}} \cdot 100 \tag{2.3}$$

$$\text{SC} = \frac{E_{\text{Load}\leftarrow\text{PV}} + E_{\text{Load}\leftarrow\text{Battery}}}{E_{\text{Load}}} \cdot 100 = \frac{E_{\text{Load}\leftarrow\text{PV}} + E_{\text{Load}\leftarrow\text{Battery}}}{E_{\text{Load}\leftarrow\text{PV}} + E_{\text{Load}\leftarrow\text{Battery}} + E_{\text{Load}\leftarrow\text{Grid}}} \cdot 100$$

$$\tag{2.4}$$

An alternative approach is the calculation over the imported energy from the utility grid (Equation 2.5).

$$\text{SC} = \frac{E_{\text{Load}} - E_{\text{Load} \leftarrow \text{Grid}}}{E_{\text{Load}}} \cdot 100 \tag{2.5}$$

Direct use and self-coverage depend on the specific PV generation profile, electrical demand profile and the specific system size:

The generation profile is specified by:

- Geographical location
- Orientation of the PV generator (azimuth, tilt angle/slope)
- Shading

A study from the University of applied Science HTW-Berlin investigated the influence of geographic location and PV generator orientation to DU and SC for PV-BESS in Germany. A PV-BESS simulation model is used to estimate the characteristic indexes for the different locations over multiple years. A specific load profile and weather data from 23 widespread weather stations in Germany was used. The PV generator is sized in the simulation to one kilowatt peak per Megawatt-hour annual electricity demand. The battery capacity is sized to one kilowatt-hour per megawatt-hour annual demand. Direct use is determined within 54 and 59% and self-coverage between 52 and 56%. Direct use decreases with higher solar irradiation and peak power of the PV generator respectively, whereas self-coverage increases (Figure 2.4). [8]

The simulation results demonstrate that the influence of the PV generator geographical location and orientation is marginal for PV-BESS installed in Germany. [20],[8],[29]. Only slight optimizations of the orientation are possible.

The demand profile is specified by:

- Persons in the household
- Electric appliances
- Special building equipment (heat pumps, air conditioner etc.)
- User behavior

The electrical demand profiles of 74 households was analyzed by the HTW-Berlin. The annual demand was categorized regarding seasonal and diurnal differences. Based on this

the self-coverage was calculated according to the previously described parametrization of the simulation model. The night fraction (sunset to sunrise) to annual electricity demand is given as follows:

- **Mean:** 49 % night fraction (Self-coverage 54 %)[8]
- **Night-active:** 61 % night fraction (Self-coverage 43 %)[8]
- **Day-active:** 32 % night fraction (Self-coverage 61 %)[8]

The summer fraction (spring to autumn) is influenced by specific building equipment and is given as follows: [8]

- **Mean:** 45 % summer fraction [8]
- **Heat Pump (HP):** 25% summer fraction (Self-coverage 45 %)[8]
- **Air Conditioning Unit (ACU):** 58 % summer fraction (Self-coverage 58 %)[8]

Self Coverage decreases for households with a high nightly demand. A higher demand in the winter months is unfavorable as solar irradiation is less available.

DU and SC are further influenced by the system sizing:

- PV Array peak power
- Battery capacity
- Maximum charge/discharge power

Direct use (self-consumption rate) and self-coverage (degree of self-sufficiency) is illustrated as a function of the system size in Figure 2.4 They do not increase proportionally with battery capacity. In order to store enough PV energy the size of the PV generator must be be increased as well.
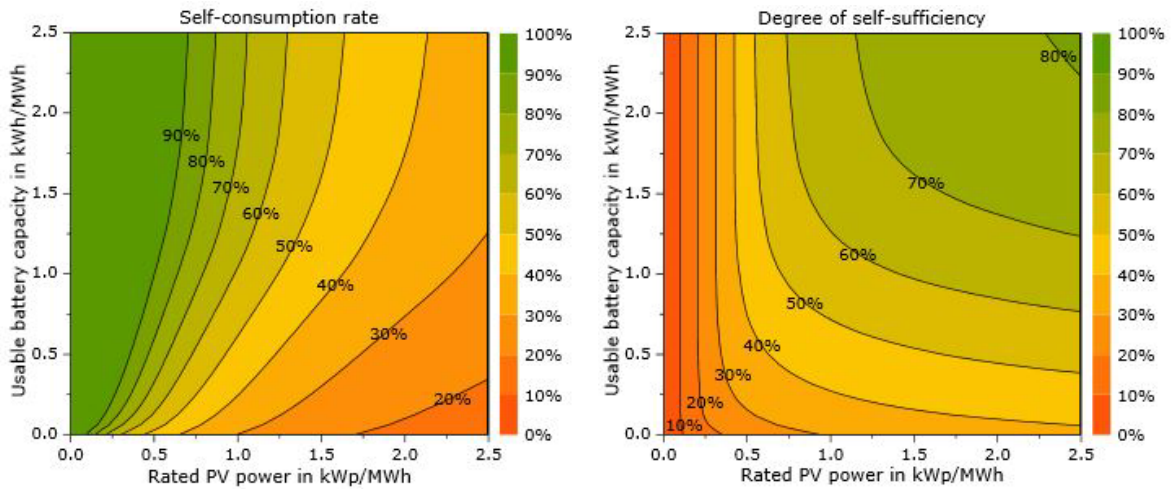
FIGURE 2.4: Mean of annual share of Direct Use (self-consumption) and Self-Coverage (self-sufficiency). PV generator peak power and battery capacity is normalized to the annual demand (Source: Economics of residential PV battery systems in the self consumption age, 2014 [26])

2.2 Power Conversion System

The PCS provides energy transfer between the PV generator, battery and the AC link. It consists of a DC/AC inverter, which transform DC generated power from PV modules or the battery into AC power. Components in PV-BESSs operate usually at different voltage levels. For instance PV input voltage (DC), battery voltage (DC) and utility grid voltage (AC) differ usually in its magnitude. Voltage adaption is performed by DC/DC converters or transformers.

2.2.1 PV Inverter

The main function is the conversion of DC generated power into grid synchronized AC power for local energy use or grid feed-in. The MPP Tracker is used to operate at the Maximum Power Point (MPP) of the PV generator. The basic electrical scheme of a PV inverter is illustrated in Figure 2.5. The specifications are found Table 2.3.
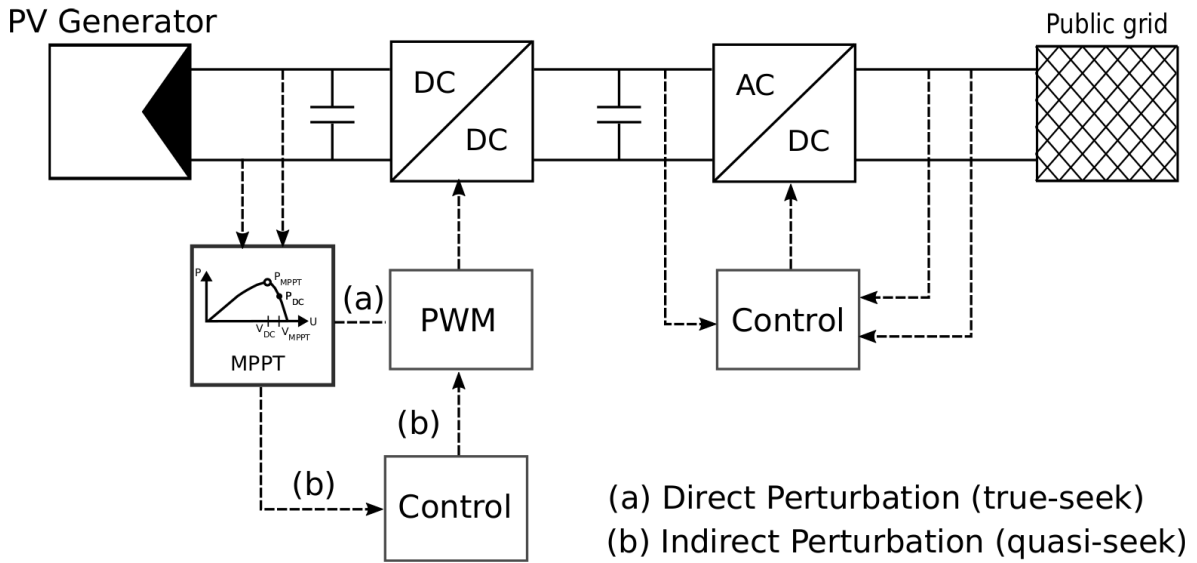
FIGURE 2.5: Double stage PV inverter (Figure adapted from 'Paja,C. et al,. Compensation of DC link voltage oscillations in grid connected PV systems, 2012 [30])

TABLE 2.3: Main specification PV inverter

Symbol	Description	Unit
$V_{\text{DC,min}}/V_{\text{DC,max}}$	minimum/maximum input voltage	V
$V_{\text{DC,r}}$	rated input voltage	V
$V_{\text{MPP,min}}/V_{\text{MPP,max}}$	minimum/maximum MPP voltage	V
$I_{\text{DC,max}}$	maximum input current	A
$P_{\text{DC,r}}$	rated input power	kW
$P_{\text{AC,r}}$	rated output power	kW

PV inverters are categorized as follows:

- Single-string inverters, typically in the 0.4 to 2 kW range for small roof-top plants with panels connected in one string [6].

- Multi-string inverters, typically in the 1.5 to 6 kW range for small roof-top plants with panels connected in one string [6].

- Mini central inverters, typically >6 kW with three phase topology and modular design for large power plants in the range of 100 kW and typical unit sizes of 6, 8, 10 and 15 kW [6].

PV inverters used for PV-BESS are mostly multi-string inverters which provide DC inputs for two PV strings. Each string might have a individual MPP tracker or one tracker is used for both strings. From the customer site a state of the art PV inverter must be high efficient in full and partial load operating area, provide a long service life and reliable operation. From the manufacturer site production costs shall be minimized. Interests in 'smart inverters', which offer ancillary services (reactive power provision / remotely controllable etc.) are observable. [28].

Maximum Power Point Tracking

Figure 2.6 illustrates the Current/Voltage Characteristic (I/V) of a PV cell. The intersection of the vertical axis with the curve, determines the short circuit current I_{SC}. The open circuit voltage V_{OC} is found at the intersection with the horizontal axis. A unique point the MPP exists for PV cells and modules respectively. It is defined by the maximum of of $P_{\mathrm{MPP}} = V_{\mathrm{MPP}} \cdot I_{\mathrm{MPP}}$.
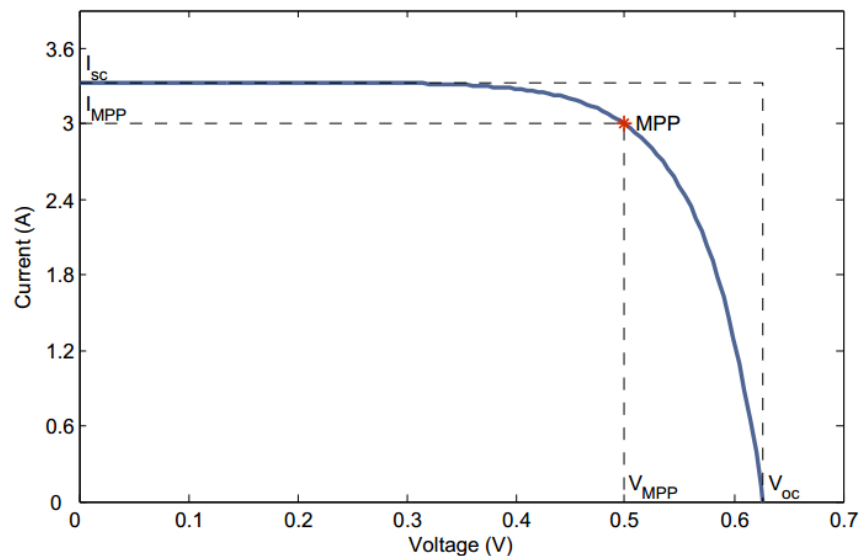
FIGURE 2.6: V/I characteristic of a $100 cm^2$ polycrystalline solar cell. (Source: Spielauer S., Evaluation of the Performance of Maximum Power Point Tracking Methods[31])

The output current of the PV generator increases with higher solar irradiation and the voltage increases with lower temperature. Figure 2.6 illustrates the dependency of power and current to solar irradiation.
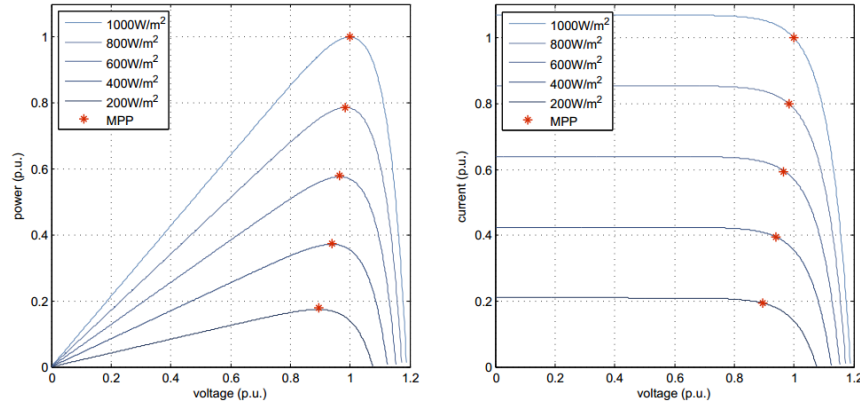
FIGURE 2.7: P/V and V/I characteristic of a PV generator for varying solar irradiation (Source: Spielauer S., Evaluation of the Performance of Maximum Power Point Tracking Methods[31])

The problem considered from MPPT techniques is to find the voltage V_{MPP} or current I_{MPP} at which a PV module must operate in order to obtain the maximum power $P_{\mathrm{PV,MPP}}$ under a given temperature and irradiation [32]. The majority of solutions, implements MPP tracking as software algorithm, which controls the input impedance of the DC/DC switched-mode, usually Pulse-width modulation (PWM) converter[33]. The control strategies of an MPP tracker are usually based on a trial and error algorithm[32]. In principle two implementation options are given:

Direct perturbation (true-seek)

Direct perturbation algorithms find the location of the MPP iteratively by drawing conclusions from the previous samples[33]. The MPP is approached by subsequent modifications of V_{DC}, resulting in oscillations around the true MPP[33]) (Figure 2.5, method-a).

Indirect pertubation (quasi-seek)

Indirect perturbation algorithms conclude the location of the MPP according to built-in knowledge and measurements of parameters other than P_{DC}[33]. The built-in settings may include specific parameters of PV generator, geographical location, climate features and meteorological measurements[33], which requires an additional controller (Figure 2.5, method-b).

Many specific MPP control methods were developed in the past. Detailed information and comparison about 15 different algorithms are found in the literature [32].

Power Conversion

The basic topology is illustrated in Figure 2.5. The PV inverter is divided into two stages. The DC input stage consists of a DC/DC converter (boost, buck or buck-boost converter [34]), the inverter stage is used for DC/AC conversion (full-bridge) and they are interconnected over a DC link (intermediate circuit). The DC/DC converter is used by the MPPT control system for adjusting the voltage at the PV generator. Additionally the boost converter might be required because the AC output voltage of commonly used inverter topologies is usually restricted to be lower than the DC input voltage [35]. Early developed PV inverters used traditionally a LF transformer at the output stage for galvanic isolation (safety requirements) and voltage adaptation. One main disadvantage is the decreased efficiency. Newer inverters are using HF transformers at the input stage and most efficient devices operate entirely transformerless. At the other hand a transformerless inverter requires more complex solutions for maintaining the saftey standards, concerning leaking currents and DC current injection.[6]

For DC/AC voltage and current transformation, traditionally a H-bridge or full-bridge (FB) is used. An implementation as half- or full-bridge is possible. [6] With the aim of increasing the efficiency enhanced versions of the traditionally H-Bridge were developed by several manufacturers.

- H-bridge H5 (SMA)
- H-Bridge HERIC (Sunways)
- H-bridge FB-DC Bypass (Ingeteam)
- H-Bridge REFU

An alternative to the H-bridge is Neutral Point Clamp (NCP). Due its principle NCP is preferable used in three phase inverters >10 kW

2.2.2 Charge Controller

The charge controller is responsible for properly charging and discharging the battery. It regulates the charging/discharging current, to provide the requested power from the EMS. Information of the BMS are used in order to prevent damage to the battery. From the technical point of view the charge controller must transform the input voltage to battery voltage. A DC coupled system uses a step-up/down DC/DC converter for discharging and charging. For isolation purpose a HF transformer might be used. The AC coupled system

requires additionally a AC/DC - DC/AC inverter stage. For voltage adaptation the battery inverter often uses a AC/AC transformer at the AC link input side.

A **non-isolated charge controller** is frequently used at high voltage battery systems (150 V to 400 V). If a LVB-BESS is used, the efficiency is decreased due to the suboptimal modulation factor of the DC/DC converter. This topology achieves a high efficiency and a low amount of semiconductors is required. A disadvantage is the missing galvanic isolation. In order to protect the battery an extra circuitry (fuses etc.) is necessary. The common DC link voltage in a tree phase system can exceed voltage levels above 800 V, which required power switches with blocking voltages of 1200 V. [25].

The **isolated charge controller** uses a transformer in order to provide galvanic isolation between battery and inverter stage. The topology is beneficial for use with low voltage battery systems (12 V to 96 V) if an a appropriate transformer ratio is set.

2.3 Battery and Battery Management System

The battery is an electrochemical storage within electricity is converted into chemical energy and vice versa. The smallest unit is the battery cell. A battery module is built up with more cells, connected in series or/and parallel. In a PV-BESS one or more standardized assembled battery modules are usually used. Cells or modules connected in parallel increase the overall capacity (Ampere-hours), whereas a series connection increases the battery voltage. The entire battery system is defined as Full Sized Battery (FSB) (Figure 2.8) [1] and includes usually a BMS and probably a Battery Support System (BSS) (fans for cooling etc.). The BMS and BSS is usually supplied from the battery. But especially for the BSS an auxiliary AC supply is possible.
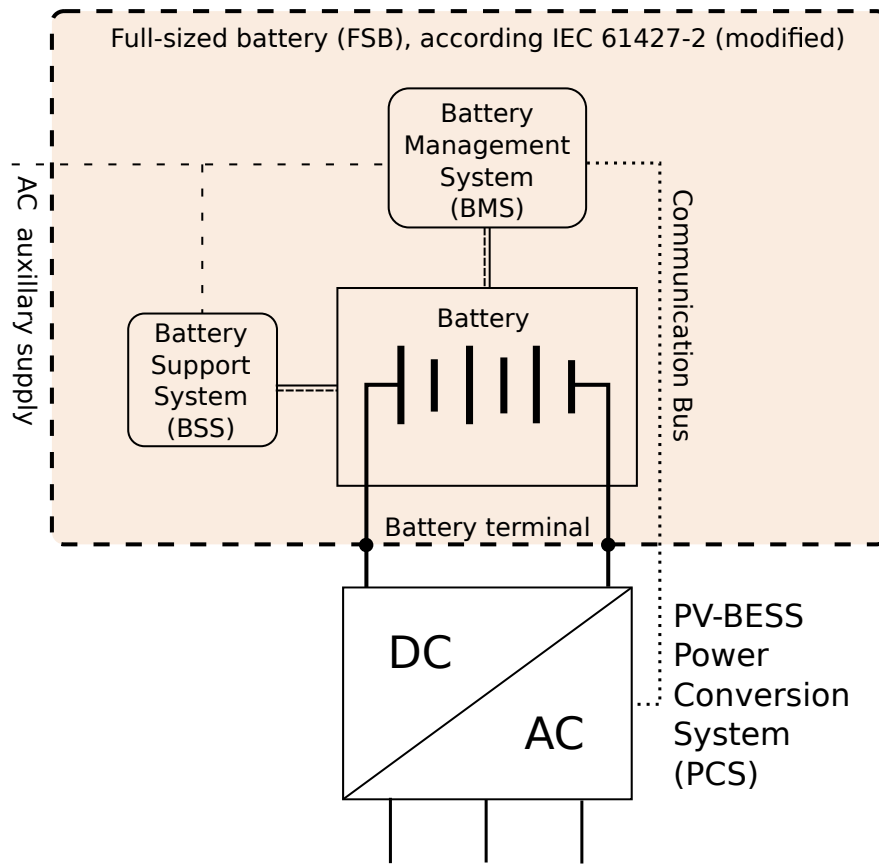
FIGURE 2.8: Description of the battery system. (Figure adapted from IEC 61427-2 [1])

The battery state is monitored by the BMS and communicated to the PCS in order to maintain charge, discharge limitations for battery protection. It monitors and controls single cells (usually for lithium-ion based systems), in order to keep them at the same charge/voltage level. The main tasks are:

- Cell protection
- Cell balancing
- SOC estimation
- Battery condition State of Health (SOH) estimation
- Thermal management
- Communication BMS to PCS

2.3.1 Battery Specifications

This section comprises a couple of indexes, used for battery specification. The definitions apply to single cells, and if not otherwise mentioned likewise to the entire module.

Capacity and SOC

The SOC is defined as an actually available amount of electrical charge (Q) in a battery, related to the maximum available amount of charge (battery capacity). The actually available amount of charge (Q) is determined by a full charge, followed by discharging the battery with a specified current until a predefined End of Discharge Voltage (EODV) at defined environmental conditions (temperature etc.) [2].

$$SOC = \frac{\text{actually available amount of charge}(Q)}{\text{maximum available amount of charge}(C)} \cdot 100 \tag{2.6}$$

Practically a fully charged battery is represented by a SOC of 100 %, whereas a entirely discharged battery is represented by a SOC of 0 %. Differences occur thereby in the definition of 'fully charged' and 'fully discharged'. A classification is done for 'fully charged'. Figure 2.9 (I-III) illustrates the difference.

Physical full means that all active masses (electrode materials) are available for charge. This should be the case for new batteries, at Beginning of Life (BOL). During lifetime, degradation occurs, and active masses are not entirely accessible for electrical charge anymore. Physical full is achieved at the point of time where further charging current is utilized 100 % into side reactions such as gassing or corrosion. [2]

Nominal full is achieved by a charge procedure prescribed by a battery manufacturer. At BOL nominal full should be quite identical to physical full. Often modified charging strategies, as Constant Current / Constant Voltage Charge (CC-CV) are required in order to achieve the physical full state [2]. The nominal full state is achieved at a predefined criterion (Section 2.3.2, Figure 2.12).

Operational full describes the highest possible charging state of a battery under field conditions in a given application. Often nominal charge conditions cannot be applied for batteries that are used in real world applications, considering the maximum charge voltage, the battery temperature and the available charging time. [2] For PV-BESS, the usable capacity is often limited by the manufacturer, for an increased battery lifetime. Limitations are performed by decreasing the End of Charge Voltage (EOCV) or increasing the EODV

The net capacity describes the maximum available amount of charge (C) in a operational fully charged battery. It is determined experimentally at BOL, by a rated power

discharge to the end of discharge voltage at a predefined temperature. The PV-BESS / BESS manufacturer must specify therefore rated discharge power, and provide a battery charge procedure to operational full state. Similar to the net capacity C_{NET} (A h), the net energy content E_{NET} (kW h) is used to express the amount of dischargeable energy at a rated power discharge from an operational fully charged battery.

The Depth of Discharge (DOD) is originally defined as the amount of charge removed from the battery at the given state, related to the total amount of charge, which can be stored in a battery, and is usually expressed as a percentage [2]. It is a measure of how deeply a battery is discharged. When a battery is 100 % full, then the DOD is 0%. Conversely, when a battery is fully discharged, the DOD is 100% (Equation 2.7) [2].

$$DOD_{actual} = \frac{\text{discharged amount of charge}(Q_{\mathrm{d}})}{\text{maximum available amount of charge}(C)} \cdot 100 = 100 - SOC [2] \qquad (2.7)$$

This definition of DOD implies that it is used as variable. By PV-BESS manufactures it is usually given as constant value, defining the ratio between net capacity and nominal capacity. In other words it is described as the maximum performable DOD of a PV-BESS, related to nominal capacity.

$$\mathrm{DOD_{NET}} = \frac{\mathrm{C_{NET}}}{\mathrm{C_{NOM}}} \cdot 100 \qquad (2.8)$$

Battery lifetime is usually expressed in years (calendar life) or the amount of performable full charge/discharge cycles (cycle life). The SOH is used to estimate the battery condition over its lifetime. In general it relates mainly to a capacity loss and furthermore to an increase of internal resistance due to degradation of materials (Equation 2.9). [2]

$$SOH = \frac{\text{actual available battery capacity}(C_{\mathrm{AV}})}{\text{nominal battery capacity at BOL}(C_{\mathrm{NOM}})} \cdot 100 [2] \qquad (2.9)$$

The SOH may be higher than 100 % at BOL. New batteries may have a slightly higher capacity, than given by the manufacturer [2]. The capacity may increase within the first cycles and decrease after a certain amount of cycles again.
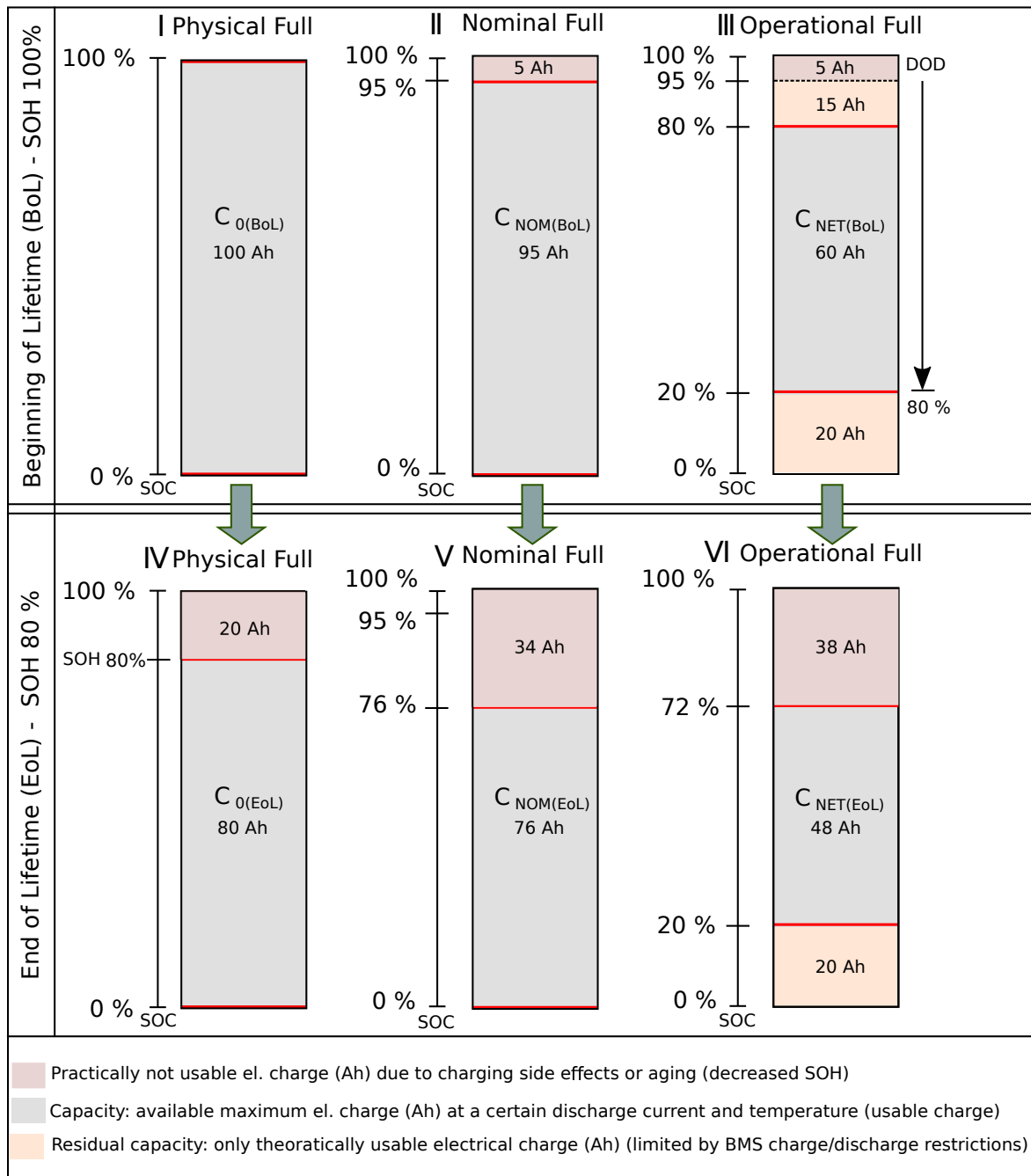
FIGURE 2.9: Battery SOC definitions [2]

Current | Power

The maximum constant charge and discharge current of a battery cell is strongly related to the cell technology and construction. Losses at the inner resistance increase with the square of the applied charge/discharge current. Higher current increases the temperature, which

reduces lifetime. The maximum current is usually limited by the technology and the manufacturer of a PV-BESS for increased lifetime. The discharge current is often expressed as C-rate and is normalized against the battery capacity. The advantage is a better comparability between different dimensioned batteries. If the battery is discharged with a constant current, corresponding to a C-Rate of one (C1) the entire battery discharge process takes approximately one hour. Table 2.4 shows the relation between C-rate, battery current and discharge time.

TABLE 2.4: Example: C-Rate, battery current and discharge time for a 60 and 120 Ah Battery

C-Rate	2C	1C	0.5C	0.1C
Battery A: 60 Ah - Discharge Current (A)	120	60	30	6
Battery B: 120 Ah - Discharge Current (A)	240	120	60	12
Battery A: 60 Ah - Discharge Time (h)	0.5	1	2	10
Battery B: 120 Ah - Discharge Time (h)	0.5	1	2	10

Voltage

In order to characterize and protect the battery from overcharge or deep discharge, the battery voltage is an important criterion.

- Open Circuit Voltage (OCV)
- Closed Circuit Voltage (CCV) (terminal voltage)
- Nominal battery voltage
- End of charge voltage (V_{EOC})
- End of discharge voltage (V_{EOD})

The OCV represents the SOC and depends on the specific battery cell type (Figure 2.10) and temperature. It is measured when no external load is connected at the battery terminals. A certain time is required after charging or discharging, until the final OCV voltage is reached (OCV relaxation). The major relaxation process is usually done after one to three hours but the entire process may take more than 10 hours. [36],[37]. It is observed that the OCV may differ slightly after charging from the OCV after discharging the battery. [36]. OCV measurements are done by the integrated BMS and cannot performed directly in PV-BESS laboratory tests. This would require to disconnect the battery from the system. Even if

no active charge or discharge is requested the battery might be unavoidable discharged for coverage of standby consumption.
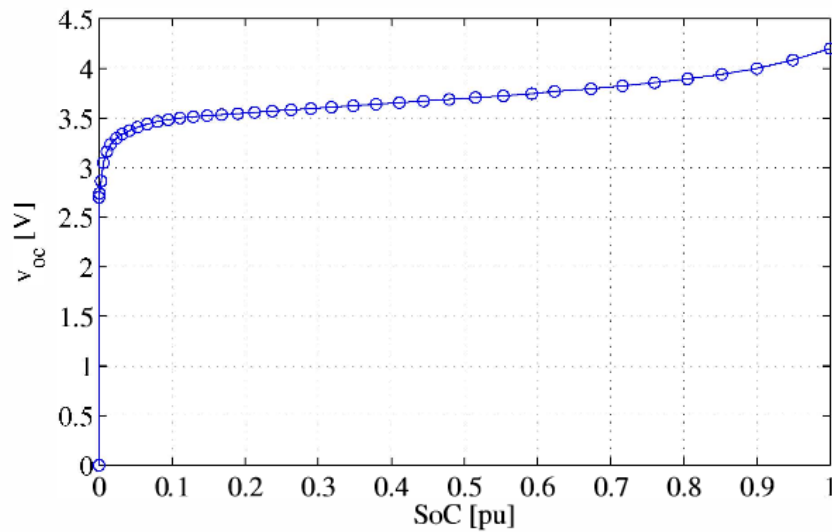
FIGURE 2.10: Measured OCV of a Lithium-ion polymer cell (Source: Comparison, Selection, and Parameterization of Electrical Battery Models for Automotive Applications[38])

The CCV is measured during charging or discharging the battery and is a function of the applied current. The charge voltage increases with higher battery current, the discharge voltage decreases. A constant EOCV limit is reached later with a lower charge current and EODV is reached later with a lower discharge current. The specific voltage profile depends strongly on the cell chemistry.

Figure 2.10 illustrates the cell voltage for a commonly used Lithium Iron Phosphate LiFePO$_4$ (LFP) cell, at different charge/discharge C-rates, as function of the specific capacity. Specific capacity can be seen as representation of the SOC. This example is used because it illustrates well the difficulty of precise SOC estimation by using the battery voltage (CCV and OCV). Especially at low charge/discharge current, only a small voltage change over a wide SOC range is seen. Small deviations of the measured voltage, for instance due to temperature, can lead to an inaccurate SOC. It would be logically that SOC is determined best at a fully or entirely discharged battery. At the other hand the EOCV and EODV is often limited in a PV-BESS to increase the battery lifetime. It implies that SOC estimation is probably done only within the flat voltage plateau.
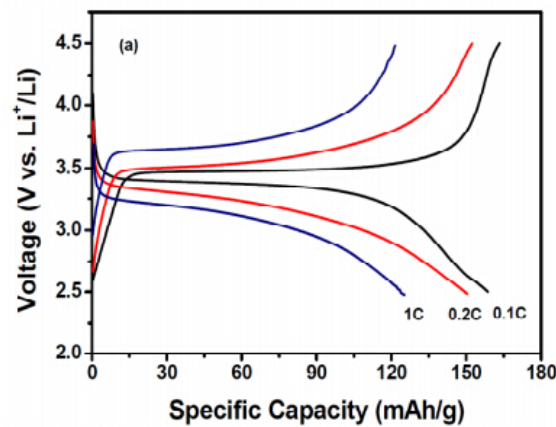
FIGURE 2.11: Example of a constant current charge/discharge profile for a LFP cell. The specific capacity corresponds in principle to the SOC (Source: Mohan,E.,et.al, Urea and sucrose assisted combustion synthesis of LiFePO4/C nano-powder for lithium-ion battery cathode application, 2014[39]).

For PV-BESS battery efficiency test procedures it is important to know that SOC estimation has some tolerances. Depending on the quality of the BMS the charged or discharged energy is not always 100% reproducible within identical charge/discharge cycles.

Similar to the C-rate the battery power can be normalized to the energy content. For instance if the battery has a net energy of $1.5\,\mathrm{kW\,h}$ it is fully discharged in 1 hour at $1.5\,\mathrm{kW}$ constant power at an E-Rate (E1).

2.3.2 Charging Procedures

A standard charge procedure is the CC-CV mode. During the constant current (CC) phase the battery is charged with constant current until a specified voltage. In the constant voltage (CV) phase the battery voltage is kept constant, by decreasing the charging current. [40] This mode allows charging the battery as full as possible, without exceeding the maximum upper voltage level. Figure 2.12 illustrates the CC-CV charging scheme.

Despite of the common CC-CV mode, a variety of different, or extended procedures are found in the literature. They can be optimized for certain battery types, chemistries or applications. It is out of the scope of this document to mention them all. More information can be found in the literature ([2], [40],[41],[42]). For commercial available PV-BESS usually a constant power charge, instead of a constant current charge is required. This implies that the current changes with SOC as function of the battery voltage. It is observed that PV-BESS often

terminate the charging process strictly when an upper voltage limit is reached, no CC-CV charge is performed.
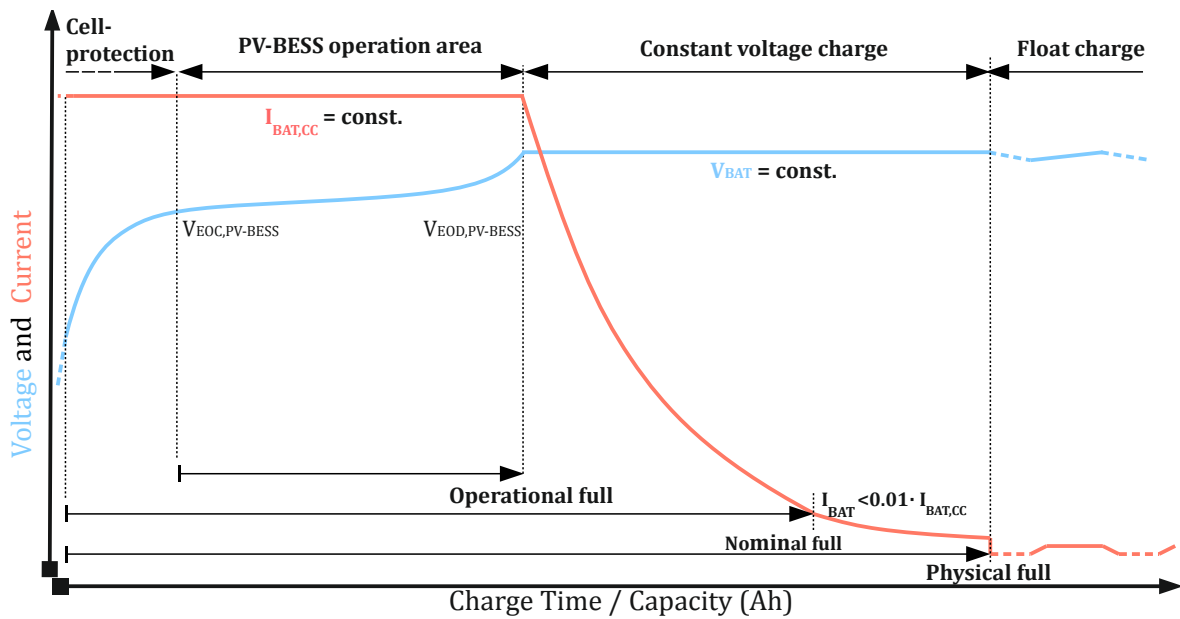
FIGURE 2.12: Constant Current - Constant Voltage charging scheme. (Figure adapted from J. Mayr [43])

2.3.3 Lead-Acid Batteries

Lead-acid batterys are well deployed and used for many years now in a lot of applications. In stationary, grid-connected PV-BESS they loose increasingly market share, with further cost reduction of lithium-ion batterys. Nevertheless a brief overview is given.

A lead-acid battery is defined by the IEC as a secondary battery with an aqueous electrolyte based on dilute sulphuric acid, a positive electrode of lead dioxide and a negative electrode of lead. Novel types of lead acid batteries incorporate various amounts of carbon or carbon structures, but the active materials are still lead, lead dioxide and sulphuric acid [44]. In lead acid batteries, the acid concentration decreases during discharge, the cell voltage is slightly above $2\,\text{V}$. Side reactions as evolving hydrogen at the negative electrode and oxygen at the positive electrode occur. Significant gassing can occur at overcharging, whereas the usual water decomposition during a normal charge is rather slow. [2] Two main types of lead-acid batteries are in use:

Flooded lead-acid batterys

Flooded lead-acid batterys (wet cell) are widespread and mostly used in many applications. They are available at a good price, related to its charge performance. Nevertheless, they need regular maintenance and have a relative high internal resistance and deficits in construction compared to sealed batteries. The electrodes are immersed in an excess of liquid electrolyte of sulfur acid. In general, the gas, produced during charge, does not recombine to liquid. The gas is vented into the atmosphere. In order to compensate the loss of the electrolyte, a filling up of water is required at regular maintenance intervals. [2].

Sealed Lead-Acid (SLA) / Valve-Regulated Lead-Acid (VRLA)

SLA use a porous matrix in order to confine the electrolyte. This separator consists of a silica, sand (Gel) or an Absorbed Glass Mat (AGM) between the plates. This types are usually maintenance free. Internally produced gas recombines again into liquid. This type of batteries contains in general a valve to release pressure produced by overcharging. Therefore it is also called valve-regulated lead-acid battery battery.

Conventional lead-acid batteries, achieve a cycle life of about 500 full charge/discharge cycles and the service life amounts to 3.4 years. [45]. The energy density, around 30-50 Wh/kg is much lower than in lithium-based systems (Section 2.3.4). For the application of stationary battery systems with deep cycles, enhanced versions of lead-acid batteries were and are available. The geometry and materials of the plates (electrodes) plays thereby a determining role. A cycle life of 2800 cycles @DOD >50 % and 17 years calendar life are achievable [2].

2.3.4 Lithium-Ion Batteries

A lithium-ion battery contains a non-aqueous electrolyte and a negative electrode of lithium or containing lithium [44].

Compared to other chemistries lithium-ion based batteries are characterized by:

- High Energy Density
- High Power Density
- High DoD
- High Cycle Life

TABLE 2.5: Types of lithium-ion based chemistries. Additional characterization parameters are found in [3].

Type	Cathode	Anode	Electrolyte	Energy density (Wh/kg)
LFP	LFP	Graphite	Li-carbonate	85-105
Lithium Manganese Oxide LiMn$_2$O$_4$ (LMO)	LMO	Graphite	Li-carbonate	140-180
Lithium Titanate Li$_4$Ti$_5$O$_{12}$ (LTO)	LMO		Li-carbonate	80-95
Lithium Cobalt Oxide LiCoO$_2$ (LCO)	LCO	Graphite	Li-polymer	140-200
Lithium Nickel Cobalt LiNiCoAlO$_2$ (NCA)	NCA	Graphite	Li-carbonate	120-160
Lithium Nickel Manganese Cobalt LiNiMnCoO$_2$ (NCM)	NMC	Graphite silicon	Li-carbonate	120-40

One of the major challenges for lithium-ion based systems are safety issues, whereas cells can overheat and produce smoke and gas venting respectively. They require a reliable, sophisticated BMS which avoids over and undercharge and cell balancing/equalization methods. Lithium-ion batterys are categorized according the specific cell-chemistry in Table 2.5.

An example is given for a modular LFP - HVB-BESS used in PV-BESS. The system consists of single modules with a nominal voltage of 51.2 V and a maximum voltage of 51.6 V per module. A single module has a nominal capacity of 1500 Wh and a usable capacity of 1200 Wh.[4] The configuriaton possibilities are listed in Table 2.6. For High Voltage Battery Systems the voltage range between fully discharged and fully charged is increased.

TABLE 2.6: Fronius Solar Battery (Source: Technical data Fronius-Solar-Battery', 2015[4])

Electrical Parameters	Battery 4.5	Battery 6.0	Battery 7.5	Battery 9.0	Battery 10.5	Battery 12.0
Nominal Capacity	4.5 kWh	6 kWh	7.5 kWh	9 kWh	10.5 kWh	12 kWh
Usable capacity (80% DOD)	3.6 kWh	4.8 kWh	6 kWh	7.2 kWh	8.4 kWh	9.6 kWh
Voltage range	120 to 290 V	160 to 230 V	200 to 290 V	240 to 345 V	280 to 400 V	320 to 460 V
Nominal charging power	2.4 kW	3.2 kW	4 kW	4.8 kW	5.6 kW	6.4 kW
Nominal discharge power	2.4 kW	3.2 kW	4 kW	4.8 kW	5.6 kW	6.4 kW
Max. charging current	16 A		16 A			
Max. discharging current	16 A		16 A			

2.4 ICT and Control System

This section describes the ICT and high level control system. Figure 2.13 illustrates the principle. The EMS is represented by a closed-loop feedback control system. The reference input represents the desired output: zero grid import and export power at the POC-GRID. The EMS receives the information about the power P_{Grid} from a sensor (electricity meter). Based on the error signal it determines the required battery charge or discharge power for grid power reduction. The BMS can overrule this set-point for battery protection issues and limits the battery current.
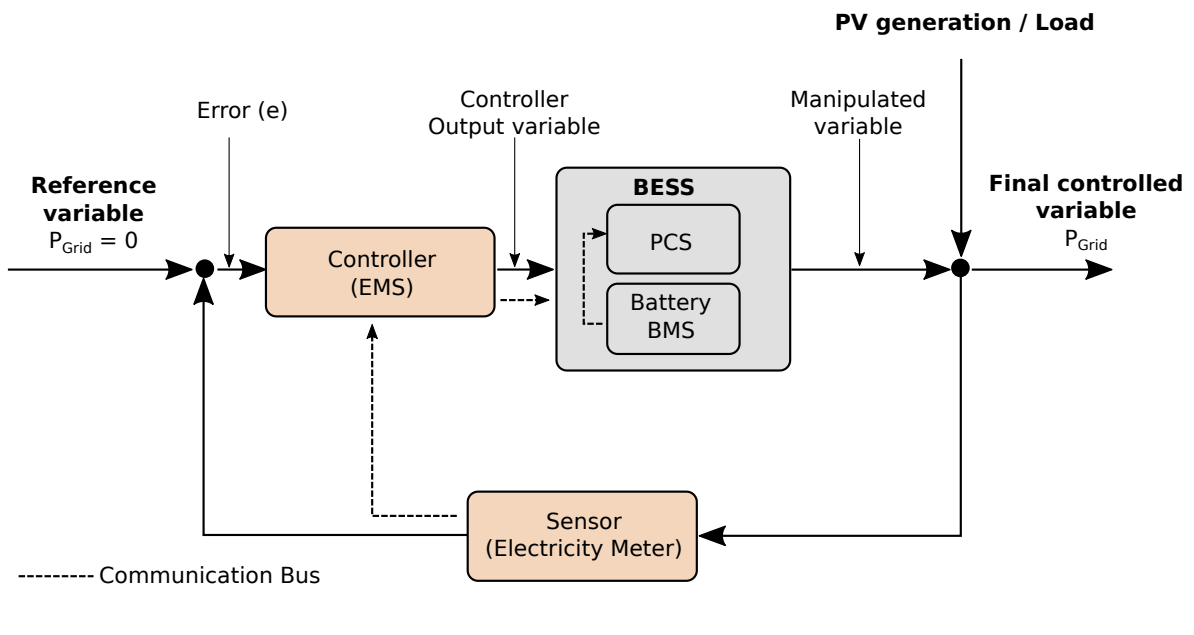
FIGURE 2.13: ICT and control sysem

A PV-BESS may use further input signals for charge/discharge decisions (price signals etc.) and alternative charge strategies. Alternative charge strategies are discussed in the literature. [46] [47]

- Fast charging with excess PV power
- Charging for maximizing battery lifetime
- Charging for maximizing Self-Consumption
- Charging for maximizing Self-Coverage
- Charging for cost minimization
- Multi-objective optimization

As required in the German incentive program for PV-BESS (KfW subsidy program 275, 2013-2015) the maximum feed in power must be reduced to 60% of the PV generator peak power. In order to reduce losses at days with curtailed feed-in power sophisticated battery charge algorithms were developed. The battery charge is shifted into times when the curtailment occurs. Weather forecasts serve often as a decision basis. Effectiveness evaluation within this thesis focuses only on PV-BESS configured for the simplest charge strategy (zero grid power).

Electricity Meter Device

The electricity meter serves as sensor at the system boundary of the residential user (household) to the utility grid (POC-GRID). Exported or imported power is measured with a bidirectional or two unidirectional devices. The measurement information is communicated to the EMS. A variety of interfaces and protocols is found for commercial available electricity/smart-meters. PV-BESS use either a proprietary or/and provide interfaces for a third-party device. The meter shall provide a high measurement accuracy, sample rate and low communication delay. Several options are available for communication between electricity meter and EMS:

Analog Signal Output A electricity meter generates a low current (mA), which is proportional to the measured power. If the measurement range is high (usually 0 to 63 A for commonly used devices) and the analog output signal is in the range of mA the high current transformer ratio may lead to inaccuracies at low electricity demand.

Pulse Output The measurement unit produces continuously a specific amount of single pulses. They correspond to the measured energy, scaled to $kW\,h^{-1}$. 1000 pulses per $kW\,h$ is a standard value. Figure 2.14 illustrates two single pulses. The time T_{high} depends on the device, usually 30 to 70ms. T_{low} is variable and changes with the amount of measured power.
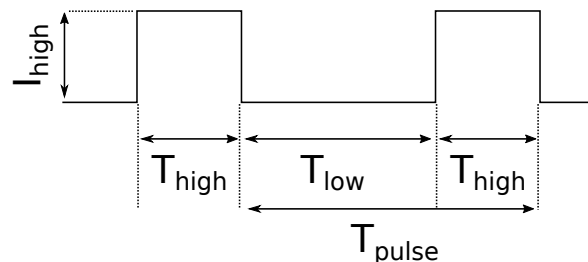
FIGURE 2.14: Pulse output signal, defined in IEC-62053[48]

Several types exist:

- Optical Output - Flashing LED

- Open Collector Output

- S0 (IEC-62053 [48])

Inputs of PV-BESSs are usually conform to the S0 interface, according IEC-62053[48]. Thereby a voltage of 27 V (Class A) or 15 V (Class B) is provided by the PV-BESS. The circuit uses an optocoupler and usually a resistance of $1\,\text{k}\Omega$ for pulse generation ($I_{\text{high}} = 15\,\text{mA to } 27\,\text{mA}$). The pulse output has a relative slow dynamic at low demand, because of long periods between single pulses . Some meters are able to sent 5 to 10000 pulses per kW h. This is preferably for a better dynamic, but might increase transmission errors.

Serial Output Electricity meters, sending their data by using a serial port, are basically standardized according IEC-62056 [49]. Herein the data model is defined by Device Language Message Specification (DLMS) and COSEM. DLMS defines the common language, which standardizes the data objects and the object identification codes. COSEM provides specific procedures for data exchange. [50]

In principle ASCII data is sent by a serial port over EIA-485 or an optical port.[50] The protocol specifies several Modes (A-E). The mode defines among others, if the data is sent on request or automatically in defined time intervals. The transmitted data is contained in standardized registers, specified by the Object Identification System (OBIS). Depending on the configuration, several registers are sent (energy / power / voltage | instantaneous, average, maximum). [51] [50]

The most used interface in commercial available smart-meters consists of a bidirectional optical interface. In order to read the data, a magnetic optical probe is placed on it and connected to the PV-BESS. In general the term D0 is used for this type of smart-meter interface. The use of commercial available smart-meters for PV-BESS is not without challenges. One reason is, that even with an obviously standardized device, the manufacturer has several degrees of freedom in its implementation:

- Data transmission intervals (i.e. 1 to 5s)

- Measurement resolution (i.e. 0.1 to 10 Wh)

- Transmitted information (OBIS registers: power or energy, instantaneous or maximum values . . .)

- Compatibility to newer smart meter protocols (Smart Meter Language (SML) etc.)[52][53]

The technical specifications are not always precisely defined by the Smart Meter manufacturer. Usually a compatibility list is provided by the PV-BESS manufacturer.

Other Protocols PV-BESS manufacturers often provide proprietary devices, based on modbus TCP/IP or modbus RTU. Several other technologies are in use, which are not further investigated within this work.

Three Phase Measurement Principle

If a three phase electricity meter is used, the sum over all phases (required in Germany, according VDE-4400 [54]) is calculated. As result information about single phases is lost. According to this principle the maximum allowed unbalance between phases (required in specific grid codes) is not guaranteed. Therefore an additional phase individual measurement device is required. This measurement principle gives a single phase BESS the possibility to compensate demand or feed in power by charging/discharging power from/to the gird at the other phases. This is frequently described as three phase compensation. An example is given in Table 2.7. At phase L2 and L3 1.8 kW is imported from the utility grid. The electricity meter measures a total import of 3.6 kW. The BESS discharges now with 3.6 kW at phase L1. The imported power at phase L2 and L3 is compensated with exported power at phase L1. The electricity meter measures zero power and the Self Coverage is increased successfully.

TABLE 2.7: Three phase accumulating measurement principle

Line	Power (+ import)	Description
Line L1	- 3.6 kW	Battery discharge with 4.6 kW
Line L2	+ 1.8 kW	Load coverage 2.3 kW
Line L3	+ 1.8 kW	Load coverage 2.3 kW
Total	0 kW	Measured power at POC-GRID is zero kW

Chapter 3

Methodology - Performance Evaluation

This chapter gives an overview about on the state of the art of existing test methods and procedures for components of PV-BESSs. Additionally the theoretical achievable efficiency of components and energy conversion paths is evaluated. Existing methods and test procedures, which are applicable to PV-BESS were developed primarily for single components, or grid-connected energy storage systems without concerns to the specific application of PV-BESS (Charge from RES and increase of direct use and self-coverage). Energy conversion efficiency, speed and accuracy of the control system is commonly evaluated in a generic approach. Proposals are given by Sandia National Laboratories [55], KEMA laboraties - USA [56] and the project DERri [57]. A proposal for performance evaluation of grid-connected PV-BESS is given by Fraunhofer IWES, presented at the PV symposium 2015 in Bad Staffelstein Germany [58].

Efficiency

Efficiency is described as the ability to avoid losses of usable energy due to conversion processes in the system. It is assignable to functions, components or energy conversion paths (component domain) and at the other hand to a specific moment or time period (time domain). The instantaneous efficiency determines the loss between an input and output of a conversion system, for a moment in time and is defined as the ratio between output to input power according to Equation 3.1. The absolute power loss is calculated according to Equation 3.2. It is used to express instantaneous PCS and MPP tracking error losses. Evaluation of the

instantaneous battery efficiency is not feasible with standard electrical power measurement devices as no power output and input exist at the same time.

$$\eta_{\text{P}}(t) = \frac{P_{\text{Out}}(t)}{P_{\text{In}}(t)} \cdot 100 \tag{3.1}$$

$$L_{\text{P}}(t) = P_{\text{In}}(t) - P_{\text{Out}}(t) \tag{3.2}$$

The efficiency for a specified time period is defined as ratio between output and input energy according to Equation 3.3). Absolute energy losses are determined according to Equation 3.4. Alternatively the efficiency for a specific time period can be given as average of instantaneous efficiency samples according Equation 3.5.

$$\eta_{\text{E}} = \frac{E_{\text{Out}}}{E_{\text{In}}} \cdot 100 = \frac{\sum_{i=1}^{n} P_{\text{Out},i} \cdot \Delta T_i}{\sum_{i=1}^{n} P_{\text{In},i} \cdot \Delta T_i} \cdot 100 \tag{3.3}$$

$$L_{\text{E}} = E_{\text{In}} - E_{\text{Out}} = \sum_{i=1}^{n} (P_{\text{In},i} - P_{\text{Out},i}) \cdot \Delta T_i \tag{3.4}$$

$$\eta_{\text{AVG}} = \frac{1}{n} \cdot \sum_{i=1}^{n} \frac{P_{\text{Out},i}}{P_{\text{In},i}} \tag{3.5}$$

Where:

n : amount of measurement samples within the measurement period T_M

ΔT_i : period between two subsequent measurement sample values $(T_{i+1} - T_i)$

The terminology static and dynamic efficiency is sometimes used describing efficiency evaluation at a specified steady-state operating point. The dynamic efficiency considers dynamic input changes and is usually refereed to energy losses due to limited dynamic of a control system (MPPT).

Effectiveness

The degree to which something is successful in producing a desired result. Effectiveness is related to the specific aim of the application. This is for grid-connected, residential PV-BESS an increase of local used PV energy and a reduction of electricity costs for the customer. Effectiveness is not only determined by the quality (high efficiency, fast and accurate control system) of the PV-BESS. For instance it is obvious that a high efficient system is useless if

generated PV energy is not used for demand coverage due to deficits of the energy management system. Effectiveness is moreover influenced by the specific sizing of the system (PV generator peak power, battery capacity etc.) and the PV and load profile of the household.

3.1 PV Inverter

The performance of the PV inverter is basically defined by the accuracy and dynamic of the MPP Tracker (Control System) and energy conversion losses (Power Conversion System). The PV inverter efficiency is content of the European Standard EN-50530. It provides a procedure for efficiency evaluation in steady-state and for dynamic changing PV irradiation input.

Static Efficiency

Static efficiency describes the accuracy of an inverter to regulate on the MPP on a given static characteristic curve of a PV generator [59]. It is subdivided in MPPT, conversion and overall efficiency. EN-50530 requires at least 48 single efficiency measurements as combination of module technology, MPP voltage and power level [59]:

- Two module technologies: Crystalline Silicon Solar Cell (C-Si),Thin-Film Solar Cell (TF)
- Three MPP input voltage levels ($V_{\mathrm{MPP,min}}$, $V_{\mathrm{MPP,rated}}$ and $V_{\mathrm{MPP,max}}$)
- Power levels: 5, 10, 20, 25, 30, 50, 75, 100% related to rated DC input power ($P_{\mathrm{PV,MPP}}/P_{\mathrm{DC,r}}$)

The efficiency is determined after the MPP is stabilized. During the measurement period the provided MPP power must not change more than 0.1% related to the specific I/V curve. The sampling and recording rate is not specified but shall be chosen high enough. The static MPP efficiency is calculated by measurements according Equation 3.6 [59]:

$$\eta_{\mathrm{MPPT,stat}} = \frac{1}{P_{\mathrm{PVS,MPP}} \cdot T_{\mathrm{M}}} \cdot \sum_{i=1}^{n} V_{\mathrm{DC},i} \cdot I_{\mathrm{DC},i} \cdot \Delta T_i \qquad (3.6)$$

Where:

$V_{\mathrm{DC,i}}$: sampled value of the inverters input voltage

$I_{\mathrm{DC,i}}$: sampled value of the inverters input current

T_{M} : overall measurement period

$P_{\text{PVS,MPP}}$: Provided MPP power by the PV simulator during T_{M}

The conversion efficiency is calculated according Equation 3.7 [59]. It is proposed to average the instantaneous input and output power over a time period of 30 seconds to properly handle AC signals, higher harmonics and DC ripples [33]. Detailed information about measurement requirements are found in the standard 'IEC-61689 Photovoltaic systems - Power conditioners - Procedure for measuring efficiency' [60].

$$\eta_{\text{CONV}} = \frac{\sum_{i=1}^{n} P_{\text{INV,AC},i} \cdot \Delta T_i}{\sum_{i=1}^{n} P_{\text{PVS,DC},i} \cdot \Delta T_i} \tag{3.7}$$

$P_{\text{PVS,DC},i}$: sampled value of the inverters input power $V_{\text{DC},i}$

$P_{\text{INV,AC},i}$: sampled value of the inverters RMS output power

The overall, or total efficiency of a PV inverter is given as product of conversion and MPPT efficiency (Equation 3.8)

$$\eta_{\text{t}} = \eta_{\text{CONV}} \cdot \eta_{\text{MPPT}} = \frac{1}{P_{\text{PVS,MPP}} \cdot T_{\text{M}}} \cdot \sum_{i=1}^{n} P_{\text{AC},i} \cdot \Delta T_i \tag{3.8}$$

Dynamic MPPT-Tracking

Static efficiency does not consider dynamic changes of PV irradiation. The dynamic MPPT efficiency is introduced to evaluate the performance of the PV inverter, adjusting to new operation points at transitions of the input. Therefore the MPP tracker must be able to find the new MPP fast and accurate as possible, after changes in the I/V curve. Depending on the quality of the used MPPT algorithm this may take up to several seconds and reduces the amount of useful PV energy. The test sequence is shown in Figure 3.1.
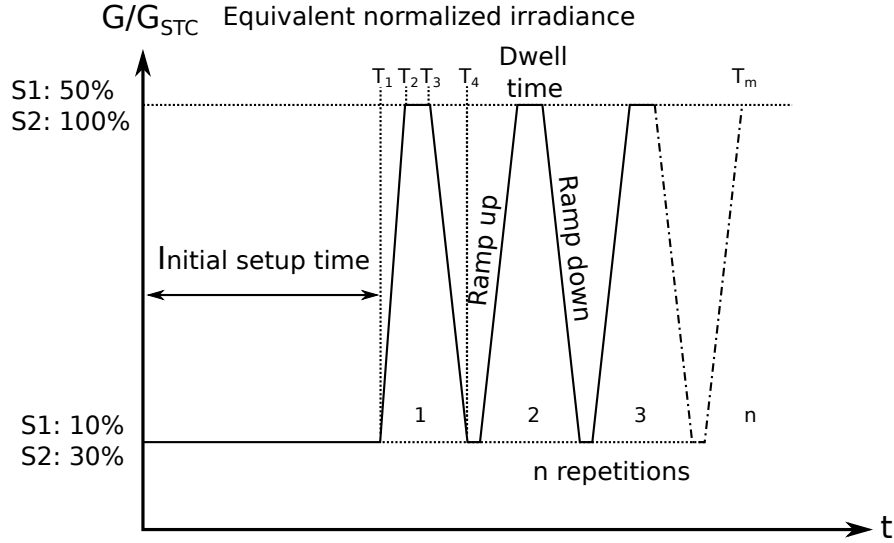
FIGURE 3.1: Dynamic MPPT sequence (adapted from EN-50530 [59])

- Phase 1: Ramp Up (T_1 to T_2)
- Phase 2: Dwell time (T_2 to T_3)
- Phase 3: Ramp down (T_3 to T_4)

The time of each phase varies between the iterations. EN-50530 defines two standardized synthetic test sequences. Once for fluctuations between small and medium (S1: 10 to 50%) and further for medium and high (S2: 30 to 100%) irradiation intensities. [59]. The efficiency is calculated according Equation 3.9 for each single phase and as mean for the entire sequence.

$$\eta_{\text{MPPT,dyn}} = \frac{1}{\sum_{j=1}^{m} P_{\text{PVS,MPP},j} \cdot \Delta T_j} \cdot \sum_{i=1}^{n} V_{\text{DC},i} \cdot I_{\text{DC},i} \cdot \Delta T_i \qquad (3.9)$$

T_j : period in which the power $P_{\text{PVS,MPP},j}$ is provided

m : m- steps of MPP power provision of the PV simulator

European- and California Energy Commission (CEC) Efficiency

The European and CEC efficiency is introduced for long-term predictions The method is described as weighted sum of power efficiency for several partial load levels[33]. The efficiency η_i at partial load is weighted with the relative frequency a_i the inverter is estimated to operate during its lifetime. The European efficiency (Equation 3.10) considers average irradiation data from Europe, CEC efficiency (Equation 3.11) from California. It is seen that the the inverter

operates mostly at 50% partial load related to rated DC input power ($P_{\mathrm{PVS,MPP}}/P_{\mathrm{DC,r}}$).

$$\eta_{\mathrm{EU}} = 0.03 \cdot \eta_{5\%} + 0.06 \cdot \eta_{10\%} + 0.13 \cdot \eta_{20\%} + 0.10 \cdot \eta_{30\%} + 0.48 \cdot \eta_{50\%} + 0.2 \cdot \eta_{100\%} \quad (3.10)$$

$$\eta_{\mathrm{CEC}} = 0.04 \cdot \eta_{5\%} + 0.05 \cdot \eta_{10\%} + 0.12 \cdot \eta_{20\%} + 0.21 \cdot \eta_{30\%} + 0.53 \cdot \eta_{50\%} + 0.05 \cdot \eta_{100\%} \quad (3.11)$$

Efficiency of State-Of-The-Art PV inverters

The maximum steady state tracking error for several MPPT control algorithms was evaluated by 'Eltawil et al., MPPT techniques for photovoltaic applications[32]'. The beta parameter based MPPT method achieves within this study the highest efficiency of 98.8 %, which means 1.2 % of the theoretical usable energy is lost. An often used algorithm is the conventional Perturb & Observe (P&O) method achieving an efficiency of approx. 98%. In a recent study (Ahmed et al., An improved P&O algorithm for higher efficiency [61]) an adaptive P&O algorithm was developed. It achieves 98.84 % efficiency and the maximum is given as 99.4% within a defined duty cycle [61]. A variety of other algorithms are available. The MPPT algorithm which is finally used does not only depend on efficiency. Several factors as maximum ripple voltage, implementation effort, number of sensors, overall costs etc. must be considered. [32]

The conversion efficiency depends on the electrical topology and voltage level between PV generator and intermediate circuit of the inverter. The influence of the specific topology (isolated, transformerless) is described as follows:

LF transformer 50 Hz By using a 50 Hz transformer a fixed transmission ratio between primary and secondary site is required. The efficiency decreases with higher input voltage. [62]

HF transformer 20-25 kHz The HF transformer achieves a higher efficiency as a LF transformer. Due to the fixed transformer transmission ratio the efficiency decreases in the same way with higher DC input voltages. [62]

HF transformer with switchover This topology provides a change of the transformer transmission ratio. Therefore the transformer utilization can be optimized and several efficiency peaks are the result. [62]

Transformerless The transformerless inverter achieves maximum peak efficiency. The DC input (PV generator) voltage must be above the gird voltage of 230 volt. The maximum

efficiency is related to a DC input voltage of approximately 350 V. This amplitude corresponds to the peak voltage of the utility grid and additional semiconductor losses about 10 V. Outside this voltage range a DC/DC converter is used, which decreases the efficiency. [62].

The efficiency is illustrated as function of DC input voltage in Figure 3.2:
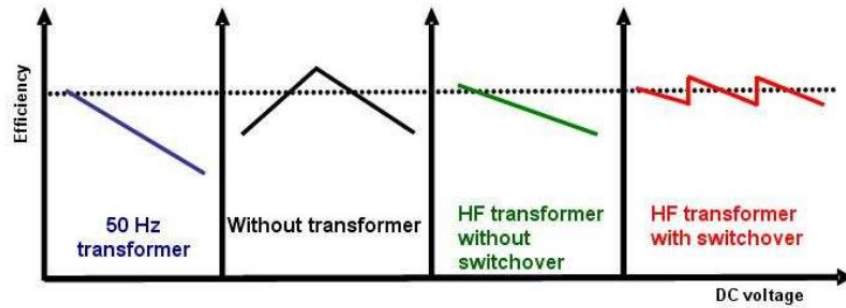
FIGURE 3.2: PV inverter Efficiency behavior (Source: Wolfahrt.J, Fronius - High Frequency Transformer with transfromer switchover,2012 [62])

The maximum efficiency of a boost converter is estimated between approx. 98% [63] and 99% [64]. For instance it is estimated in a simulation approach by 'Frisch M et. al, High Efficient Topologies for Next Generation Solar Inverter[64]' for a converter with following characteristics: $P_{\mathrm{IN}} = 2\,\mathrm{kW}$, $f_{\mathrm{PWM}} = 16\,\mathrm{kHz}$, $V_{\mathrm{PV}} = 300\,\mathrm{V}$, $V_{\mathrm{DC}} = 400\,\mathrm{V}$. An efficiency above 99% is achieved from 10 to 100% of P_{IN} and a maximum efficiency of 99.6 % is given. The simulation considered only switching losses of semiconductors. Losses in passive components, boost inductors and output filters are not considered. [64] As a rough estimation a doubling of losses is assumed herein, for this specific boost converter. The estimation based on the distribution of losses for a rectifier unit, found in the literature [65]. The maximum efficiency decreases to 99.2 %. It demonstrates that DC/DC converters can maintain a high efficiency.

The inverter stage performs the DC/AC and in case of a bidirectional device AC/DC power conversion. The efficiency of DC/AC inverter bridges is determined by losses in semiconductors (conduction, switching, blocking/leakage losses). The efficiency varies between the specific bridge designs and the type of used semiconductors (IGBT, diodes etc.). The European efficiency is determined within a simulation approach by 'Martino et al., Efficiency Analysis of Single Phase Photovoltaic Transformerless Inverters [5]' and is listed in Table 3.1:

TABLE 3.1: European Efficiency for DC/AC bridge topologies[5]

	Full H-Bridge	Half H-Bridge	Heric	H5-5	NPC
STGW35NB60S IGBT + Si diode	98 %	98.3 %	98.5 %	98.2 %	98.5 %
STGW35NB60S IGBT + SiC diode	98.1 %	98.3 %	98.6 %	98.3 %	98.6 %
STGW20NC60V + Si diode	98.3 %	99.3 %	99.7 %	99.6 %	98.9 %
STGW20NC60V + SiC diode	98.4 %	99.4 %	99 %	98.7 %	99 %

Figure 3.3 shows the simulated efficiency, for the H5-bridge topology, as function of the output power.
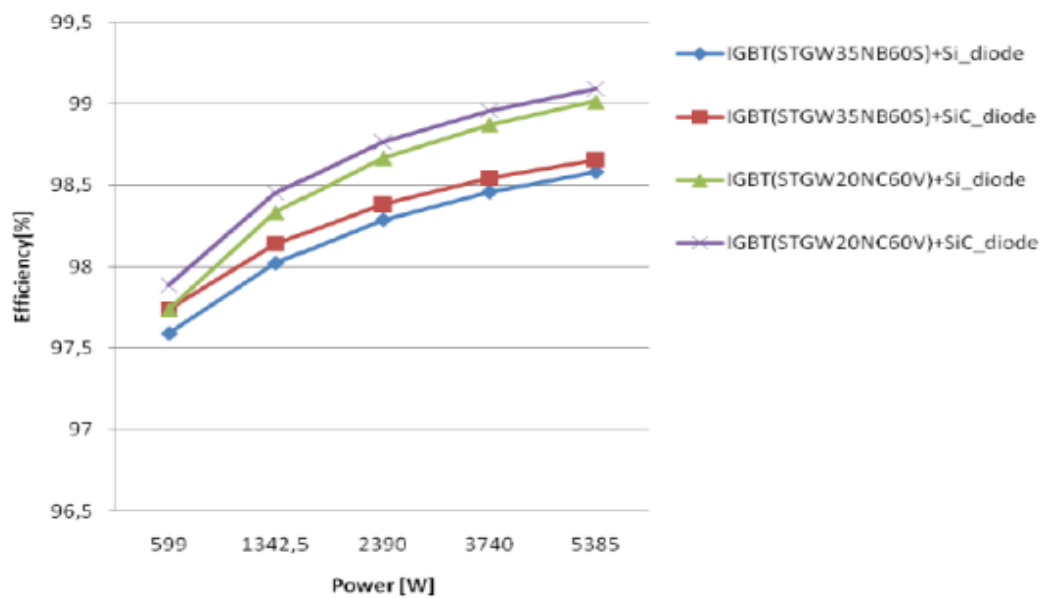
FIGURE 3.3: Efficiency DC/AC inversion H5-bridge (Source: Martino et al., Efficiency Analysis of Single Phase Photovoltaic Transformerless Inverters,2012 [5])

The European and maximum efficiency for the different types of H-bridges are given in the literature [6] according Table 3.2.

TABLE 3.2: H-bridge maximum and weighted European efficiency [6]

Name	η_{EU} / Maximum efficiency
H-bridge H5 (SMA)	97.7 / 98 %
H-Bridge HERIC (Sunways)	97.5 / 98 %
H-bridge FB - DC Bypass (Ingeteam)	95.1 / 96.5 %
H-Bridge REFU	97.5 / 98 %

NCP topologies achieve an efficiency between 95 and 98% [6].

3.2 Charge Controller

The standard **IEC-62509 Battery Charge Controllers for Photovoltaic Systems - Performance and Functioning [66]** was developed for PV systems with a Battery Charge Controller (BCC) connected to lead acid batteries. The standard applies to charge controllers, directly connected to a PV module and electrical loads. The test procedure requires a battery simulator, in order to emulate the appropriate battery voltage. The test procedures determine standby consumption and efficiency as follows:

Standby Consumption The aim of this test is to determine the consumption of the battery charge controller in standby mode (no PV input or load)[66].

The standby consumption is determined at a cell voltage of 2.1 V/cell $\pm2\%$ and 25 °C ±2°C. Acceptance criteria are given by the standard. The maximum accepted standby consumption current depends thereby on the nominal charge current, which is defined by the manufacturer.

Efficiency The aim of this test is to determine the efficiency of the BCC over the range from 10% to 100% of the rated charging current at an ambient temperature of 25 °C ±2°C and 40 °C ±2°C. [66]. The test procedure requires exact adjustment of the battery voltage, for efficiency determination in one specified operating point.

The **California Energy Commission** provides several documents, comprising test procedures for charge controllers. The initial proposal was initially published in 2008 [67], the procedures vary for charge controllers below and more than 2 kW of rated DC or AC input. In the year 2011 a further document, declared as 'Appendix Y to Subpart B of Part

430-Uniform Test Method for Measuring the Energy Consumption of Battery Chargers [68]'
was published with newer test procedures. In addition a proposal exists for external power
supplies in general [69]. A brief overview will be given about the content of the different
documents.

The procedures, described by 'Energy Efficiency Battery Charger System Test Procedure'[67]
in the year 2008 are described as follows (charge controller $> 2\,\mathrm{kW}$):

A battery conditioning is required for new batteries before the actual test is started. Therefore
some preparatory cycles are performed on the battery and charger. The test starts with the
discharge of a fully charged battery. Estimating the SOC at full charge depends on the
battery type: Flooded cells require specific gravity measurements of the electrolyte, whereas
for VRLA batteries voltage measurement is recommended. [67]

The test sequence starts with a battery discharge (no sooner than 3 hours and no more than
24 hours after the last full charge). The constant current discharge, expressed as C-rate must
not deviate $\pm$ 3% of the declared current. The appropriate discharge rate is determined
by the area of application within the charge controller is used (electric vehicles, industrial
equipment). The battery shall be discharged to 100% DOD with a measurement accuracy of
1% or to the specified end of discharge voltage. The battery must be recharged within 1 to
6 hours, depending on the battery temperature.

This charge/discharge sequence is iterated three times, whereas the second discharge is per-
formed to 40% DOD and the third to 80% DOD ($\pm$ 10%) determined by voltage measure-
ments, Ah counter, specific gravity measurements, or discharge meter reading of the Ampere-
hour capacity [67]. After the cycle tests, the battery is left connected, AC- and DC delivered
energy to the charger shall be recorded further over a 72h period. The next step is to discon-
nect the battery and measure the demand of the charger at the AC side for a period of up to
one hour. [67]

The performance indicators are described as follows:

- Charge Return Factor (C_{rf}): The number of Ampere-hours charged, divided by the
  number of Ampere-hours delivered by the battery during discharge. $C_{\mathrm{rf}} = 1/\eta_{\mathrm{C}}$

- Power Conversion Efficiency ($\eta_{\mathrm{PCS,conv}}$): The instantaneous DC output power of the
  charger divided by the simultaneous utility AC input power

Further changes in the test procedure lead to 'Appendix Y to Subpart B of Part 430', published in 2011. The test sequence is briefly described as follows: Battery conditioning is not required anymore for lead-acid or lithium-ion batteries. In the pretest phase the battery is discharged and must maintain a rest period of 1 to 24 hours. The test starts with fully charging the battery. The duration of the charge time is determined, by use of a integrated indicator (SOC gauge etc.) or an estimated charge time declared by the manufacturer. If none of this is present the charge time is calculated according to Equation 3.12. [68]

$$\text{Duration} = 1.4 \cdot \frac{\text{Rated Charge Capacity (Ah)}}{\text{Charge Current (A)}} + 5 \text{hours} \tag{3.12}$$

After a full charge a rest-period ot 1 to 4 hours is given and then the battery is discharged again. The standby consumption of the battery charge controller is measured over a period of 24 hours [68].

An acceptance criteria is given by CEC for battery chargers $>2\,\text{kW}$ after July 1, 2013 (Table 3.3.

TABLE 3.3: CEC acceptance criteria battery charge controllers $>2\,\text{kW}$

Charge Return Factor (C_{rf})	100 %, 80 % DOD: ($C_{\text{rf}} \leq 1.10$)
	40 % DOD $C_{\text{rf}} \leq 1.15$
Power Conversion Efficiency	≥ 89 %
Maintainance Power	20 W
No Battery Power	10 W

The document 'Test Procedures for External Power Supply' of the United States Department of Energy (DOE)[69] recommends efficiency determination for several power levels: 10% (optional), 25%, 50%, 75% ,100% of its nameplate output current. The average value of 25 to 100% is declared for the overall Power conversion efficiency. In addition the power consumption at no load shall be determined as well. The document references to 'Test Procedures to AC Power Supplies August 11, 2004 (incorporated by reference, see §430.3)'. The procedures were originally given for AC/DC or AC/AC power suppliers. They are theoretically applicable for PV (DC/DC) charge controllers as well.

The proposed procedures are not directly applicable for charge controllers integrated in a PV-BESS among others, due to following reasons:

- The procedures require constant current charge/discharge. PV-BESS are performing usually constant power charge/discharge.

- In an AC coupled PV-BESS the maximum power of the battery inverter is limited by the used battery. Therefore it is not always possible to test the entire operating area of a charge controller without a battery simulator. At the other hand the system shall be tested without use of a battery simulator. A wide range of voltage levels are used in PV-BESS battery systems (40 to 450 V). This might require a battery simulator for low and high voltage systems. In addition the BMS and communication to the PCS has to be emulated as well. This efforts shall be avoided in the first development stage of test procedures.

- For DC hybrid coupled systems measurements at the input and output of the charge controller might not be available (Current flows over conductor tracks at a Printed Circuit Board (PCB) in the DC link).

Further investigation of the described test procedures are necessary. It would be useful if manufacturers of charge controllers test their devices according a standard procedure and provide information about the overall efficiency. The charge controller is an important device in the PV-BESS. A high efficiency is therefore desirable. Efficiency testing of standalone charge controllers is not further considered for the development of test procedures for an entire PV-BESS.

The efficiency of a charge controller used in a DC coupled is a function of:

- Topology (isolated, transformerless)
- Charge/discharge current
- Voltage difference between DC Link and battery
- Switching frequency (lower ripples, less effort for filters)

Figure 3.4 shows the efficiency of a **Non Isolated Charge Controller (NICC)** as a function of the charging current. For the efficiency evaluation a DC link voltage of 400 V and a battery voltage of 150 V is assumed. The maximum charge/discharge efficiency is approximately 98 % for a switching frequency of 20 kHz. [25] The efficiency of a non isolated 5 kW charge controller, connected to a three phase inverter was given by 'Dr. Scarpa. V, Lopes P., Matching Circuit Topologies and Power Semiconductors for Energy Storage in Photovoltaic,2014 Systems [25]'. A half-bridge DC/DC converter with 1200V CoolSiC JFET power

module is used and a high efficiency >99 % is achieved at 650 V DC link voltage from 30 to 100% of maximum output power and 40 kHz switching frequency.
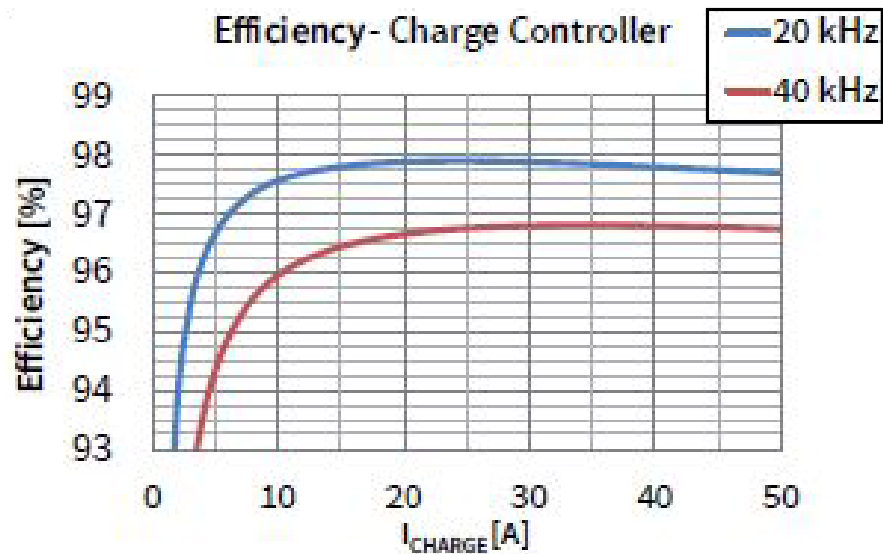
FIGURE 3.4: Efficiency results of a non-isolated 50A 650V IGBT device from the TRENCH-STOP 5 family based on IKW50N65H5 devices (Source: Dr. Scarpa. V, Lopes P., Matching Circuit Topologies and Power Semiconductors for Energy Storage in Photovoltaic,2014 Systems,2014[25])

Efficiency of an **isolated charge controller**, using Zero Voltage Switching (ZVS) techniques is given between 95 to 96% from 25 to 100% of rated (2kW) power [25].

If an AC coupled system is used an additionally inverter/rectifier stage is necessary. A 3.3 kW MOSFET rectifier can achieves a maximum efficiency of 99.2%. The distribution of the losses is given as follows [65]:

- 50 % MOSFET
- 25 % Boost Inductors
- 8 % Output Capacitors
- 5 % Gate Drivers
- 7 % Digital Signal Processor (DSP) and Complex Programmable Logic Device (CPLD)
- 10 % Zero curent instant detector and current measurement

The overall efficiency of an AC coupled Low Voltage Battery System inverter is illustrated in 3.5. The efficiency decreases with higher battery voltage. This is typical for a topology, where the battery is directly connected to the inverter stage (bridge) and voltage is adapted by a glos:lftrans.
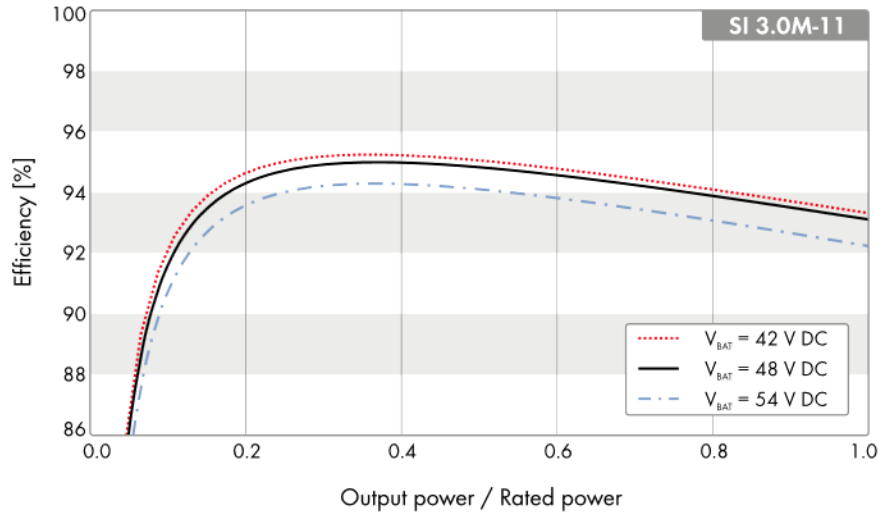
FIGURE 3.5: Efficiency curve for the AC coupled battery inverter Sunny Island 3.0M-11 (Source: Technical data-sheet Sunny Island 3.0M / 4.4M For on-grid and off-grid applications,2015 [70])

3.3 Battery

This section comprises regulatory framework, related to a full sized battery, without concerns to the PCS. Regarding performance testing, standards are available primarily for the automotive sector and batteries used in off-grid systems. But due to higher penetration of grid-connected battery systems more standardization effort is recently seen within this field. The difference between stationary and automotive sector are basically different charge/discharge profiles and environment (temperature, vibrations etc.). Battery efficiency is principally given as coulombic, voltaic and energy efficiency:

Battery Coulombic Efficiency (BCE)

The BCE is the ratio between dischargeable and chargeable coulombs (ampere-hours) within a battery (Equation 3.13). The BCE is reduced for lead-acid batteries especially due to electrolysis of water at the end of charge (gassing). The efficiency is given to be around 90% for a nominal charged battery. [71]. Lithium-ion cells achieve a very high BCE above 99.8%. The coulomb efficiency is an important factor for precise SOC estimation, based on the ampere-hour method. [72]

$$\eta_\text{C} = \frac{Q_\text{d}}{Q_\text{c}} = \frac{\int_0^{T_\text{d}} I_\text{d}}{\int_0^{T_\text{c}} I_\text{c}} \tag{3.13}$$

Where:

Q_d :discharge capacity (Ampere-hours)

Q_c :charge capacity (Ampere-hours)

I_c :charge current (Ampere)

I_d :discharge current (Ampere)

T_c :required time for a full battery charge

T_d :required time for a full battery discharge

Battery Voltaic Efficiency (BVE)

The voltaic efficiency is described as ratio between discharge and charge voltage (Equation 3.14) at a specified current, temperature and OCV/SOC. It results from internal resistance and polarization losses at the electrodes. The CCV is higher as the OCV during charging and lower during discharging. The deviation to the OCV depends on the battery current and internal resistance ($V_\mathrm{BAT} = R_\mathrm{BAT} \cdot I_\mathrm{BAT}$).[73]. Practically the BVE is not directly used for efficiency evaluation.

$$\eta_\mathrm{V} = \frac{V_\mathrm{d}}{V_\mathrm{c}} \tag{3.14}$$

Where:

V_d :discharge voltage

V_c :charge voltage

Battery Energy Efficiency (BEE)

The energy efficiency is defined as product of voltage and coulombic efficiency (Equation 3.15)

$$\eta_\mathrm{E} = \eta_\mathrm{V} \cdot \eta_\mathrm{C} = \frac{V_\mathrm{d}}{V_\mathrm{c}} \cdot \frac{Q_\mathrm{d}}{Q_\mathrm{c}} \tag{3.15}$$

Energy efficiency is influenced by:

- **Cell Temperature**: The internal battery resistance is affected by temperature and differs between cell chemistries.
- **Battery current**: Loss at the internal resistance is increased with higher battery current ($P_\mathrm{loss} = I_\mathrm{BAT}{}^2 \cdot R_\mathrm{BAT}$)

- **State of Charge**: The internal battery resistance varies with the SOC. The deviation is different for charging and discharging specific cell chemistries. [74]

Self-discharge Self-discharge is described as capacity loss when the battery is not connected (open circuit) or active discharged from a load. The self-discharge rate depends on the chemistry and temperature. Higher temperatures increases the self-discharge rate.

- Lithium-ion based: 1 to 2% per month plus 3% for safety circuit (BMS)[75].
- Lead-acid based: 5% per month[75].

Round Trip Efficiency

The round trip efficiency is introduced for energy efficiency evaluation during a specific charge/discharge cycle. It is defined as ratio between discharged and charged energy (Equation 3.16). The RTE is in principle determinable for the battery only and for the whole system, including charge and discharge losses of the PCS. This section comprises only standards or methods proposed for battery efficiency evaluation only. Section 3.6 includes generic proposals for RTE test procedures with concern to PCS and battery losses. The International Electrotechnical Commission (IEC) provides a standard for efficiency evaluation of grid-connected battery systems in combination with RESs.

- IEC 61427-2 (2013) Secondary cells and batteries for Renewable Energy Storage - General Requirements and methods of test - Part 2: On-grid application [76]
- IEC 61427-2 (2015-08) Ed. 1.0. Secondary cells and batteries for Renewable Energy Storage - General Requirements and methods of test - Part 2: On-grid application [1]

Only a draft in advanced stage, but not the finally published 2015 version was available until the end of this work. The described procedure relates to the 2013 version as only minor changes were observed in the draft. A grid-connected PV-BESS was evaluated according IEC-61427-2 Ed.1.0 (2013) in recent research activity by the technical university of Madrid (IES-UPM), and was presented at the EU PVSEC 2015 'Makibar,A.,Narvante,L. Characterization and Efficiency Test of a Li-ion Energy Storage System for PV Systems' [77]. The procedure is basically described, based on this work.

The efficiency is determined by performing a full charge/discharge cycle. It is specified as ratio between net discharged to the amount of charged energy (Equation 3.16). Energy consumption of auxiliary battery systems (Figure 2.8), as BMS or BSS (e.g. ventilation etc.)

are taken into account.

$$\eta = \frac{E_{\text{Out}}}{E_{\text{In}}} = \frac{E_{\text{discharged}} - E_{\text{aux,discharge}}}{E_{\text{charged}} + E_{\text{aux,charge}}} \qquad (3.16)$$

The sequence is described at a 16h duty-cycle (8h discharging / 8h charging), starting and terminating at SOC 100%. The appropriate discharge and charge power must be calculated, in order to recharge to a SOC level of 100% and perform SOC stabilization. The required charge parameters are specified by the manufacturer.[77]

1-Initial Phase Full battery charge

2-Full Discharge Discharge for 480 minutes with constant DC power until V_{BAT} reaches lower limit set by $V_{\text{cell,min}}$ In order to perform a full discharge during 8 hours[77]. The system must provide a certain discharge power. The calculation is not further explained and is referenced to the standard [76].

3 - Full Charge Charge for around 480 minutes with constant DC power $P_{\text{BAT,charge}}$ [77]. The battery shall reach 100% SOC again.

As not the entire standard and only a draft of a newer version was available, further investigation is necessary about the content of the recently published version [1]. The draft proposed to charge the battery with two power levels, within one full charge/discharge cycle. It was seen that required power form the standard might be higher as maximum discharge power of most small/scale PV-BESS. The generic approach of efficiency evaluation by a full charge/discharge cycle is pursued within this work and further described in the methodology in Section 3.6 and is content of the test portfolio in Section 4.3.

Alternative Efficiency Evaluation Methods

It is seen that PV-BESS manufacturers provide sometimes information about their battery efficiency. The test procedure is not always described and the used methods may be applicable only for single cells. An increase of losses for the entire module due to contacts, wiring, and a series connection of cells is probably not considered. A brief overview about several methods is given.

OCV method

The efficiency is determined by charging and discharging the battery with identical, predefined power and time. The difference to the RTE test routine is that charge/discharge time is constant and not a function of battery voltage or SOC. It is calculated by using the difference of SOC at the beginning and the end of the test. Instead of the SOC it is recommended to use the difference between the open circuit voltage (Equation 3.17) which shall avoid SOC estimation inaccuracies of an integrated BMS. The test procedure is describes as follows:

1. Measure the OCV ($V_{\text{OCV,}start\text{-}charge}$) after an appropriate rest period for voltage stabilization

2. Charge a specified time T_m with defined power level P_m at temperature T_m

3. Allow a rest phase for voltage relaxation (optional)

4. Discharge with the same time T_m, power level P_m and temperature T_m as the battery was charged

5. Measure OCV ($V_{\text{OCV,}end\text{-}discharge}$) after an appropriate rest (voltage relaxation) period

$$\eta_{bat} = \frac{V_{\text{OCV,}end\text{-}discharge} - V_{\text{OCV,}start\text{-}charge}}{V_{\text{OCV,}start\text{-}charge}} \tag{3.17}$$

The test is performable in any SOC range the battery is charged and discharged with the specified power and time. Following restrictions are given for tests on PV-BESS:

- If the battery is connected to the PV-BESS the OCV cannot be necessarily measured.

- SOC is related to the OCV of single cells. In a series connection the OCV at the battery terminal must not represent the SOC of each cell.

- Detailed knowledge about the relation between OCV and State of Charge is required (battery characterization).

- OCV does not represent the internal resistance and ability to deliver current of a battery. For instance an aged battery has a higher internal resistance but the OCV does not change. This implies that only the BCE is determined. [78]

Internal Resistance

This method determines the internal resistance of battery cells. The internal resistance is a good indicator for energy losses within the battery. In addition the energy loss is assignable

to charge and discharge separately and the instantaneous efficiency could be determined. Nevertheless this method requires additional efforts in battery characterization [74] and is not considered for PV-BESS battery efficiency evaluation.

Equivalent Ampere-hour charge/discharge

For types of lithium-ion based batteries the coulomb efficiency is assumed to be closely 100%. This implies that charging a certain amount of electric charge (Ampere-hours) and discharging the same electrical charge results in losses only affected by the internal resistance and polarization effects. In order to perform the test procedure for a PV-BESS the charged and discharged ampere-hours are determined in real time. The discharge is terminated when the same amount of ampere-hours is withdrawn as it was previously charged.

1 Charge X ampere-hours and record the charged energy
2 Discharge X ampere-hours and record the discharged energy
3 The BCE is calculated as ratio between discharged to charged energy

As this method is not elaborated enough, it is not used for test procedures developed within this work.

3.4 ICT and Control System

The electrotechnical vocabulary provided by the IEC uses a step response to define the speed (dynamic) and accuracy of a control system (Figure 3.6. [44]). The step response for performance evaluation in a PV-BESS is basically a change of demand or PV generation resulting in grid import or export.
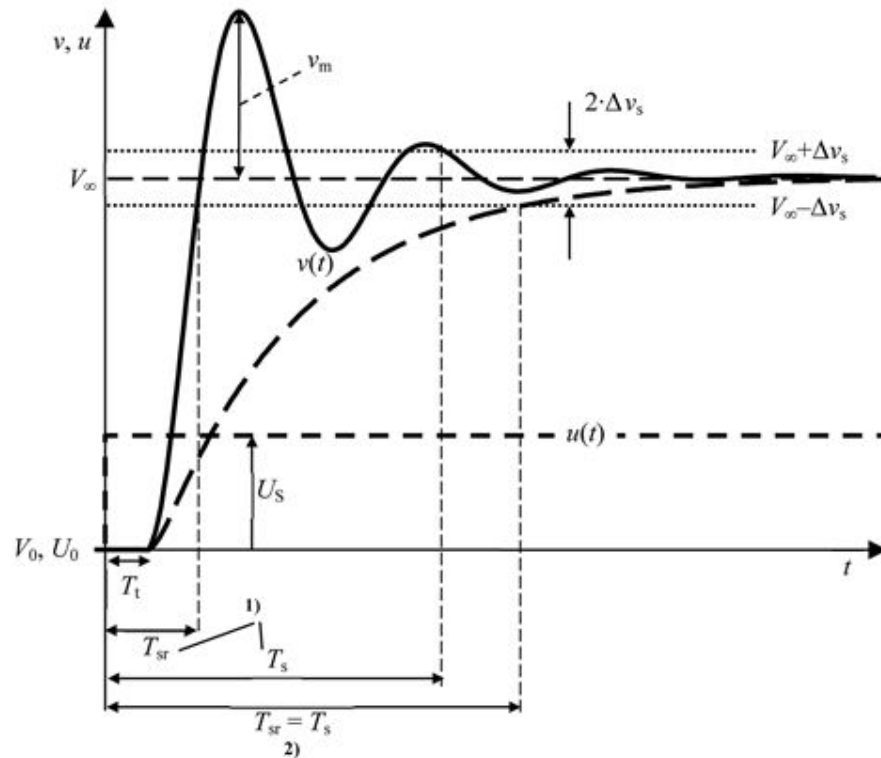
FIGURE 3.6: Typical step responses of a control system 1) for periodic 2) for aperiodic behavior. (Source: IEC/IEV ref. 351-45-36 [44]).

Where:

- u = Input variable

- U_0 = Initial value of the input variable

- U_s = Step height of the input variable

- v = Output variable

- V_0 V_∞= Steady-state values before and after the application of the step

- V_m = Overshoot (maximum transient deviation from the final steady-state value)

- $2 \cdot \Delta v_s$ = Specified tolerance limit

- T_{SR} = Step response time
- T_{S} = Settling time
- T_{t} = Dead / Delay time

Following classification is applicable for performance evaluation of PV-BESS:

Delay Time T_{t}

The duration of the time interval by which the output variable is shifted relative to the input variable [44]. It is characterized by the time energy is exported or imported from the utility and the battery starts increasing its output power. The delay results eventually from limited high-level control processing speed but this is assumed to be negligible. Communication delays between electricity measurement and EMS are seen as largest influence factor.

Step Response Time T_{SR}

For a step response the duration of the time interval between the instant of the step change of an input variable and the instant when the output variable reaches for the first time a specified percentage of the difference between the final and the initial steady-state value [44]. According this definition the document 'Criteria and procedures for performance testing[57] from the Distributed Energy Research Infrastructure (DERri) project, describes it as time in which 95% of the request power is reached. The step response time may differ for the specific operating mode of the PV-BESS[57]:

- Time to switch from charge to discharge and vice-versa
- Time to start from a standby mode

In addition the ramp time is defined within the step response between an increase of 5 to 95% of rated power.[57] The power ramp rate is expressed similarly but in units of $\mathrm{kW\,s^{-1}}$. The ramp time and ramp rate is seen more important for storage systems with a higher power rating as small-scale PV-BESS used in single family households. Therefore it is not considered in the development of test procedures for PV-BESS.

Settling Time T_{S}

For a step response the duration of the time interval between the instant of the step change of an input variable and the instant, when the difference between the step response and their steady state value remains smaller than the transient value tolerance [44]. The settling time is an important criteria as charge/discharge oscillations of battery power and grid power respectively shall be reduced.

Steady State Error Difference between requested and measured power at steady-state operation. It evaluates the ability to fulfill a specific set point[57].

It is proposed from [57], to determine the minimum time requested, between two successive orders (Set successively ten operating point in charge and discharge as fast as possible) [57]. This could be fast switching/changing of demand or PV generation. Further investigation is necessary, concerning the dynamic behavior of PV and load profiles in households.

The Sandia National Laboratories proposed in the document 'Protocol for Measuring and Expressing the Performance for Energy Storage Systems [55]' a reference signal tracking test for the application of frequency regulation. This procedure can be used in principle for PV-BESS as well. The reference signal tracking test determines the ability of the BESS to respond to a reference signal. The characteristic indexes are determined by error calculation. The deviation between a reference signal P_{Signal} and the manipulated variable P_{BESS} are described by SANDIA according Equations 3.18, 3.21 and 3.24. The characteristic indexes are adopted herein for performance evaluation of PV-BESS.

Sum of Square Errors (SSE) The sum of the square of errors between the reference signal ($P_{\text{Reference}}$) and the power delivered or absorbed by the BESS (P_{BESS}) [55].

$$SSE_{\text{BESS,P}} = \sum \left(P_{\text{Reference}} - P_{\text{BESS}} \right)^2 \tag{3.18}$$

$$SSE_{\text{PV-BESS,P}} = \sum \left(P_{\text{Load}} - P_{\text{PV-BESS}} \right)^2 \tag{3.19}$$

$$SSE_{\text{PV-BESS,P}} = \sum \left(0 - P_{\text{Grid}} \right)^2 \tag{3.20}$$

Where

$P_{\text{PV}-\text{BESS}}$: Power at POC-AC, considering PV and battery charge/discharge power

P_{Grid}: Power at POC-GRID

P_{Load}: Demand of electrical appliances in the household

Sum of absolute magnitude of difference in power The sum of the absolute magnitude of the difference between reference signal ($P_{\text{Reference}}$) and the power delivered or

absorbed by the BESS (P_{BESS}) [55].

$$SAE_{\text{BESS,P}} = \sum |P_{\text{Reference}} - P_{\text{BESS}}| \tag{3.21}$$

$$SAE_{\text{BESS,P}} = \sum |P_{\text{Load}} - P_{\text{PV-BESS}}| \tag{3.22}$$

$$SAE_{\text{PV-BESS,P}} = \sum |0 - P_{\text{Grid}}| \tag{3.23}$$

Sum of absolute magnitude of difference in energy The sum of the absolute magnitude of the difference between the reference signal and BESS to account for the inability for the system to meet high energy half cycles due to the system reaching the SOC limits [55].

$$SSE_{\text{BESS,E}} = \sum |E_{\text{Reference}} - E_{\text{BESS}}| \tag{3.24}$$

$$SSE_{\text{PV-BESS,E}} = \sum |E_{\text{Load}} - E_{\text{PV-BESS}}| \tag{3.25}$$

$$SE_{\text{PV-BESS,E}} = \sum |0 - E_{\text{Grid}}| \tag{3.26}$$

The described equations do not provide separation of the error between charge or discharge or grid import or export respectively. It seems useful to introduce the Mean Signed Error (MSE). This is basically the average of measured gird power during a specific test sequence. The mean deviation to zero grid power is given according Equations 3.27 to 3.28. It gives insight about the trend if more energy export or import was present during a specific test sequence. Equation 3.29 and 3.30 are defined as average deviation of imported or exported power only to zero grid power. The higher the deviation to zero the less the performance of the control system, thereby the test sequence is designed with respect to SOC and charge/discharge power limitations. The MSE for power is calculated as follows:

$$MSE_{\text{total}} = \frac{1}{n} \cdot \sum_{i=1}^{n} (P_{\text{Load}i} - P_{\text{PV-BESS},i}) \tag{3.27}$$

$$MSE_{\text{total}} = \frac{1}{n} \cdot \sum_{i=1}^{n} P_{\text{Grid},i} \tag{3.28}$$

$$MSE_{\text{export}} = \frac{1}{n} \cdot \sum_{i=1}^{n} P_{\text{Grid,export},i} \tag{3.29}$$

$$MSE_{\text{import}} = \frac{1}{n} \cdot \sum_{i=1}^{n} P_{\text{Grid,import},i} \tag{3.30}$$

Control System Performance PV-BESS

The control system in a PV-BESS is divided in a low-level control system for current and power regulation. The EMS represents a high-level control system, which is responsible for charge/discharge decisions. It is assumed that the performance of the control system is not limited by low-level control and high-level processing speed but mostly due to communication delays between electricity measurement and signal processing. The determining factor is usually the sample rate at which the electricity measurement is transmitted to the EMS. The accuracy is determined by the resolution of power (W) or energy (W h) and electricity measurement tolerances of the metering device. Especially for commercial available smart-meters it is observed that a high resolution is usually not limited by the device itself. Moreover the digital output format is limited by the smart-meter manufacturer (amount of delimiters - 0.xxx kWh). The time until the battery is charged or discharged results in grid feed-in or grid imported power. This is shown in Figure 3.8 and 3.8. The response of a steady state charging PV-BESS to a change of PV generation is illustrated in Figure 3.8. Figure 3.8 illustrates the adequate situation for changing demand, during a steady state battery discharge.
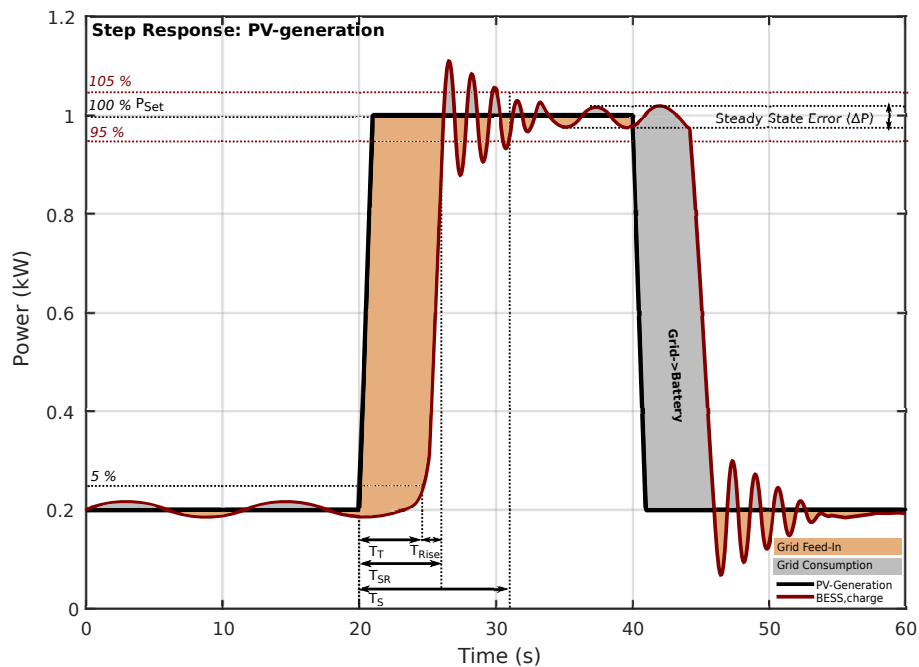
FIGURE 3.7: Step response PV generation
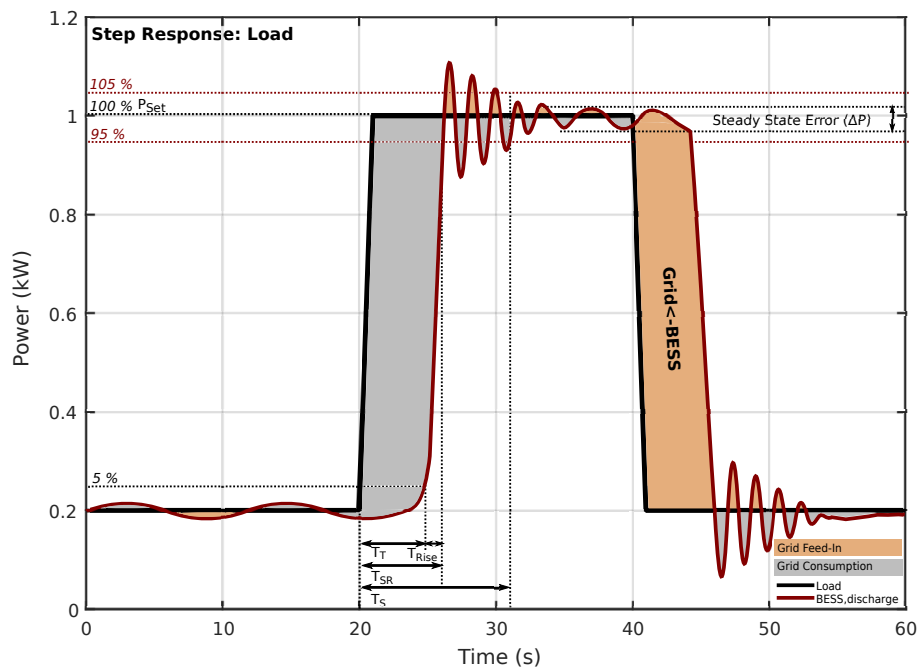
FIGURE 3.8: Step response demand

The time the storage and the inverter needs to start from a standby state is considered in the delay time. The DC coupled system allows theoretically a faster response to changes of PV irradiation. The generated power is measured directly at the DC input and not at the POC-GRID.

3.5 Standby Consumption

The supply for coverage of standby consumption of the PCS and BMS, may change if the battery is empty or fully charged. If the battery is fully charged, energy for PCS, protection devices, BMS etc. can be consumed from the DC battery side. If the battery is empty the system must import power from the utility grid. Different notations are found in technical data-sheets:

Idle Mode In idle mode the system must be able to respond quite instantaneous to feed in, charge or discharge requests. Standby consumption in idle mode is highest.

Night / Sleep / Silent mode The night or sleep mode is given for PV inverters during the night and is usually very low. The inverter is activated again when PV irradiation

is available. For the battery system, depending on the SOC different levels of standby modes might be available, where the PCS is sequentially shut down or the supply of standby power switches from DC to AC supply. Various options are observed to decrease the standby consumption. Three-phase systems change operation mode to single-phase during periods without or very low output power. Some systems shut the PCS entirely down, but still some energy is required for protection and monitoring devices. The BMS must avoid deep discharge during longer periods, therefore standby consumption must be obtained from the utility grid, if the system is not turned off.

A procedure for standby consumption measurements for auxiliary devices (energy meter, external supported EMS etc.) is defined in 'DIN EN 50564:2011-12 (IEC-62301:2011, modified) electrical and electronic household and office equipment Measurement of low power consumption'. The standard addresses electrical standby power measurements for AC powered electrical appliances. It describes testing requirements primarily for single phase systems but theoretically also applicable to three phase products with some adoptions. It describes that the energy consumption of the devices is related to their operating mode. As examples the off-mode, standby-mode and active mode are used as a reference. It is declared that the specific operation mode is not subject of the standard itself. [79]

The measurement of standby consumption over was proposed from CEC for battery charge controllers at connected and disconnected battery. DERri proposes to leave a fully charged ESS in a rest mode for a longer time period (days, weeks), depending on the standby losses rate. Afterwards the system shall be discharged entirely. The discharged rest energy is compared with the dischargeable energy without rest period. [57].

3.6   System Performance Evaluation

The evaluation of the system performance considers efficiency and effectiveness observation. The efficiency is determinable as one way and round trip efficiency for specified power levels. The effectiveness evaluation observes the characteristic indexes Direct Use and Self Coverage for application related input profiles (electrical demand and PV irradiation) of single family households.

Related Standards and Guidelines

This section comprises Related Standards and Guidelines for efficiency evaluation of single energy conversion paths, PV-BESS round trip efficiency and an approach for evaluation of the overall system performance.

One Way Efficiency (PCS)

The one way efficiency determines power or/and energy losses of the Power Conversion System. The efficiency is evaluated for single energy conversion paths at full and partial load power.

- PV Feed-In Efficiency
- PV Charge Efficiency
- Discharge Efficiency
- Grid Charge Efficiency

Grid Charge Efficiency is not further considered as it is not within the application of PV-BESS. It is indirectly determined for an AC coupled system during PV charge efficiency evaluation.

Figure 3.9 illustrates the energy conversion paths for an AC coupled system. Figure 3.10 for a DC hybrid coupled and in Figure 3.11 for a DC generator coupled system.
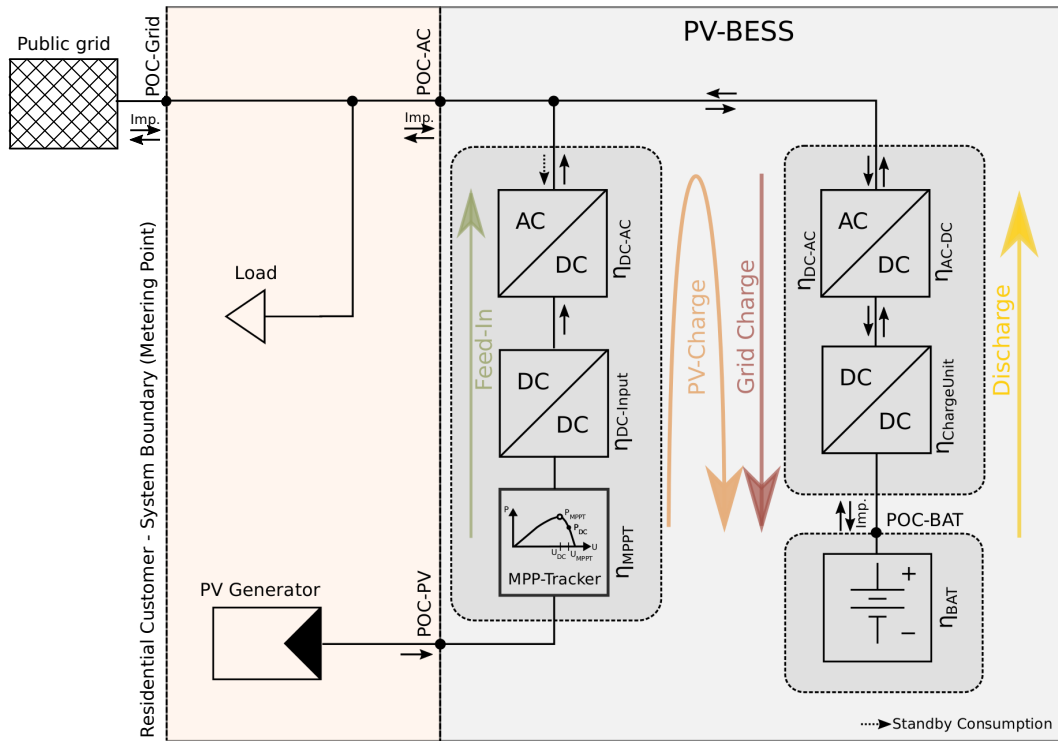
FIGURE 3.9: Energy conversion paths and and component efficiency in an AC coupled system
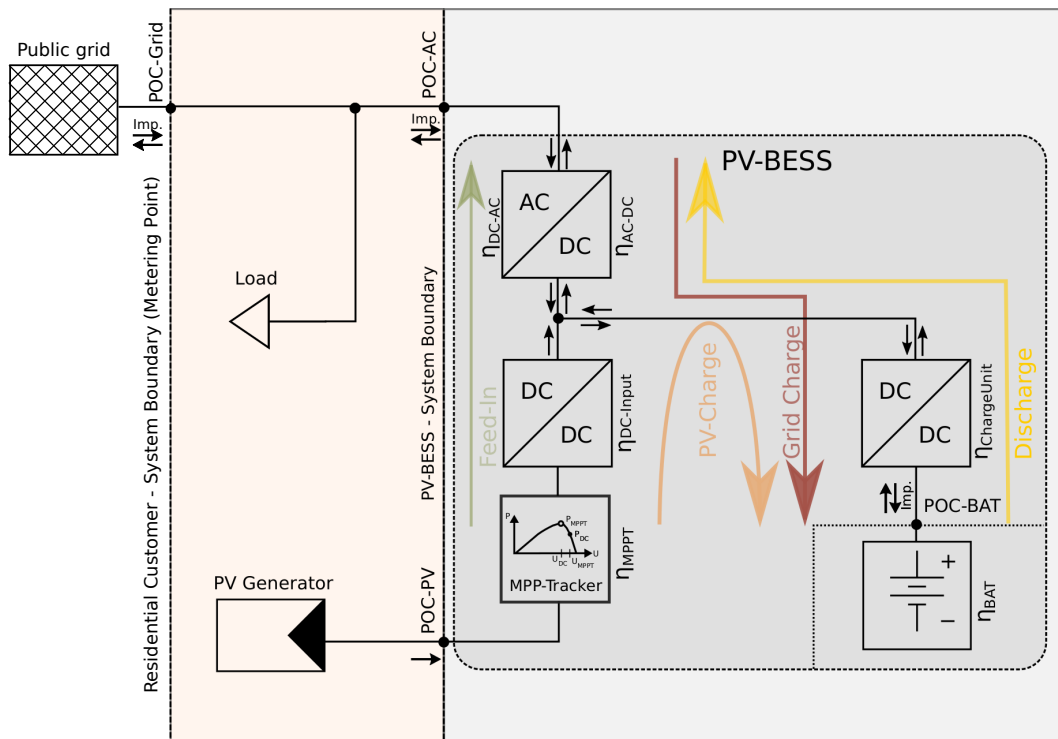
FIGURE 3.10: Energy conversion paths and and component efficiency in a DC hybrid coupled system
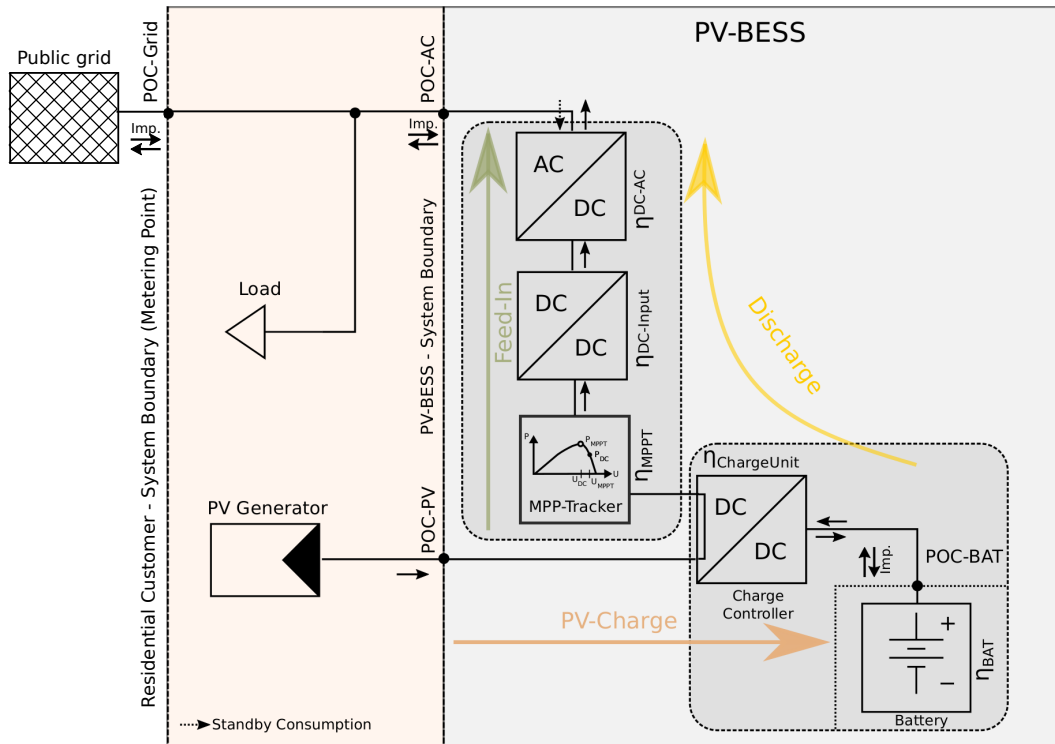
FIGURE 3.11: Energy conversion paths and and component efficiency in a DC generator coupled system

An approach for one way (modular [7]) efficiency evaluation was presented by Fraunhofer IWES at the 30. PV symposium in Bad Staffelstein, Germany. The required measurement points are declared as follows:

TABLE 3.4: Measurement points (Fraunhofer-IWES[7])

Measurement points	
MP_{PVS}	PV generator | PV inverter input
MP_{BAT}	Battery DC terminals | charge controller
MP_{LOAD}	Load (Emulated electical demand)
MP_{GRID}	POC between residential customer and the utility grid
MP_{BESS}	AC coupled: charge controller, connected to the AC link
$\text{MP}_{\text{DCL-Bat}}$	DC coupled: charge controller connected to the DC link

PV Feed-In efficiency is determined at a fully charged battery and no demand (load). The calculation is given for an AC (Equation 3.31 [7]) and DC coupled system (Equation 3.32 [7]). PV generation power (total input power) is added or decreased by the output/input power

of the charge controller. This seems not correct as PV generation and BESS power are not connected at a Point of Common Coupling (PCC) because of losses between. This implies that they cannot be simply summed up.

$$\eta_{\text{Feed-In}}(P_{\text{PV}}) = \frac{P_{\text{Grid}}}{P_{\text{PV}} + P_{\text{DCL-Bat}}} \tag{3.31}$$

$$\eta_{\text{Feed-In}}(P_{\text{PV}}) = \frac{P_{\text{Grid}}}{P_{\text{PV}} + P_{\text{BESS}}} \tag{3.32}$$

P_{Grid} : Grid power (sign convention not given in [7])

P_{PV} : PV power (sign convention not given in [7])

$P_{\text{DCL-Bat}}$: DC link battery charge controller power (sign convention not given in [7])

P_{BESS} : Charge controller AC power (sign convention not given in [7])

PV Charge Efficiency (Equation 3.33 [7]) is determined at a fully discharged battery and no load. The equation contains the previous determined Feed-In efficiency if PV power is fed into the utility grid during charging. The sign convention is not given in the original document but exported grid power (P_{Grid}) must correspond to negative values.

$$\eta_{\text{PV-Charge}}(P_{\text{PV}}) = \frac{P_{\text{BAT}}}{P_{\text{PV}} + \frac{P_{\text{Grid}}}{\eta_{\text{Feed-In}}(P_{\text{Grid}})}} \tag{3.33}$$

Discharge Efficiency (Equation 3.34)[7]) is determined at a fully charged battery and the discharge power is controlled by the demand (emulated demand of electrical appliances in the laboratory by a single phase or three phase load).

$$\eta_{\text{Discharge}}(P_{\text{Load}}) = \frac{P_{\text{Load}}}{P_{\text{BAT}}} \tag{3.34}$$

Round trip efficiency

Test procedures for round trip efficiency evaluation are proposed in the literature for grid-connected BESS, charged from the grid and discharged to the grid. Therefore a slight variation is required for PV-BESS, as the battery is charged from PV generated power. It is determinable for the whole system in the same way as for battery efficiency evaluation only. Equation 3.35 [55] presents a generic approach for grid-connected BESS. It is adopted herein for PV-BESS round trip efficiency evaluation according Equation 3.36.

$$RTE_{\text{generic}} = \frac{\sum_{2}^{X} E_{\text{Output},i}}{\sum_{2}^{X} E_{\text{Input},i}} \tag{3.35}$$

$$RTE_{\text{PV-BESS}} = \frac{\sum_{2}^{X} E_{\text{Load}\leftarrow\text{Bat},i}}{\sum_{2}^{X} E_{\text{PV}\rightarrow\text{Bat},i}} \tag{3.36}$$

Where:

> X: Number of charge/discharge cycle iterations
>
> $E_{\text{Output},i}$: Energy (watt-hours) delivered (discharged) by the system, where 'i' is the cycle number.
>
> $E_{\text{Load}\leftarrow\text{Bat},i}$: Energy (watt-hours) delivered (discharged) from the battery to supply AC powered loads
>
> $E_{\text{Input},i}$: The energy input (watt-hours) into the system during charging, including all parasitic losses, where 'i' is the cycle number.
>
> $E_{\text{PV}\rightarrow\text{Bat},i}$: The energy input (watt-hours) charged from PV generation, where 'i' is the cycle number.

The proposed test procedure from **Sandia National Laboratories [55]** reads as follows:

1. The ESS shall be discharged to its minimum SOC level in accordance with the system manufacturers specifications and operating instructions[55].

2. The ESS shall be charged in accordance with the system manufacturers specifications to full SOC in less than 12 hours. The energy input $E_{\text{Input},i}$, into the system during system charging, including all parasitic losses, shall be measured and recorded[55].

3. The system shall be left at rest in an active standby state for 30 minutes[55]

4. The system shall be discharged in accordance with the system manufacturers specifications and operating instructions to the minimum SOC associated with the practical SOC range as defined by the system manufacturer and provided in the system manufacturers specifications. The discharge rate shall be chosen to the specific application the BESS is used. The energy output from the system $E_{\text{Output},i}$ shall be measured and recorded during discharge.[55]

5. The system shall be left at rest in an active standby state for 30 minutes[55]

6. Steps 1 to 5 above shall be repeated at least eight times, 1 through the number of test repeats X. The reference performance test value shall be calculated as the mean of the second through Xth values of $E_{\text{Input},i}$ as measured in item 2 above, with the standard deviation also calculated and reported[55].

7. The system shall be recharged in accordance with step 2 and the system left in a fully charged state. The energy input for this step will not be used for calculation of the RTE.[55]

In addition to the standard cycle test the efficiency shall be evaluated during a specific, application related duty-cycle.

1 The ESS shall be fully charged in accordance with the manufacturers specifications. The system shall be brought to the initial desired SOC in accordance with the applicable duty cycle by removing the necessary amount of energy at the rate provided in the system specifications provided by the manufacturer or alternatively brought to the desired starting SOC in accordance with a vendor specified procedure [55].

2 The ESS shall then be subjected to the applicable duty cycle [55].

3 At the end of the duty cycle, the system shall be returned to the initial SOC just prior to the application of the duty cycle [55].

4 The RTE shall be determined in accordance as the total energy output divided by the total energy input measured between the same SOC end points associated with the application of the duty cycle during the test[55].

The RTE standard procedure evaluates the efficiency for only one specific charge and discharge power level. At the other hand at least eight iterations are proposed. This is time consuming and it is questionable if this is necessary for a good reproducibility and accuracy of the result. For the RTE duty-cycle test a corresponding sequence must be generated. It may give insight about the efficiency in an application related operation.

'**DERri, Criteria and procedures for performance testing - grid-connected storage [57]**' proposes to evaluate the RTE for four full charge/discharge cycles. The charge power is the same for each cycle but the discharge power varies. The procedure reads as follows:

1 Standard charge until 100% State of Energy (SOE)[57].

2 Discharge at the nominal power and record the energy discharged[57].

3 Definition of the 4 constant discharge power levels (P_{rated} , $3/4 P_{\text{rated}}$, $1/2 P_{\text{rated}}$, $1/4 P_{\text{rated}}$)[57].

Where the terminology is described as follows:

State of Energy DERri introduces, comparable with the SOC the SOE (expressed as energy content in watt-hours). It is determined as the amount of stored energy in the battery, normalized to the net energy.[57]. An approach is done herein to define the described SOE by Equation 3.37.

$$SOE = \frac{E_{\text{Bat}}}{E_{\text{Net}}} = \frac{Q_{\text{Bat}}(Ah) \cdot V_{\text{Bat,OCV}}}{E_{\text{Net}}} \tag{3.37}$$

Standard Charge The normal charge is defined as the charge process used by the manufacturer in order to reach 100% SOE. The End of Charge (EOC) criterion is given as follows:[57]

- 100 % SOE
- Specific variable detects EOC
- The delta SOE is below 1% per hour at maximum continuous charging power.

Standard Discharge The nominal discharge is defined as a complete discharge using the nominal power.[57]. The End of Discharge (EOD) criterion is given as follows:[57]

- 0 % SOE
- Specific variable detects EOD.
- The delta SOE is below -1% per hour at maximum continuous charging power.

The proceeding recommends to estimate both, the Round Trip and One Way Efficiency for charging and discharging (e.g $\eta_{charge} = \Delta SOE/\text{energy charged}$). This would require an accurate SOE estimation. As example it is proposed for lead-acid batteries to measure the acid concentration. No detailed descriptions about feasibility is given for more complex electrochemical systems (e.g. lithium-ion batteries). Therefore the SOE is not considered for efficiency evaluation within this work. End of charge and discharge criteria is given from the internal BMS or specific V/I characteristics at the battery terminal.

A redefinition of the chosen levels for discharge power may be useful. This is because of lower discharge power in a household at the evening and during the night ($<350\,\text{W}$). If a system has a rated discharge power of $2\,\text{kW}$ $1/4 \cdot P_{rated}$ corresponds to $500\,\text{W}$. This probably does not represent well enough the application of PV-BESS in single family households.

No iterations of identical cycles are performed within this test sequence, this seems necessary for reproducibility of test results, because SOC or SOE estimation has tolerances. The amount of charged and discharged energy may therefore vary, between two identical full charge/discharge cycles.

In general the test time effort increases if more cycles are performed and especially a low power charge/discharge takes longer. A compromise between enough performed charge/discharge power levels and iteration of identical cycles must be found.

System Efficiency / Effectiveness / Control System Performance

A first approach for overall PV-BESS performance evaluation was done by Fraunhofer IWES (Test Procedures for grid-connected, residential PV Battery Systems (2013) [80]). It requires the generation of a matrix, containing full and part load efficiency, related to the main energy transfer paths within the system (Table 2.2, Section 1.4). The partial load efficiency for each energy transfer path is first determined by laboratory measurements. In principle it relates to the one way efficiency described in Section 3.6. The next step is to weight the partial load efficiencies with the relative frequency of power and energy during an application related test (Emulation of real PV generation and electrical demand of households in a laboratory environment).

The efficiency matrix includes battery charge/discharge efficiency as square root of the round trip efficiency [80]:

$$
\eta_{modular} =
\begin{matrix}
\eta_{\text{PV-Charge}}(P_1) \cdot \sqrt{\eta_{\text{RTE,Bat}}(P1)} & \eta_{\text{Feed-In}}(P_1) & \cdots & \eta_{\text{Discharge}}(P_1) \cdot \sqrt{\eta_{\text{RTE,Bat}}(P1)} \\
\eta_{\text{PV-Charge}}(P_2) \cdot \sqrt{\eta_{\text{RTE,Bat}}(P2)} & \eta_{\text{Feed-In}}(P_2) & \cdots & \eta_{\text{Discharge}}(P_2) \cdot \sqrt{\eta_{\text{RTE,Bat}}(P2)} \\
\cdots\cdots\cdots\cdots\cdots\cdots\cdots\cdots\cdots\cdots\cdots\cdots\cdots\cdots\cdots\cdots\cdots\cdots\cdots\cdots\cdots \\
\eta_{\text{PV-Charge}}(P_n) \cdot \sqrt{\eta_{\text{RTE,Bat}}(Pn)} & \eta_{\text{Feed-In}}(P_n) & \cdots & \eta_{\text{Discharge}}(P_n) \cdot \sqrt{\eta_{\text{RTE,Bat}}(Pn)}
\end{matrix}
$$

$$(3.38)$$

Where:

$P_1 \ldots P_n$: Full and partial load power related to rated power of the specific energy
transfer path.

The power distribution (divided into classes), is given by the weighting factors according Matrix 3.39 [80]:

$$F_{\text{modular}} = \begin{matrix} F_{\text{PV}\to\text{Bat}}(P_1) & F_{\text{PV}\to\text{AC}}(P_1) & \dots & F_{\text{Bat}\to\text{AC}}(P_1) \\ F_{\text{PV}\to\text{Bat}}(P_2) & F_{\text{PV}\to\text{AC}}(P_2) & \dots & F_{\text{Bat}\to\text{AC}}(P_2) \\ \dots\dots\dots\dots\dots\dots\dots\dots\dots\dots\dots\dots\dots\dots\dots \\ F_{\text{PV}\to\text{Bat}}(P_n) & F_{\text{PV}\to\text{AC}}(P_n) & \dots & F_{\text{Bat}\to\text{AC}}(P_n) \end{matrix} \tag{3.39}$$

The energy distribution is expressed as weighting vector (Equation 3.40).

$$a_{\text{modular}} = \begin{matrix} a_{\text{PV}\to\text{Bat}} & a_{\text{PV}\to\text{AC}} & \dots & a_{\text{Bat}\to\text{AC}} \end{matrix} \tag{3.40}$$

The efficiency factors are now weighted with the given energy and power distribution, determined during an application related test. The result corresponds to the overall system efficiency (Equation 3.41).

$$\epsilon_{\text{System}} = (F_{\text{modular}} \cdot \eta_{\text{modular}}) \cdot a_{\text{modular}} \tag{3.41}$$

The application related test was further developed and published within the 30. PV symposium in Bad Staffelstein, Germany ('Test Procedures for Grid-Connected Residential PV-Battery Systems (2015) [7]') An index portfolio is proposed for evaluating the overall PV-BESS performance during an application related test. Within this portfolio not only the system efficiency is taken into account but moreover effectiveness (self-coverage) and performance of the control system.

The sequence consists of PV irradiation data of Germany (Nordhessen). Corresponding load profiles were measured at single family households with children. Both are sampled at one second and the described profiles have have a duration of four days. The first and third day consists of high solar irradiation and low fluctuations. The second and fourth day is represented by low solar irradiation and high fluctuations. Demand is mostly low (approx. 100 W) during the night and shows maximum peaks of 5000 W during the day. [7] The test starts at midnight with an empty battery, at the end of the sequence the battery must be at its initial state (empty) again. This is required for battery and PV-BESS efficiency evaluation.

The index portfolio is given as follows:

- Energy Efficiency (ϵ_{AC})
- Control System (ϵ_{Load})
- Effectiveness (ϵ_{SC})

Energy Efficiency ϵ_{AC} is determined as ratio between total AC energy expenditure and DC input energy (Equation 3.42 [7]).

$$\epsilon_{\text{AC}} = \frac{E_{\text{Load}\leftarrow\text{PV}} + E_{\text{Grid}\leftarrow\text{PV}} + E_{\text{Load}\leftarrow\text{Battery}}}{E_{\text{PV}}} \tag{3.42}$$

$$\tag{3.43}$$

The Control System Performance ϵ_{Load} compares the load coverage from the laboratory test with results from an ideal (endless fast and accurate) modeled control system. It is configured that a surplus of PV power is stored in the battery, and a deficit is compensated by immediately discharging the battery (with respect to SOC range and power limits). The system efficiency (energetic losses) is considered in the calculation by ϵ_{AC} (Equation 3.44).

$$\epsilon_{Load} = \frac{E_{\text{Load}\leftarrow\text{PV(Laboratory)}} + E_{\text{Load}\leftarrow\text{PV(Laboratory)}}}{E_{\text{Load}\leftarrow\text{PV(Simulation)}} + E_{\text{Load}\leftarrow\text{Bat(Simulation)}}} \cdot \frac{1}{\epsilon_{\text{AC}}} \tag{3.44}$$

The effectiveness of the system is given by the Self-coverage, calculated according Equation 3.45 [7].

$$\epsilon_{\text{SC}} = \frac{E_{\text{Load}\leftarrow\text{PV}} + E_{\text{Load}\leftarrow\text{Bat}}}{E_{\text{Load}}} \tag{3.45}$$

It is proposed to rate the system in classes from A to E according Table 3.5 by using the combination of all individual performance indicators. For instance a system achieving a high efficiency $\epsilon_{\text{AC}} = 95\%$, a control performance $\epsilon_{\text{Load}} = 92\%$ and self coverage $\epsilon_{\text{SC}} = 60\%$ is rated as ACD[7].

TABLE 3.5: Possible rating of grid-connected residential PV-BESS.[7]

Rating group	Energy Conversion ϵ_{AC} (%)	Control System ϵ_{Load} (%)	Self-Coverage ϵ_{SC} (%)
A	>90	>97	>80
B	80 - 90	94 - 97	70 - 80
C	70 - 80	91 - 94	60 - 70
D	60 - 70	88 - 91	50 - 60
E	<60	<88	<50

Comparison Round Trip efficiency AC and DC coupled system

A theoretical charge/discharge efficiency is calculated for a DC and AC coupled system. The comparison does not takes dependencies from voltage or power into account. Differences in the voltage transformer ratio are neglected. No losses are considered for cooling, protection devices and control systems.

It is assumed that the charge controller and DC/AC and AC/DC inverter stage has the same topology and efficiency in both systems. A high and moderate efficiency scenario is observed. According to the previous section the high efficient system uses mainly transformerless topologies, the moderate efficiency scenario assumes a system using HF transformers for galvanic isolation. Assumed values are found in Table 3.6. One way efficiency of the battery is calculated simplified as square root of the RTE.

TABLE 3.6: High- and moderate efficiency scenario PV-BESS (theoretical values)

	High Efficiency	Moderate Efficiency
MPPT	0.98	0.98
InputStage	0.99	0.96
charge controller	0.98	0.95
Battery (One Way)	0.98	0.96
Inverter unit (bidirectional)	0.99	0.98

Feed-in efficiency is determined for both systems according Equation 3.46. Charge efficiency for the DC coupled system according Equation 3.47 and for the AC coupled system according 3.48. The discharge efficiency is determined by using Equation 3.49.

$$\eta_{\text{Feed-In}} = \eta_{\text{MPPT}} \cdot \eta_{\text{DC-Input}} \cdot \eta_{\text{DC/AC}} \tag{3.46}$$

$$\eta_{\text{PV-Charge}} = \eta_{\text{MPPT}} \cdot \eta_{\text{DC-Input}} \cdot \eta_{\text{ChargeController}} \tag{3.47}$$

$$\eta_{\text{PV-Charge}} = \eta_{\text{MPPT}} \cdot \eta_{\text{DC-Input}} \cdot \eta_{\text{DC/AC}} \cdot \eta_{\text{AC/DC}} \cdot \eta_{\text{ChargeController}} \tag{3.48}$$

$$\eta_{\text{Discharge}} = \eta_{\text{ChargeController}} \cdot \eta_{\text{DC/AC}} \tag{3.49}$$

The total charge (Equation 3.50) and discharge (Equation 3.51) efficiency considers an estimated one way battery efficiency:

$$\eta_{\text{Charge,BAT\&PCS}} = \eta_{\text{PV-Charge}} \cdot \sqrt{\eta_{\text{RTE,Bat}}} \tag{3.50}$$

$$\eta_{\text{Discharge,BAT\&PCS}} = \eta_{\text{Discharge}} \cdot \sqrt{\eta_{\text{RTE,Bat}}} \tag{3.51}$$

The PV to Battery to AC round trip efficiency is determined according Equation 3.52. This assumption requires that the total PV generated energy is charged and no feed-in occurs.

$$\eta_{\text{RTE,PV-BESS}} = \eta_{\text{Charge,BAT\&PCS}} \cdot \eta_{\text{Discharge,BAT\&PCS}} \tag{3.52}$$

The results are given in Table 3.7:

TABLE 3.7: Efficiency evaluation based on the values from Table 3.6

Efficiency (%)	High Eff. Scenario 1		Moderate Eff. Scenario 2	
	DC coupled	AC coupled	DC coupled	AC coupled
Feed In	98		94.1	
Discharging (PCS)	97.0		93.1	
Discharging (Total)	96.0		89.4	
Charging (PCS)	96	94.1	89.4	85.8
Charging (Total)	95.1	93.2	85.8	82.4
Round Trip	91.3	89.5	76.7	73.6

Chapter 4

PV-BESS Test Portfolio and Analysis

This chapter comprises an approach for a test portfolio, based on the described methodology of the Art in Chapter 3. The first section describes the Laboratory Framework at the AIT research test bed. The test portfolio is described in the next sections and examples of test results are given.

4.1 Laboratory Framework

The AIT research test bed consists of following components:

- PV Simulator 12 kW per string
- Electrical Load 11 kW
- Measurement Devices and Data Acquisition System (DAQ)

Table 4.1 lists the available current and voltage measurement points at the test stand:

TABLE 4.1: Measurement points at the main unit of the research test bed

Symbol	Descripton	Measurement
PVS,MPP	PV Simulator MPP power	Provided MPP power
PVS,DC	PV Simulator DC power	DC voltage and current (+/-)
GRID	Utility grid or simulator	AC voltage and current (1/3 ph)
INV	Inverter ouptut	AC voltage and current (1/3 ph)

State of the Art PV simulators were developed for evaluation of feed-in efficiency according EN-50530. The conversion efficiency and MPPT efficiency is usually determined separately and overall efficiency is given as a product of both. Direct determination of the overall efficiency is not necessarily possible, because no time synchronous measurement of AC inverter output power (INV) and MPP power is given. For PV-BESS efficiency evaluation the same approach is done. Instantaneous overall efficiency is not defined if no time synchronous measurement of provided MPP power from the PV simulator and DAQ for PV-BESS power measurements exists.

The emulated load is not measured directly but calculated according Table 4.2 for DC and AC coupled systems. For this reason the standby consumption of the electrical metering device is included in the calculation. Further developments of the research test bed shall allow direct power measurements of the emulated load.

TABLE 4.2: The demand of the electrical load is calculated, according Krichhoff's nodal rule

	Nodal rule
DC coupled	$P_{\text{Inv}} + P_{\text{Grid}} + P_{\text{Load}} = 0$
AC coupled	$P_{\text{Inv}} + P_{\text{Grid}} + P_{\text{BESS}} + P_{\text{Load}} = 0$

4.1.1 Requirements on Test Equipment and Environment

The test procedures are based on the assumption that no communication from the DAQ system to the control system (Load control, PV Simulator) is available. The operation points during the tests are set only by adjustment of PV simulator and load power. All power measurements must be time synchronous for instantaneous efficiency evaluation $\eta(t)$. Due to the specific properties of the used devices (bridges, step-up and step-down converter) DC voltages and currents are usually superposed with a ripple (i.e. double of the mains frequency: 100 or 120 Hz). Therefore an average over at least 50 to 100 ms or more is recommended for power calculation [81]. For long-term PV-BESS tests a maximum sample rate as moving average of 1s is preferable.

The Californian Energy Commission sets requirements for efficiency evaluation of charge controllers and power supplies. These could be adopted for PV-BESS laboratory test, but are not investigated in detail within this work.

Test equipment

The requirements for the test equipment are defined by CEC as follows[68]:

- Power Measurement Accuracy: $\leq 0.1\,\text{W}$ (10 to 100 W) $|\leq 1\,\text{W}$ (over 100 W)

- Energy: $\leq 1\%$

- Voltage and Current Measurement: uncertainty $\leq 1\%$

- Temperature measurement $\leq 2\,°\text{C}$

The requirements for the test room are defined by CEC as follows[68]:

Test room

The ambient temperature shall be maintained at $20\,°\text{C} \pm 2\,°\text{C}$ throughout the test. Air speed near the UUT of $\leq 0.5\,\text{m/s}$. No intentional cooling.

A PV-BESS operates usually at room temperature between 15 to $25\,°\text{C}$. For maximum reproducibility (battery capacity decreases with higher temperature, efficiency may increase) a limitation of the ambient temperature to $20\,°\text{C} \pm 2\,°\text{C}$ is recommended herein for laboratory testing.

4.1.2 System Under Test

The system under test is illustrated for the AC coupled system in Figure 4.1 and for the DC coupled system in Figure 4.2 It is divided schematically into the power conversion system (PCS), communication and controls and the battery system. The illustrations comprise the use of a grid simulator and additional control possibilities of the equipment under test (EUT). The efficiency and effectiveness test procedures, described in this thesis do not require a grid simulator and enhanced control possibilities. For systems, which allow direct control of charge/discharge set points, a simplification of the procedures could be done in future development steps. A standardized interface for test or certification purpose would be preferable.

AC coupled System

The setup for the AC coupled storage system is illustrated in Figure 4.1. Two energy meters are installed. One at the connection point to the grid (POC-GRID), which transmits the measured data to the EMS. The second meter measures the PV generation, the information

is required for internal calculations of the PV-BESS and logging of Direct Use and Self-Coverage. This data is accessible for the customer at a web portal.

Voltage and current measurement is done at the AC and DC terminal of the battery inverter (Table 4.3, Figure 4.1)
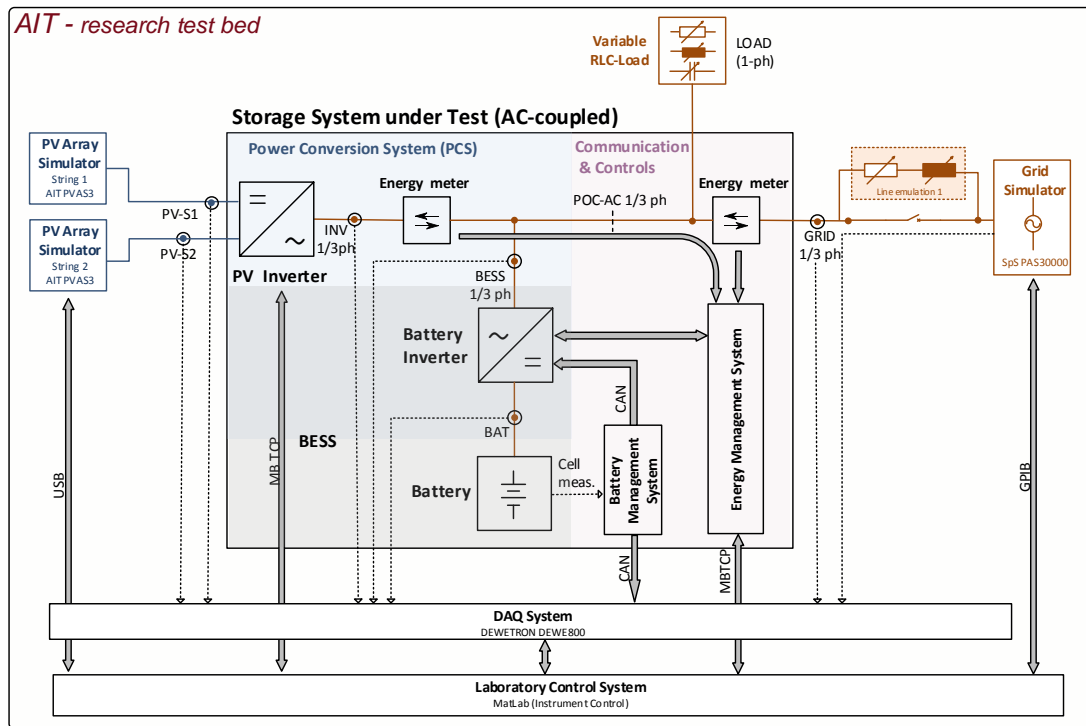
FIGURE 4.1: AIT research test bed (AC coupled PV-BESS under test)

TABLE 4.3: Additional measurement points for the AC coupled system

Symbol	Descripton	Measurement
BESS	Battery inverter, AC terminal	AC voltage and current (1/3 ph)
BAT	Battery DC terminals	DC voltage and current (+/-)

DC hybrid coupled system

The DC hybrid coupled system could provide theoretical three measurement points within the DC-link. It is not guaranteed that measurements are available if current flows over conductor tracks at a PCB. The illustration shows one available measurement point connected to the

TABLE 4.4: Additional measurement points for the DC coupled system (Note: If optional measurement points are available within the DC Link, at least one voltage measurement is required. The power is calculated as a product of current and common DC Link voltage)

Symbol	Descripton	Measurement
BAT	Battery pack DC-terminals	DC- voltage and current (+/-)
DCL-Ipt	DC Link input stage	DC voltage or current (+/-)
DCL-Inv	DC Link inverter stage	DC voltage or current (+/-)
DCL-BESS	DC Link charge controller	DC voltage or current (+/-)

daq. Power measurements at the DC link require a voltage measurement point and current measurements between the junction point and the different stages (DC input, inverter, charge controller). If the current flows over integrated conductor tracks shunts of current transformers are not installable without usual methods. If not at least two measurement are available within the DC link it implies that the exact power distribution within the system (described in Figure 2.3 and Table 2.2) is not feasible. It is assumed that a measurement point at the battery DC terminal is always available.
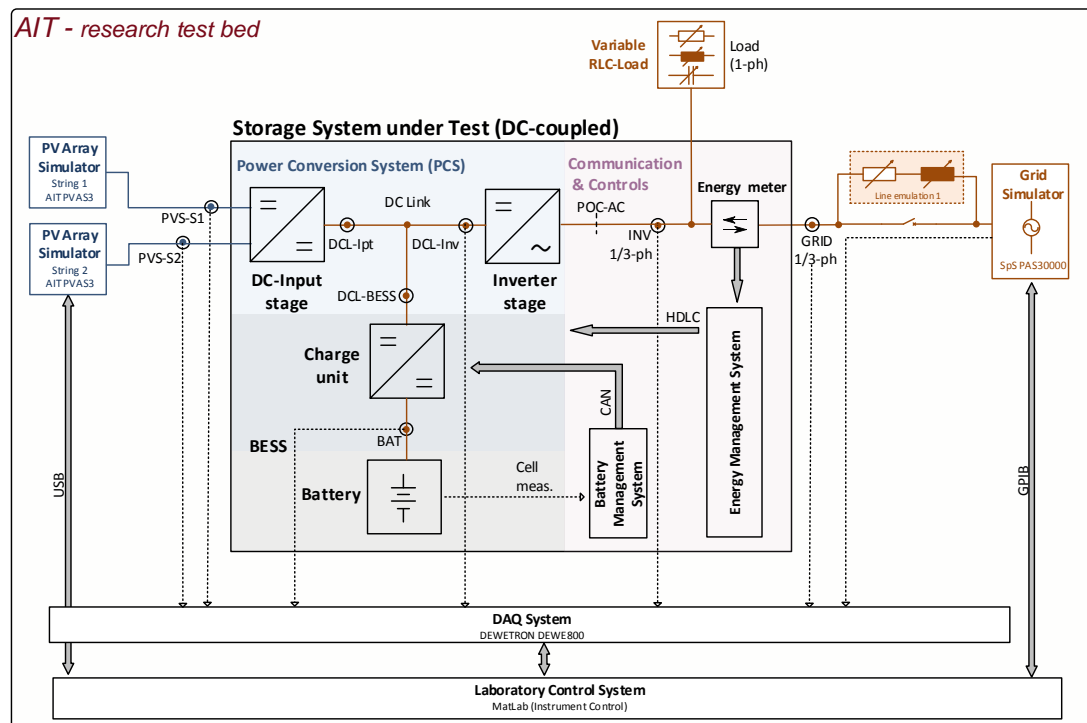
FIGURE 4.2: AIT research test bed (DC hybrid coupled system under Test)

4.1.3 Pretest and Definition of Standard Procedures

A pretest shall validate the basic functionality of the PV-BESS and measurement equipment. An example of a possible pretest is illustrated in Figure 4.3. If the load power exceeds the generation battery discharge is expected. If generation exeeds the load power a battery charge shall be observed (SOC range must allow battery charge/discharge).
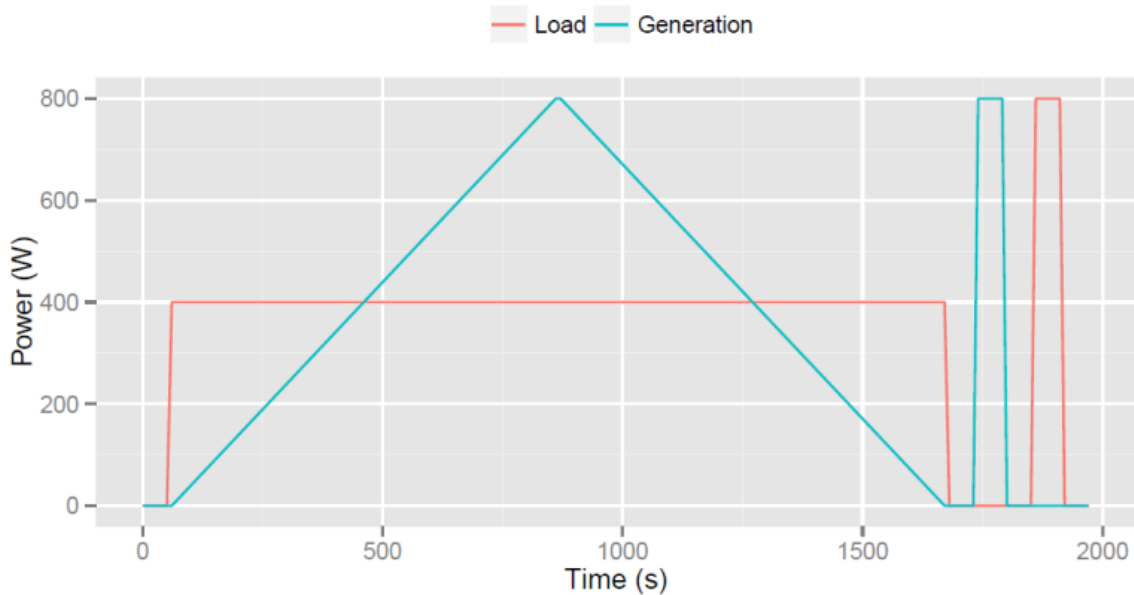
FIGURE 4.3: Pretest

Efficiency evaluation requires knowledge about the set points at the PV simulator and load for automatically adjustment of a desired DC battery power. For instance for evaluation the charge efficiency power the MPP power set at the PV simulator must be known at which maximum/rated battery DC power is adjusted, but no additional power is fed into the utility grid. A manually performed pretest determines the maximum PV (MPPT) power $P_{\text{PVS,MPP(max,charge)}}$ where the battery is charged only and no feed-in is observable. The same applies to the maximum load power $P_{\text{Load(max.discharge)}}$ where no additional grid import is required for demand coverage. The procedure reads as follows:

1 Determine the output power of the PV simulator $P_{\text{PVS,MPP(max,charge)}}$ at $V_{\text{MPP,r}}$, the battery is charged with maximum/rated DC power and no additional feed-in is observable. This is done at approximately 50% SOC. The information about SOC is provided by the PV-BESS (it is assumed that every PV-BESS has a built-in SOC gauge).

2 Determine the load power $P_{\text{Load(max.discharge)}}$, the battery is discharged with maximum/rated DC power and no additional power is imported from the grid for load coverage. This is done at approximately 50% SOC.

3 Information if the PV-BESS decreases discharge power automatically at low SOC levels shall be given by the manufacturer or determined at the pretest.

4 Information if the system decreases charge power automatically with increasing SOC shall be given by the manufacturer or determined at the pretest.

Test procedures for battery efficiency evaluation start preferable at a fully charged or discharged battery. A standardized charge/discharge procedure could be defined as follows:

1 Full battery charge/discharge with maximum power until the PV-BESS terminates the charge/discharge process.

2 Rest phase of $T_{\text{REST},1}$ (recommended: 1.5 hours) for OCV relaxation and SOC recalibration. (A fully charged battery might be slightly discharged during this phase due to standby consumption).

3 If possible, charge/discharge the battery again with 10% of rated charge power until the PV-BESS terminates the charge/discharge process again.

4 Rest phase of $T_{\text{REST},2}$ (recommended: 15 minutes) until the actual test sequence starts.

If the test starts at a specific SOC or must be performed within a specific SOC range the integrated indicator (SOC gauge) at the PV-BESS is used. A fully charged battery corresponds to 100% SOC and a fully discharged battery to 0% SOC. It was observed that PV-BESS sometimes indicate only the SOC related to a nominal but not operational fully charged battery. For instance the battery is fully charged at indicated $SOC_{\text{EOC}} = 95\%$ and fully discharged ad indicated $SOC_{\text{EOD}} = 5\%$. If the SOC range is limited it can be converted according Equation 4.2 to be convenient to the 0 to 100% (operational full) definition.

$$SOC_{\text{range}} = SOC_{\text{EOC}} - SOC_{\text{EOD}} \tag{4.1}$$

$$SOC_{\text{PV-BESS}} = SOC_{\text{EOD}} + SOC_{\text{range}} \cdot \frac{SOC_{\text{Test}}}{100} \tag{4.2}$$

Where:

SOC_{range} : SOC range PV-BESS (Min. to Maximum SOC gauge)

SOC_{EOC} : SOC indicated at the PV-BESS SOC gauge at End of Charge

SOC_{EOD} : SOC indicated at the PV-BESS SOC gauge at End of Discharge

$SOC_{\text{PV-BESS}}$: Indicated SOC at the PV-BESS converted to a SOC range between 0 to 100%

SOC_{Test} : SOC level required from the test procedure.

4.2 One Way Efficiency (PCS)

The test procedures determine the full and partial load efficiency for components of the PCS and energy conversion paths. One way efficiency does not comprise battery efficiency. Efficiency evaluation is done under steady state condition or for dynamic changing input profiles during a specific test sequence (An example is given in Section 4.6: Application related System Performance).

The instantaneous or time period conversion efficiency of the whole PCS is determined according Equation 4.3. The calculation corresponds to the relation between output and input of power or energy. In Table 4.5 all related input and outputs at the PCS of a PV-BESS are listed. The absolute power or energy conversion losses are determined by the difference of input and output power/energy. If no PV generation and battery discharge for load coverage is present the losses consist of DC (Battery) or AC (Grid) supplied energy for coverage of standby consumption.

$$\eta_{\text{PCS}} = \frac{\sum_{i=1}^{n} P_{\text{Out},i} \cdot \Delta T_i}{\sum_{i=1}^{n} P_{\text{In},i} \cdot \Delta T_i}$$

TABLE 4.5: Inputs and Outputs at the PV-BESS Power Conversion System

Power Input (PCS)	Power Output (PCS)
Import at POC-AC	Export at POC-AC
Battery discharge	Battery charge
PV generation (MPPT or DC power)	

$$\eta_{\text{PCS,conv}} = \frac{\sum_{i=1}^{n} (P_{\text{POC-AC,export},i} + P_{\text{Bat,charge},i}) \cdot \Delta T_i}{\sum_{i=1}^{n} (P_{\text{PVS,DC},i} + P_{\text{POC-AC,import},i} + P_{\text{Bat,discharge},i}) \cdot \Delta T_i} \tag{4.3}$$

The overall efficiency is defined herein as efficiency considering conversion and MPPT losses of the PCS. Equation 4.4 is used for static (steady-state) efficiency evaluation and Equation 4.5 for profiles with dynamic changing PV input (MPP power provided by the PV simulator) during a specific test sequence.

$$\eta_{\text{PCS,t,static}} = \frac{\sum_{i=1}^{n}(P_{\text{POC-AC,export},i} + P_{\text{Bat,charge},i}) \cdot \Delta T_i}{P_{\text{PVS,MPP}} \cdot T_{\text{M}} + \sum_{i=1}^{n}(P_{\text{POC-AC,import},i} + P_{\text{Bat,discharge},i}) \cdot \Delta T_i} \tag{4.4}$$

$$\eta_{\text{PCS,t,dyn}} = \frac{\sum_{i=1}^{n}(P_{\text{POC-AC,export},i} + P_{\text{Bat,charge},i}) \cdot \Delta T_i}{\sum_{i=1}^{m} P_{\text{PVS,MPP},j} \cdot \Delta T_j + \sum_{i=1}^{n}(P_{\text{POC-AC,import},i} + P_{\text{Bat,discharge},i}) \cdot \Delta T_i} \tag{4.5}$$

This equations allow efficiency evaluation of the PCS for more than one active energy conversion paths at the same time. For instance PV feed-in and PV battery charge. The subsequent efficiency evaluation of single energy conversion paths (charge / discharge / feed-in) is based on the previously described equations for the entire PCS. The test sequence must provide that only one single energy conversion path is actively used during the power measurement for efficiency evaluation.

Charge and discharge efficiency are influenced by the battery voltage. During a constant power charge the battery voltage increases and the current decreases. During a constant power discharge the voltage decreases and current increases. Both affects the efficiency as a function of SOC. The impact on the efficiency depends strongly on the specific configuration. In Section 2.3.4, Table 2.6 an example is given for a modular HVB-BESS. Depending on the amount of used modules battery voltage and therefore the difference to the DC link voltage varies for one PV-BESS with identical PCS. Assuming a constant power charge/discharge the battery current is decreased for configurations with more modules or higher SOC levels. At the other hand it was shown that the voltage profile depends on the used chemistry and that especially for LFP batteries the voltage does not change strongly within a wide SOC range. Lower voltage transformation ratio and battery current hypothetically increases the efficiency of the DC/DC converter.The efficiency of an AC coupled system LVB-BESS inverter is shown in Figure 3.5. The losses are increased for this specific topology (LF transformer at the AC input and battery connected to DC link of the bridge) with higher battery voltage.

4.2.1 PV Feed-In Efficiency

The static feed-in efficiency evaluation is done basically according the EN-50530 (MPPT, conversion, overall and EU/CEC efficiency)[59] as described in Section 3.1. For an AC coupled system in principle any PV inverter can be used. The feed-in efficiency is therefore not defined. It is specified by the efficiency of the used inverter in the household of the residential customer. If the PV-BESS manufacturer provides a product which contains PV and battery inverter the PV inverter efficiency shall be declared in the test report.

The test starts with a fully charged battery and no electrical load power (demand) is active. Figure 4.4 shows an example of an automatic performable test sequence. The entire procedure is illustrated for efficiency evaluation at $V_{\mathrm{MPP,min}}$ and $V_{\mathrm{MPP,rated}}$ and the required power steps from EN-50530. It is recommended to evaluate the efficiency for more power and voltage levels as declared in the standard as State of the Art PV inverters allow fast MPP stabilization. The overall test time is therefore reduced. The duration of the timing parameters is not specified herein. T_{Prepare} must allow MPP stabilization, if no stabilization is observed the efficiency is evaluated manually and for maximum five minutes. The efficiency is determined during T_{Meas} for a recommended period of 30 seconds.
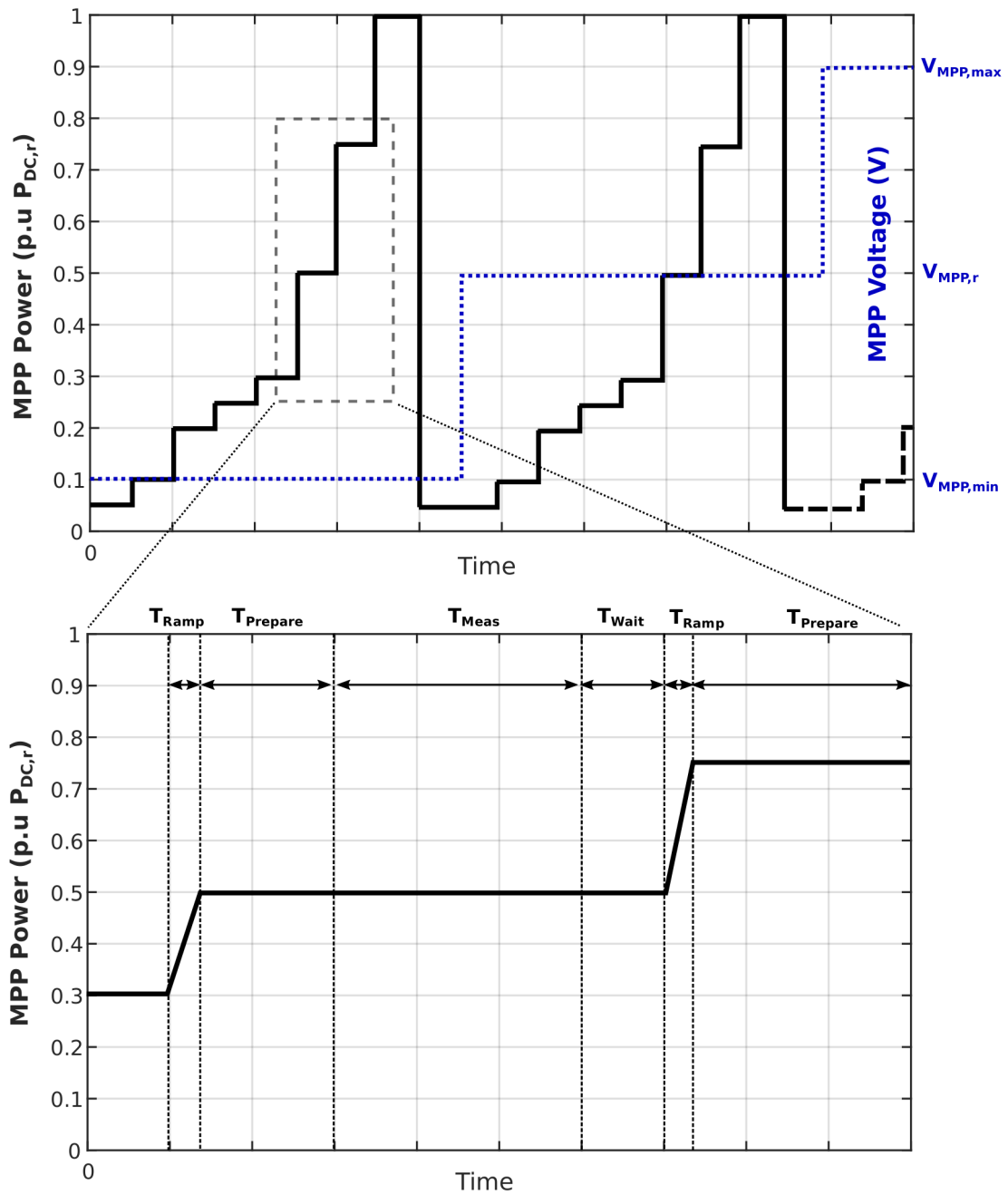
FIGURE 4.4: Automatic test sequence for the determination of feed-in efficiency. Power and voltage levels are adopted from EN-50530. The test is performed for two PV cell technologies

It was observed for a DC hybrid coupled system that the fully charged battery was slightly but unavoidable discharged during feed-in (1.5% of maximum feed-in power). Therefore battery power is considered as an additional input for the calculation of the feed-in efficiency.

If discharge is observed during the test it shall be reported as average over the corresponding measurement period T_M (T_{Meas}) in the test report. Conversion efficiency is determined according Equation 4.6, and overall efficiency according to Equation 4.7. Dynamic MPPT (feed-in) is determined according to the described procedure within EN-50530 and Equation 4.8 is used for efficiency calculations.

$$\eta_{\text{Feed-in,conv}} = \frac{\sum_{i=1}^{n} P_{\text{POC-AC,export},i} \cdot \Delta T_i}{\sum_{i=1}^{n} (P_{\text{PVS,DC},i} + P_{\text{Bat,discharge},i}) \cdot \Delta T_i} \tag{4.6}$$

$$\eta_{\text{Feed-in,t,static}} = \frac{\sum_{i=1}^{n} P_{\text{POC-AC,export},i} \cdot \Delta T_i}{P_{\text{PVS,MPP}} \cdot T_M + \sum_{i=1}^{n} P_{\text{Bat,discharge},i} \cdot \Delta T_i} \tag{4.7}$$

$$\eta_{\text{Feed-In,t,dyn}} = \frac{\sum_{i=1}^{n} P_{\text{POC-AC,export},i} \cdot \Delta T_i}{\sum_{j=1}^{m} P_{\text{PVS,MPP},j} \cdot \Delta T_j + \sum_{i=1}^{n} P_{\text{Bat,discharge},i} \cdot \Delta T_i} \tag{4.8}$$

The European/CEC conversion and overall efficiency does not fit for DC coupled systems because estimated feed-in power vin EN-50530 varies due to changed power distribution. The fed-in power is reduced for charging the battery. MPPT European/CEC efficiency only can be further used. The restrictions are not given for an AC coupled system.

4.2.2 PV Charge Efficiency

The efficiency is evaluated for charging the battery at full and partial load from PV power. As for feed-in efficiency, a subdivision in MPPT, conversion and overall charge efficiency is done. A measurement point at the DC battery terminal is required. For an AC coupled system the efficiency is basically determined by the single efficiency of the battery inverter and PV inverter. If no PV inverter is provided by the PV-BESS manufacturer the test is performed with an average efficient State of the Art inverter. The test report comprises total charge efficiency and PV inverter and battery inverter efficiency separately. A tolerance shall be declared for the case that a low or high efficient PV inverter is used from the customer. This approach shall make charge efficiency for AC and DC coupled systems comparable.

The MPPT, conversion and overall charge efficiency is evaluated basically in the same way as feed-in efficiency according EN-50530. The power input is PV generated power, the output DC battery charge power. No load is active during the procedure and PV power is limited that no additional feed-in occurs during the measurement period T_M. The overall efficiency is defined according Equation 4.4 for static (steady-state) evaluation and Equation 4.5 can be

used for profiles with dynamic changing PV input (MPP power provided by the PV simulator) during a specific test sequence.

$$\eta_{\text{PV-Charge,conv}} = \frac{\sum_{i=1}^{n} P_{\text{Bat,charge},i} \cdot \Delta T_i}{\sum_{i=1}^{n} (P_{\text{PVS,DC},i}) \cdot \Delta T_i} \tag{4.9}$$

$$\eta_{\text{PV-Charge,t,stat}} = \frac{\sum_{i=1}^{n} P_{\text{Bat,charge},i} \cdot \Delta T_i}{P_{\text{PVS,MPP}} \cdot T_{\text{M}}} \tag{4.10}$$

$$\eta_{\text{PV-Charge,t,dyn}} = \frac{\sum_{i=1}^{n} P_{\text{Bat,charge},i} \cdot \Delta T_i}{\sum_{i=1}^{m} P_{\text{PVS,MPP},j} \cdot \Delta T_j} \tag{4.11}$$

Where:

$$P_{\text{POC-AC,export},i} = 0 \text{ No feed-in shall occur during evaluation of charge efficiency}$$

The static efficiency is evaluated only at $V_{\text{MPP,r}}$. It does not seem necessary to test charge efficiency for different DC input levels, because its influence is already evaluated for feed-in efficiency. The power levels set by the PV simulator are recommended as follows: 5, 10, 20, 30, 50, 60 ,70 ,80, 90 100% of $P_{\text{PVS,MPP(max,charge)}}$. Similar to the weighted European MPPT efficiency, a weighted charge efficiency should be introduced. Assuming a basic charge strategy and an empty battery in the morning the battery starts charging when PV power exceeds the electrical demand. The battery capacity and concurrency between PV generation (as function of the PV generator size) and electrical demand determines the charge time. With longer charge time the PV profile and battery DC charge profile changes. Further investigation of measurement data of PV-BESS installed in the field is necessary if such an approach is possible.

Charge efficiency may be influenced by the battery voltage as function of SOC and charge power. For the design of an automatic test procedure with the only adjustable parameters of PV and load power it is not feasible to determine the partial load efficiency exactly at a predefined battery voltage level. This would increase the test effort enormous, as the battery voltage is not only a function of the SOC but furthermore of the charge/discharge current. The influence of the SOC to the charge efficiency of the PCS is determinable during the the RTE test procedure (Section:4.3). The battery is charged with rated power ($P_{\text{PVS,MPP(max,charge)}}$ at $V_{\text{MPP,r}}$) from fully discharged to a fully charged battery state. It can be used as a first indicator if charge efficiency differs between low and high SOC levels. It does not provide an efficiency evaluation at all desired power levels from 10 to 100% of rated charge power.

The following options could be an approach for charge efficiency evaluation at several power levels:

Option 1

Full and partial load efficiency evaluation during a battery charge from fully discharged to fully charged using a iterating stair profile and changing power levels. The evaluation of the efficiency is performed with the described stair profile sequence for feed-in efficiency (Figure 4.4) within the measurement period T_{Meas}. The time T_{Prepare} must allow the system to achieve the new set-point for steady-state operation. The average time can be estimated within the control test, described in Section 4.4. Figure 4.5 shows in a simulation approach the influence battery voltage during the sequence. The voltage profile differs if the stair profile starts with high or low power.

Option 2

Full and partial load efficiency evaluation within several SOC/battery voltage ranges. Table 4.6 shows a possible approach.

TABLE 4.6: PCS charge efficiency evaluation

SOC range	$V_{\text{MPP,r}}$ | **P1,P2...Pn**
$SOC_{\text{Start}} = 85\%$ and $(80\% < SOC_{j=3} < 90\%)$	$\eta_{\text{PV-Charge}}(V_{\text{MPP,r}}, SOC_{j=3}, P_{i=1} \ldots P_n)$
$SOC_{\text{Start}} = 50\%$ and $(45\% < SOC_{j=2} < 55\%)$	$\eta_{\text{PV-Charge}}V_{\text{MPP,r}}, SOC_{j=2}, P_{i=1} \ldots P_n)$
$SOC_{\text{Start}} = 0\%$ and $(0\% < SOC_{j=3} < 10\%)$	$\eta_{\text{PV-Charge}}(V_{\text{MPP,r}}, SOC_{j=1}, P_{i=1} \ldots P_n)$

The average charge efficiency $\eta_{\text{PV-Charge,AVG}}$ over the entire SOC is given according Equation 4.12.

$$\eta_{\text{PV-Charge,AVG}} = \frac{1}{3} \cdot \sum_{j=1}^{3} \eta_{\text{PV-Charge}}(V_{\text{MPP,r}}, SOC_j, P_i) \quad (4.12)$$

It is required to keep the voltage and SOC in the specified range. This can be done with an iterating charge/discharge profile illustrated in Figure 4.6).

Option 3

Full and partial load efficiency evaluation only at one SOC range. For instance at a fully discharged battery e.g. $<5\%$ SOC
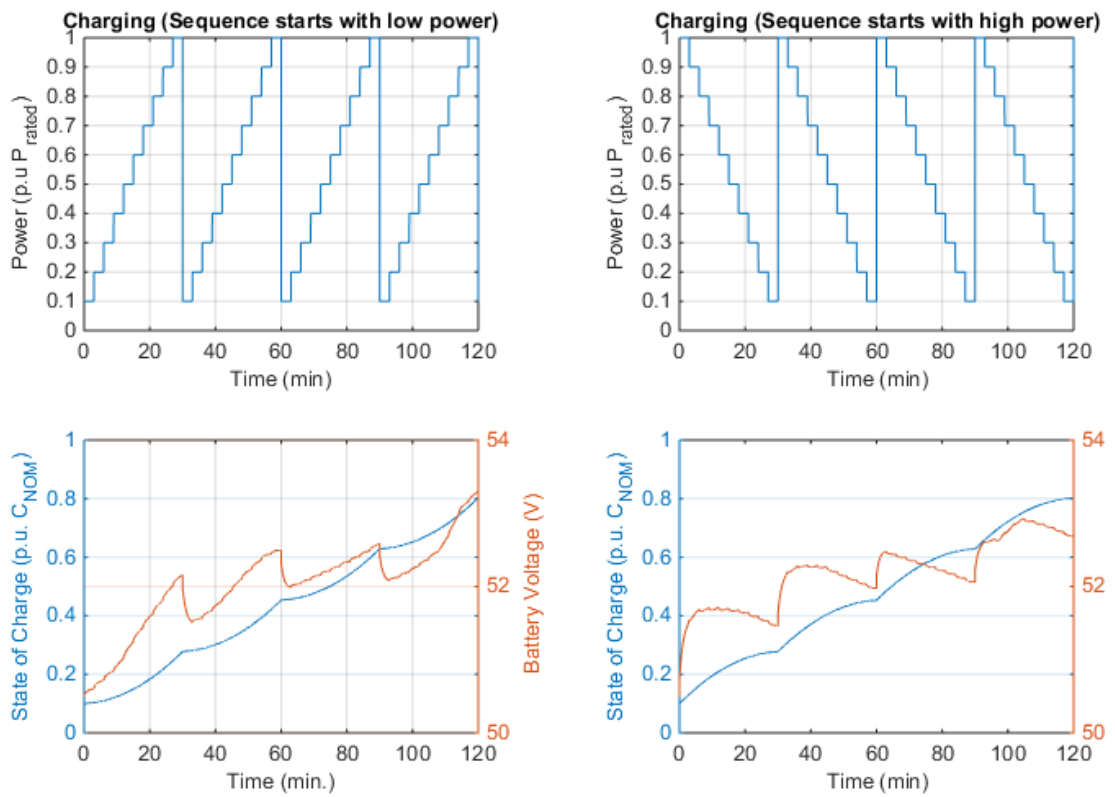
FIGURE 4.5: Simulation for a LiFePO4 battery (51V/30 Ah):Battery charge (20 to 90% SOC) using a stair profile.
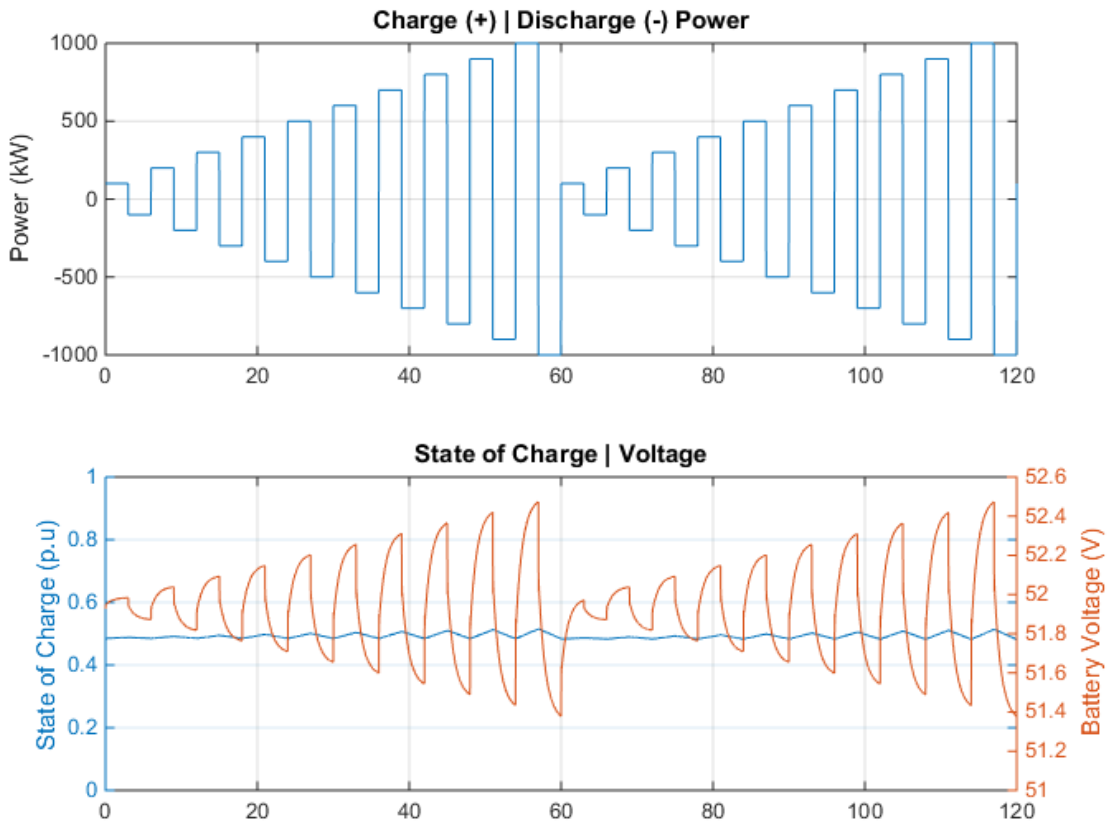
FIGURE 4.6: Simulation for a LiFePO4 battery (51V/ 30 Ah): Charge/discharge profile, with the aim to keep the SOC level constant. Note: The simulation shows idealistic behavior (no time delay until charge/discharge).

4.2.3 Discharge Efficiency

The discharge efficiency is evaluated basically according to Equation 3.34 in Section 3.6 . The equation is changed, that not the load power but the power at the POC-AC is used (Equation 4.13). This convention is useful if in further development of test procedures discharge power of a PV-BESS is adjustable by direct commands and no load is required to start the charge/discharge process. This is already possible for several commercial available systems. Moreover load power can exceed the maximum battery discharge power and imported energy from the grid is not considered in the calculation.

$$\eta_{\text{Discharge}}(P_{\text{Load}}) = \frac{\sum_{i=1}^{n} P_{\text{POC-AC,export},i} \cdot \Delta T_i}{\sum_{i=1}^{n} P_{\text{Bat,discharge},i} \cdot \Delta T_i} \tag{4.13}$$

The test is performed so that the maximum adjusted load power can be covered entirely by battery discharge power (See Pretest Section 4.1.3) and no grid import occurs during the measurement time. The test is performed at several partial load power levels (recommended: P_{Load}: 5, 10, 20, 30, 40, 50, 60, 70 ,80 ,100% of $P_{\text{Load(max.discharge)}}$). In addition it is recommended to perform the test at several load power levels, which are frequently observed in single family households. This is proposed because efficiency is decreased especially at low power levels. If normalized power is used systems with a high power rating may not be tested for real field conditions. For instance the test could be performed at P_{Load}: 250 W, 500 W, 1000 W, 1500 W 2000 W .... A weighted discharge efficiency for these power levels could be used to represent overall efficiency for single family households better. It must consider the individual size of the PV generator (peak power) because discharge power is influenced by the direct matched demand. Further investigation and analyses of household profiles is necessary if such an approach is feasible.

If the discharge efficiency is influenced by the SOC, the RTE can be estimated first during several full discharge cycles within the RTE test procedure, as described in Section 4.3. It does not allow PCS discharge efficiency evaluation for all desired power levels. An automatically performable test sequence can be designed similar to one way charge efficiency evaluation.

Option 1

> Full and partial load efficiency evaluation during a battery discharge from fully discharged to fully charged using a iterating stair profile and changing power levels. The measurement is done in steady state after the demand is covered entirely from battery discharge power within the measurement period T_{Meas}. Figure 4.7 shows the influence if discharging the battery starts with maximum or minimum power level.

Option 2

> Full and partial load discharge efficiency evaluation within several SOC voltage ranges. (See Option 3 PCS charge efficiency evaluation)

Option 3

> The test is performed only within one SOC range.
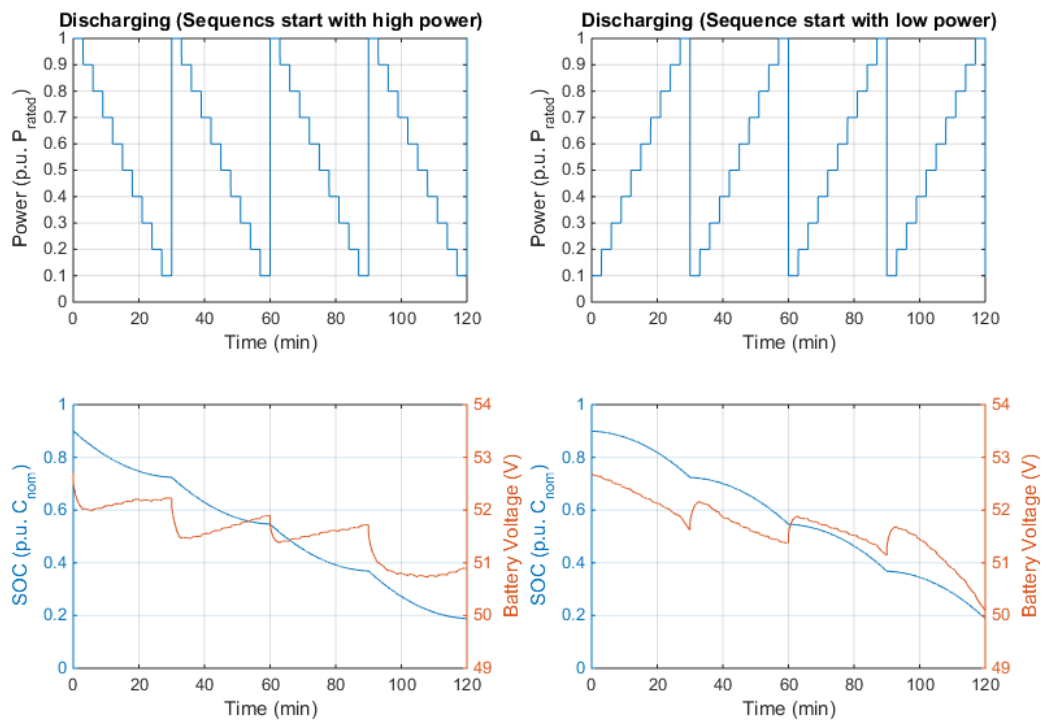
FIGURE 4.7: Simulation for a LiFePO4 battery (51V/30 Ah): Battery discharge (90 to 20% SOC) using using a stair profile.

4.2.4 Example of Test Results

Test results for charge/discharge efficiency of a DC hybrid coupled low voltage battery PV-BESS are shown. The charge/discharge efficiency was determined during a full charge/discharge using an iterating stair profile (Option 3). The charge efficiency is illustrated in Figure 4.8 as function of power and the difference between DC link and battery voltage. It is determined at V_{MPP}. The power is normalized to rated charge power and the difference between DC link and battery voltage is expressed by using a color map.
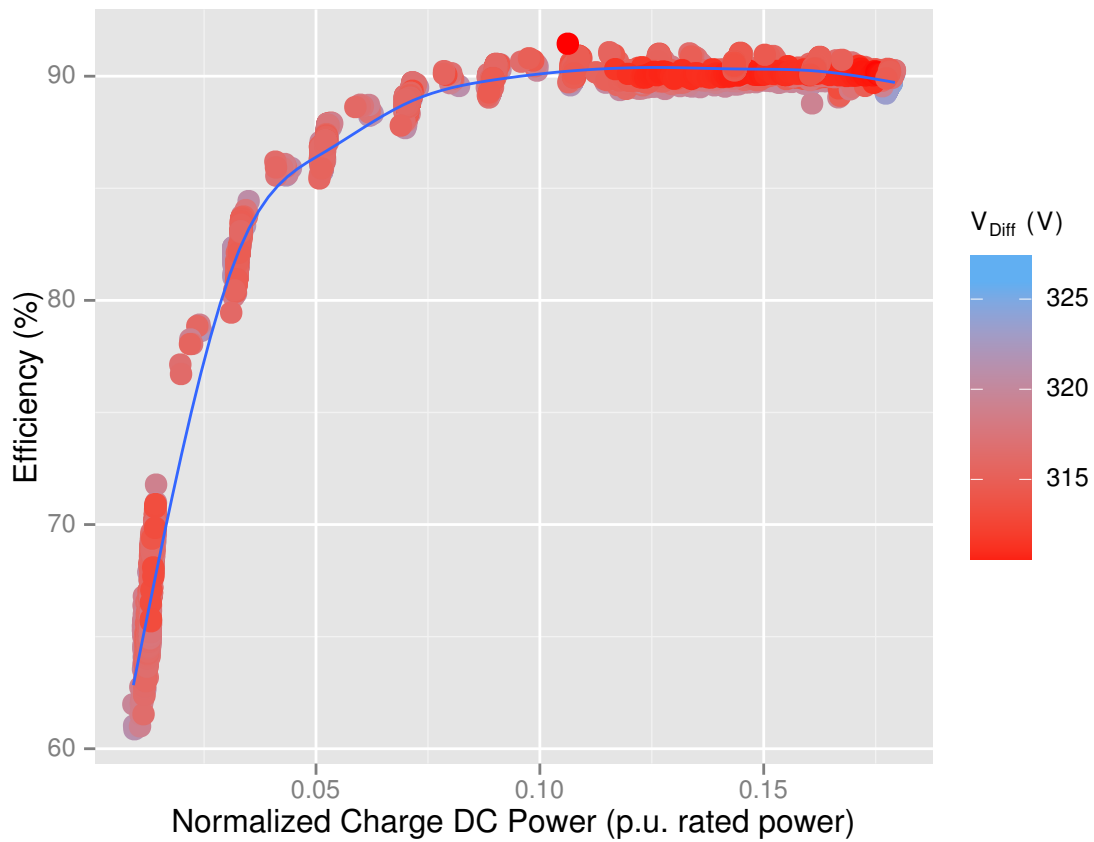
FIGURE 4.8: Charge conversion efficiency of a DC hybrid coupled system LVB-BESS (V_{Diff} = Difference between inverter DC link and battery voltage).

The discharge efficiency is illustrated in Figure 4.9. Below 10 % of P_{rated} efficiency decreases strongly. Load coverage in the area below 200 W is quite inefficient. Figure 4.10 shows only values >80%. The efficiency deviation for different voltage levels is approx. $\pm$ 1.5 % to the mean efficiency at a specific power level. The difference between DC link and battery voltage is expressed by using a color map.
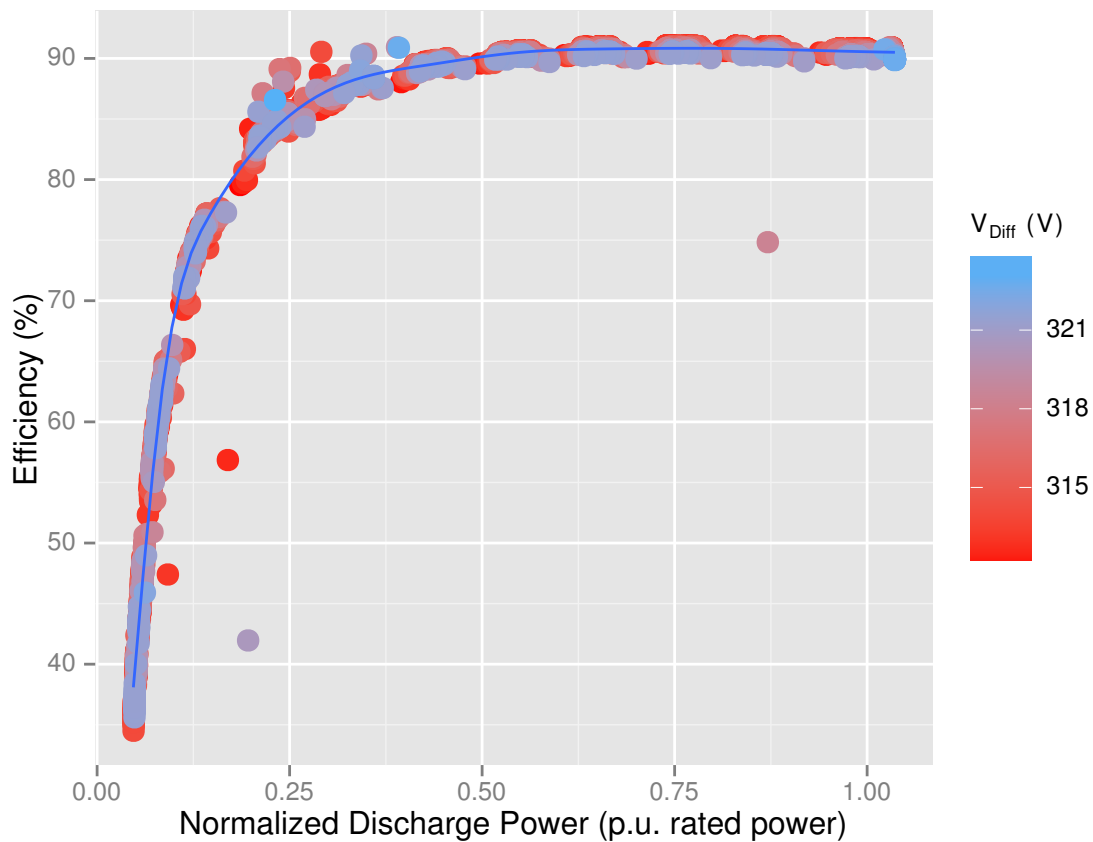
FIGURE 4.9: Discharge efficiency to the AC link of a DC hybrid coupled system LVB-BESS (V_{Diff} = Difference between inverter DC link and battery voltage).
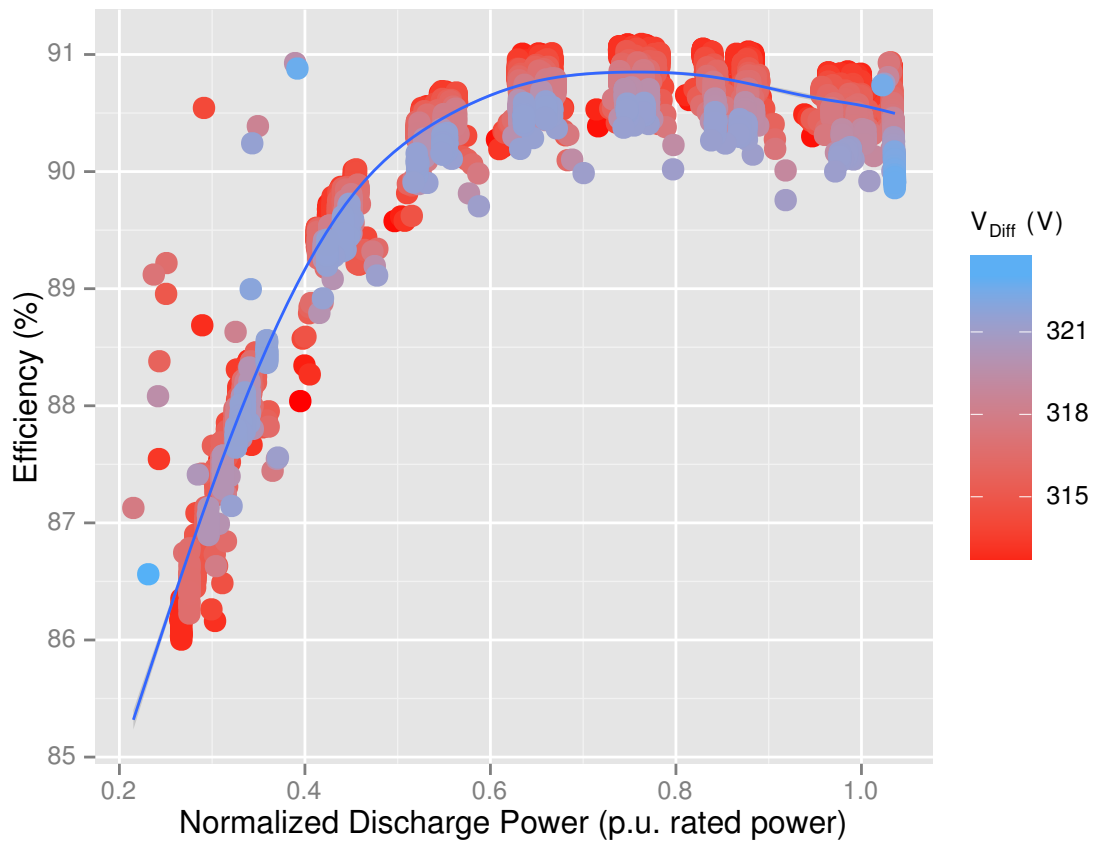
FIGURE 4.10: Discharge efficiency to the AC link of a DC hybrid coupled system LVB-BESS (V_{Diff} = Difference between inverter DC link and battery voltage)

Efficiency was determined in detail for components within the DC hybrid coupled system. The evaluation does not include the MPPT efficiency. The tested system did not provide required measurements within the DC link when it operated at MPP. If the system did not operate in the MPP, current measurements could be done by using current transformers at bypass lines. If it operated at MPP the current was lead over conductor tracks at the PCB. The system showed problems at several input voltage levels, where MPP tracking efficiency was <90%. Figure 4.11 shows feed-in, charge and discharge efficiency. For comparison PV charge and feed-in efficiency is determined at the same absolute power levels. Feed-in power is normalized to rated charge power. Therefore it is only shown at about the half of maximum possible feed-in power in the efficiency chart. If the measurement allowed its determination, AC/DC and DC/DC (feed-in: input boost converter | discharge: DC/DC charge controller) efficiency is given.
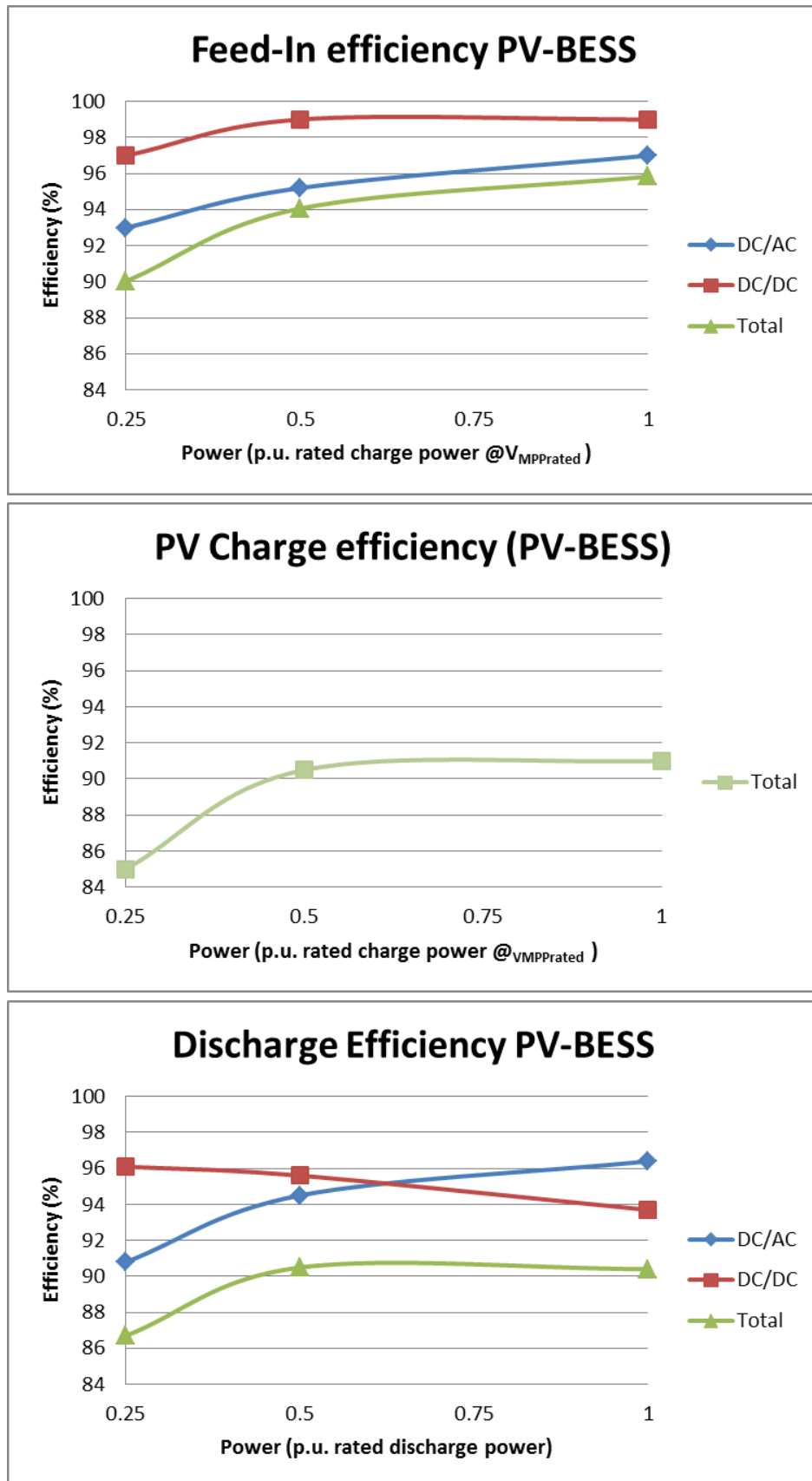
FIGURE 4.11: Static conversion efficiency for a DC hybrid coupled system. (The test was performed at a mid SOC range)

In addition the efficiency for charging from the grid (AC link) is determined. Theoretically the system could be used as an AC coupled system, if the energy management allows to charge a surplus of local generated AC energy. Figure 4.12 show the efficiency chart.
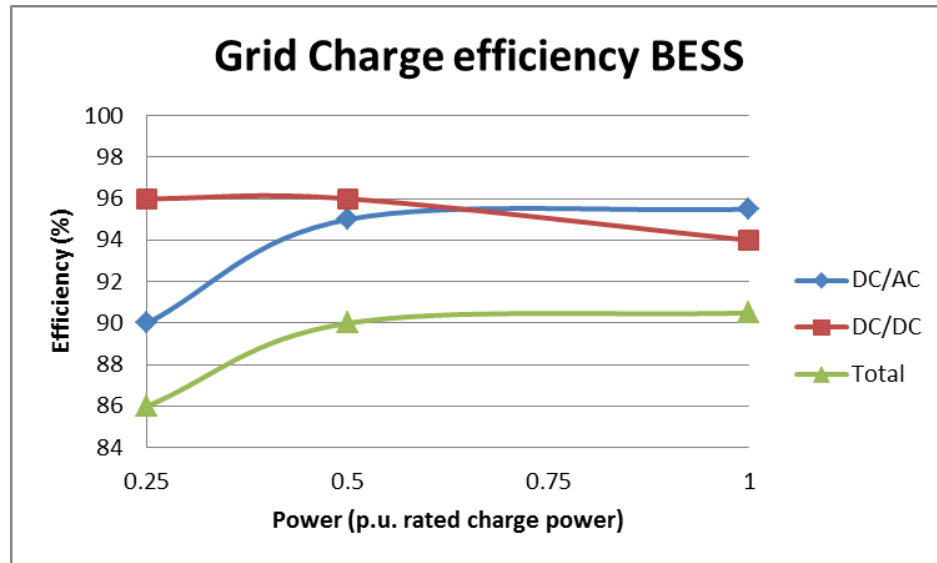
FIGURE 4.12: Grid charge efficiency for a DC hybrid coupled system (Theoretically usable as AC coupled system at this operation mode). The test was performed at a mid SOC range)

4.3   Round Trip Efficiency (PCS and battery)

The round trip efficiency evaluation for the whole PV-BESS follows the described methodology in Section 3.6. It is evaluated by a PV battery charge, followed by a discharge to supply AC loads. The measurement point $\mathrm{MP_{BAT}}$ and therefore intervention in the PV-BESS is not necessarily required. It is only required if a separation in PCS and battery efficiency is done. RTE can be evaluated within two sequence types.

- RTE Option 1: Full charge/discharge cycles performed with constant power levels.
- RTE Option 2: Specific duty cycle

This section describes basically Option 1. The efficiency evaluation for a specific duty cycle (Option 2) is done in principle identically, with the only difference that the battery power changes dynamically (See: System Performance Evaluation Section 4.6).

4.3.1 RTE Sequence

The test starts with a fully charged or discharged battery, which is brought to the initial test state, according to a predefined charge/discharge procedure. The sequence is controlled by adjustments of PV Simulator and load power. No feedback signal of the battery current/voltage/SOC is used to control the input profiles. The sequence consists of full constant charge/discharge cycles. Figure 4.13 shows an example for three RTE evaluation at three discharge power levels. A single cycle is defined by DC battery charge power as function of MPP power of the PV simulator and DC battery discharge power as function of load power. Table 4.7 shows the chronological sequence of one cycle. The test can be started in principle with fully discharged or fully charged battery.

TABLE 4.7: RTE test sequence

Phase	Description	Time
Phase 1	PV generation, battery charge	T_1 to T_3
Phase 2	Active standby	T_3 to T_4
Phase 3	Load, battery discharge	T_4 to T_7
Phase 4	Active Standby	T_7 to T_8

The RTE is evaluated for the entire test sequence and an iteration of cycles ($\eta_{X=1}, \eta_{X=2} \cdots \eta_{X=m}$) with the same charge/discharge power. The first cycle of each iteration is not used for the calculation, because it was observed that efficiency is influenced by the previous cycle charge or discharge power. For instance discharging is terminated earlier at a high power discharge or charge.

Test Sequence: Input Profile PV Simulator / Load

Overall RTE efficiency η_{Total}

Iteration i = 1	Iteration i = 2	Iteration i = 3 ...
$\eta_{i=1}$	$\eta_{i=2}$	

$P_{\text{PVS-MPPT}}$ (p.u. $P_{\text{MPPT(charge,r)}}$)

1
0.8
0.6
04
02
0

P_{Load} (p.u. $P_{\text{Load(discharge,r)}}$)

0.2
0.4
0.6
0.8
1.0

Time

Detail: Input Profile and Battery power

$P_{\text{PVS-MPPT}}$ (kW)
$P_{\text{Bat-DC(charge)}}$ (kW)

T_1 | T_{Gen} | T_3 | T_{Pause1} | T_4 | T_{Load} | T_7 | T_{Pause2} | T_8

PV generation | No PV No Load | Load activated | No PV No Load

PCS charging loss

0

PCS discharging loss

P_{Load} (kW)
$P_{\text{Bat-DC(discharge)}}$ (kW)

$T_{\text{M(charge)}}$ | $T_{\text{M(discharge)}}$

Active battery charge | Bat. rest time | Active discharge | Bat. rest time

T_1 | T_2 | T_5 | T_6

State of Charge

100%

0%

Time

$$\eta_{\text{RTE,PV-BESS}} = \frac{E_{\text{Load}\leftarrow\text{Bat}}}{E_{\text{PV}\rightarrow\text{Bat}}} \qquad \eta_{\text{RTE,BAT}} = \frac{E_{\text{Bat-DC (discharged)}}}{E_{\text{Bat-DC (charged)}}} \qquad \eta_{\text{RTE,PCS}} = \frac{\eta_{\text{RTE,PV-BESS}}}{\eta_{\text{RTE,BAT}}}$$

FIGURE 4.13: Example of round trip efficiency evaluation with varying charge/discharge power and iterations of single cycles

The time the PV and load power is applied is determined by one of following options:

- Manufacturer provides information about charge/discharge time at rated power.
- Pre-test determining rated charge/discharge time
- Pre-simulation or Pre-calculation

If a pre-calculation is done the theoretical charge time is calculated by the relation between net energy capacity and required MPP power for rated DC power battery charge (Equation 4.15). The discharge time is calculated according to Equation 4.17. The calculated charge time is increased by a certain percentage (e.g. 15%) to ensure a full charge is preformed (Charge time is e.g increased due to battery losses and increased PCS losses at partial load power). The discharge time decreases with higher PCS losses because more energy is drawn at the battery DC terminals. Nonetheless it is recommended to prolongate the theoretical calculated time, ensuring a full battery discharge. Between battery charge and discharge the system rests in an active standby phase (No PV generation, no load). The time is defined as a constant value (recommended 30 min to three hours) or as percentage to the previous charge/discharge power level. Higher power requires longer time for battery relaxation.

$$T_{\text{PV,r}} = \frac{\text{E}_{\text{NET}}}{P_{\text{BAT}}(P_{\text{PVS,MPP(max,charge)}})} \cdot 1.15 \tag{4.14}$$

$$T_{\text{PV}} = \frac{T_{\text{Gen,r}} \cdot P_{\text{PVS,MPP,x-cycle}}}{P_{\text{PVS,MPP(max,charge)}}} \tag{4.15}$$

$$T_{\text{Load,r}} = \frac{\text{E}_{\text{NET}}}{P_{\text{BAT}}(P_{\text{Load(max.discharge)}})} \cdot 1.15 \tag{4.16}$$

$$T_{\text{Load}} = \frac{T_{\text{Load,r}} \cdot P_{\text{PVS,MPP,x-cycle}}}{P_{\text{PVS,MPP(max,charge)}}} \tag{4.17}$$

The RTE is determined as ratio between energy output during $T_{\text{M,discharge}}$ and input during $T_{\text{M,charge}}$. If efficiency is evaluated over more cycles the total measurement time is used. The Round Trip Battery Efficiency is calculated according to Equation 4.18.

$$\eta_{\text{RTE,Bat}} = \frac{\sum_{i=1}^{n} P_{\text{Bat,discharge},i} \cdot \Delta T_i(T_{\text{M,discharge}})}{\sum_{i=1}^{n} P_{\text{Bat,charge},i} \cdot \Delta T_i(T_{\text{M,charge}})} \tag{4.18}$$

Where:

$\eta_{\text{RTE,Bat}}$: Round trip efficiency battery

$P_{\text{Bat,charge},i}$: Sampled value of the battery charge power within TM,charge

$P_{\text{Bat,charge},i}$: Sampled value of the battery charge power within TM,discharge $P_{\text{POC-AC,export},i}$

n : amount of measurement samples

ΔT_i : period between two subsequent measurement samples

The rountrip conversion efficiency is determined according Equation 4.19 and overall PV-BESS round trip efficiency according Equation 4.20.

$$\eta_{\text{RTE,PV-BESS,conv}} = \frac{\sum_{i=1}^{n} P_{\text{POC-AC,export},i} \cdot \Delta T_i(T_{\text{M,discharge}})}{\sum_{i=1}^{n} P_{\text{PVS,DC},i} \cdot \Delta T_i(T_{\text{M,charge}})} \tag{4.19}$$

$$\eta_{\text{RTE,PV-BESS}} = \frac{\sum_{i=1}^{n} P_{\text{POC-AC,export},i}(T_{\text{M,discharge}})}{P_{\text{PVS,MPP}} \cdot T_{\text{M,charge}}} \tag{4.20}$$

Where:

$\eta_{\text{RTE,PV-BESS}}$: round trip efficiency PV-BESS including PCS and battery efficiency

$\eta_{\text{RTE,PV-BESS}}$: round trip efficiency PV-BESS including MPPT, PCS and battery efficiency

$P_{\text{POC-AC,export},i}$: Sampled value of the PV-BESS output power at POC-AC TM,discharge

$P_{\text{PVS,MPP,x-cycle}}$: Provided MPP power from the PV simulator

The round trip efficiency of the Power Conversion System only is determined by Equation 4.21.

$$\eta_{\text{RTE,PCS}} = \frac{\eta_{\text{RTE,PV-BESS}}}{\eta_{\text{RTE,Bat}}} \tag{4.21}$$

It is useful to additionally determine the BCE. It gives insight about the accuracy of the SOC estimation. It was observed during testing that for single cycles the BCE was sometimes higher than 100%. This means more ampere-hours were discharged as charged. The BMS compensated the missing charge usually within the next performed charge/discharge cycles. It shows the importance that not only a single cycle is considered in the efficiency evaluation but moreover the average efficiency of more than one cycle.

4.3.2 Example of Test Results

A test was performed for a lithium-ion based DC coupled PV-BESS. The test sequence is shown in Figure 4.14. Each cycle is charged with maximum power. The test was performed at 100 % 50% and 25% of rated discharge power. Each unique cycle is iterated four times for reproducibility and minimizing errors, resulting from tolerances in SOC estimation. The illustration shows losses during charge and discharge. It is seen that after the end of charge the battery is discharged with low power during feed-in.
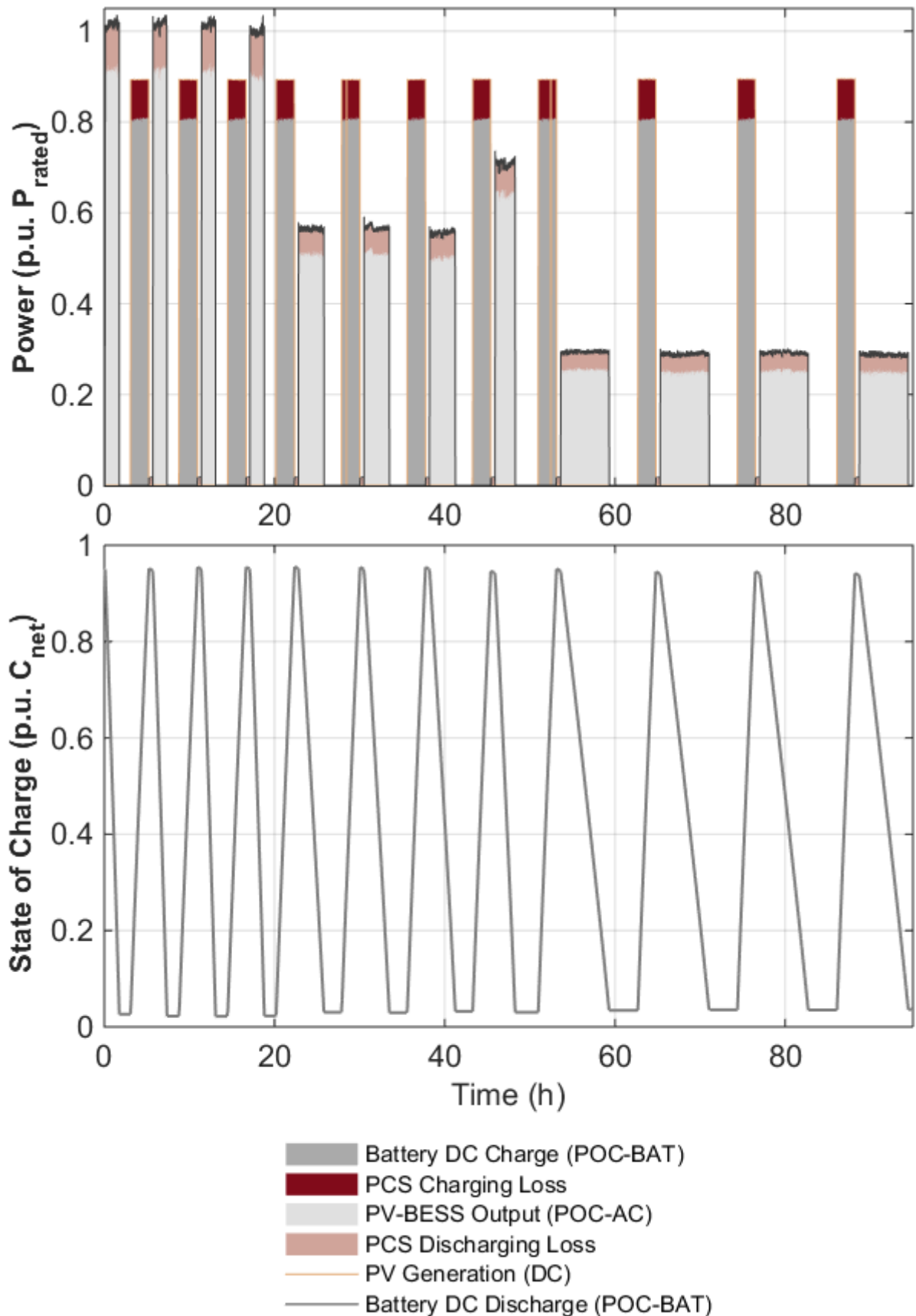
FIGURE 4.14: Performed sequence for RTE evaluation at a DC hybrid coupled LVBS (The load at the 4th cycle at $0.5 \cdot P_{rated}$ resulted from an error in the automatic load control.)

The battery efficiency is very high and increases slightly with lower discharge power (average C_{rate}: 0.5, 0.25, 0.125). The overall PV-BESS efficiency is best at $P/2$. At $P/4$ it is lower due to the low efficiency of the PCS at this operating point.
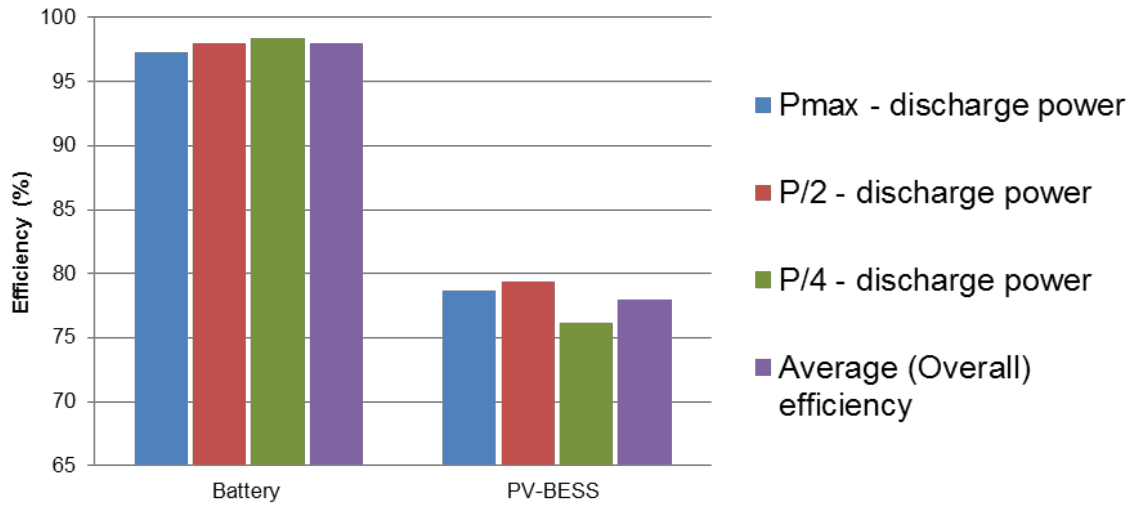
FIGURE 4.15: Results of the RTE of the cycle test in Figure 4.14 for a DC coupled, lithium based LVBS. (MPPT efficiency not considered)

The RTE of the PV-BESS is compared in a theoretical approach with the product of the determined one way efficiency and estimated battery RTE for the specific power levels. PV-BESS Round Trip Efficiency is given between 70 and 80%. Figure 4.16 shows the result. Deviations to the result of the cycle test are content of further investigation. One reason might be, that the cycle test determines One Way PCS efficiency for the entire SOC range, whereas the theoretical approach evaluates efficiency only for one point of battery voltage.
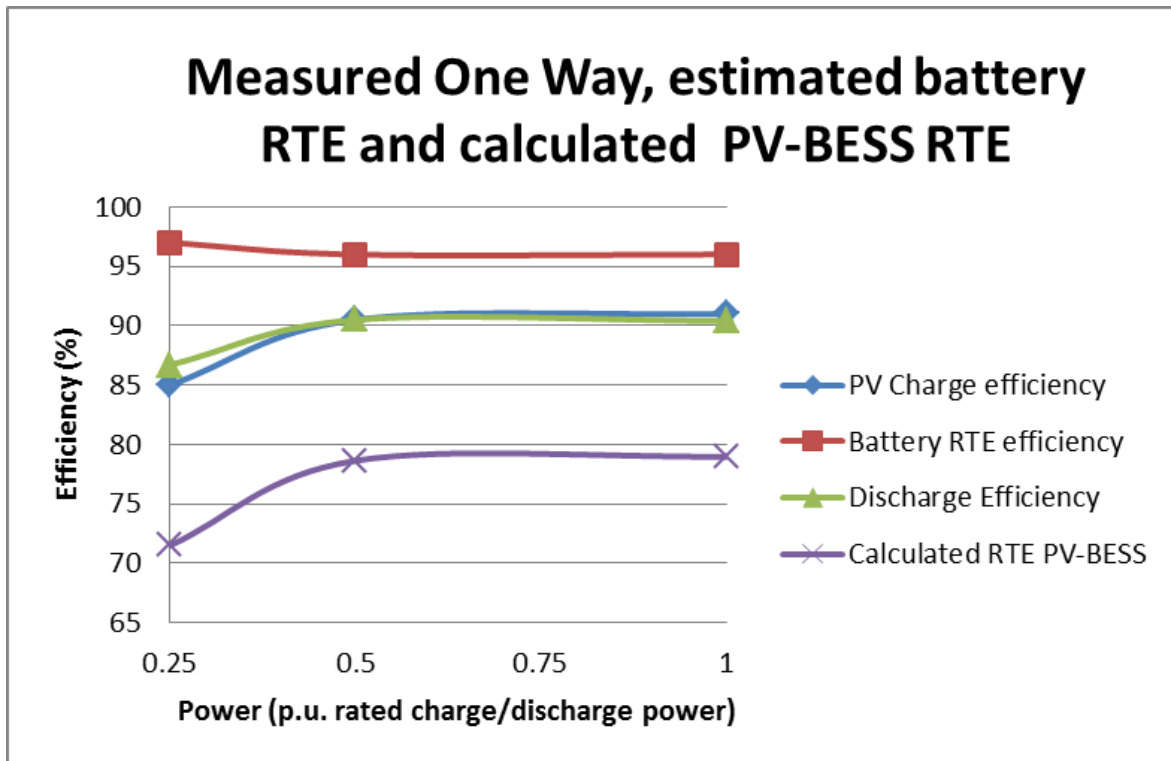
FIGURE 4.16: PV-BESS RTE, as result of determined One Way charge/discharge efficiency and estimated battery RTE for the specific power level

Several full cycle tests were performed for an AC coupled system with a 1.5 kWh/30 Ah lithium-ion (LFP) based battery connected to a single-phase battery converter. The BMS allowed a discharge rate of max. 1C for test purpose (mostly limited in PV-BESS below 0.75C for increased lifetime). The charge process is done by a CC/CV procedure. An example of a performed sequence is illustrated in Figure 4.17. It shows that the the amount of charged and discharged ampere-hours is not identical for each single cycle. It can be seen at the SOC, which is determined by the coulomb-counting method (charged/discharged Ah are normalized to the battery capacity). The battery is discharged with 30 A (1C) constant current and charged with 28 A constant current (until CV phase) at the first two cycles . The highest amount of ampere-hours was charged and discharged at the third cycle x=3 at 15 A (0.5C) charge/discharge power. This is an important insight for efficiency evaluation, as efficiency would not be properly calculated if the discharged energy from cycle x=3 and charged energy from cycle x=2 is set in relation (analysis of charge/discharge sequence instead of discharge/charge sequence for this specific case). An indicator is the coulomb efficiency because it is $\eta_C = Q_{\text{discharged,x=3}}/Q_{\text{charged,x=2}}$ >100% for this specific charge/discharge cycle.
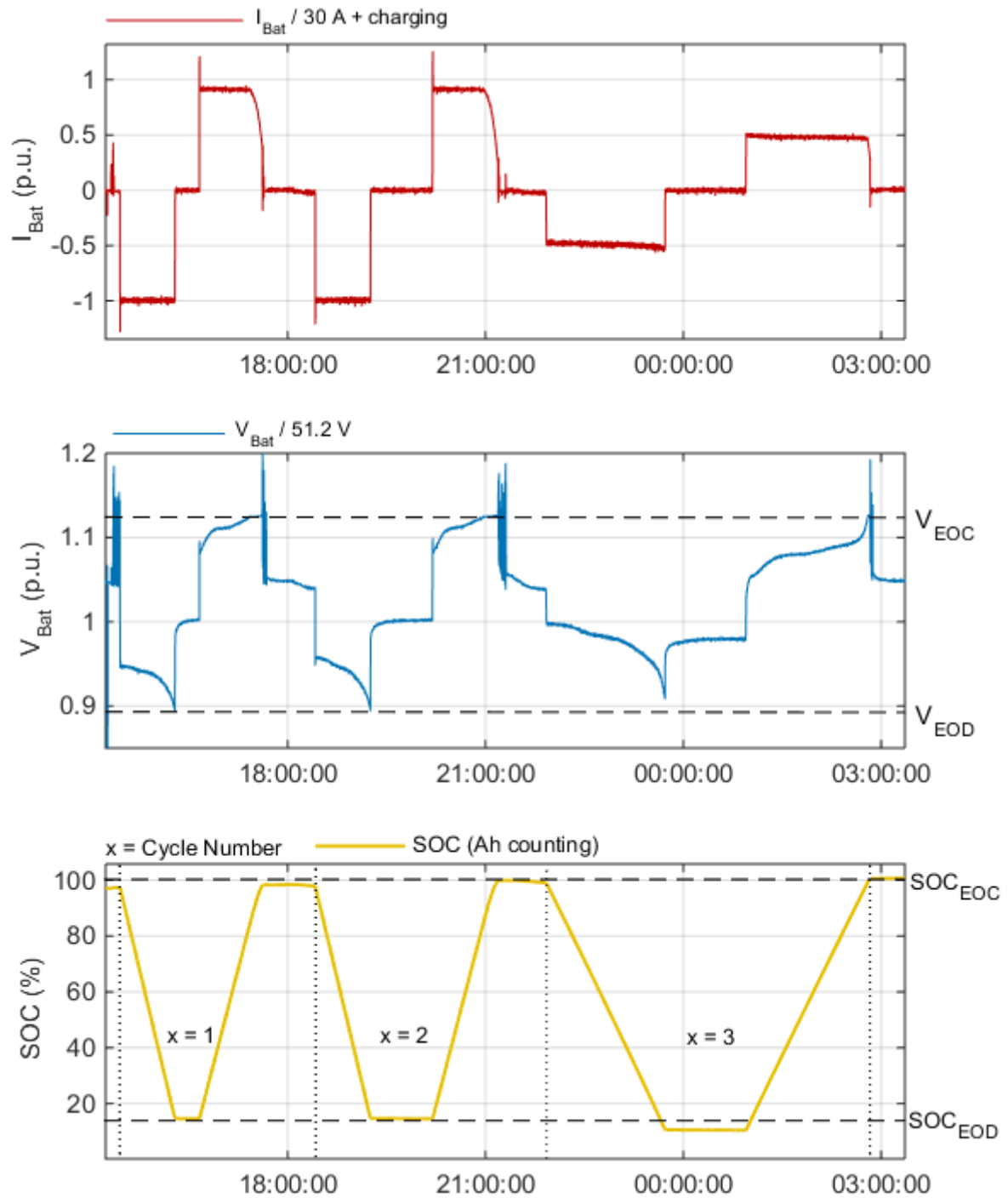
FIGURE 4.17: Discharge/Charge Sequence for RTE evaluation

Figure 4.18 shows the results for this AC coupled system. The battery efficiency was determined between 89% and 91% for several cycles at a 0.5C discharge rate. It decreases strongly at a C_{rate} of 1C. The PCS (single phase PV inverter and battery inverter) operated at a power of approximately 30% and 15% normalized to 4.6 kW. The battery inverter efficiency was relative constant within this range. The overall PV-BESS efficiency is 69%. Assuming a

higher battery efficiency (97% as for the DC coupled system) PV-BESS efficiency would be increased to 74%, which is close to the efficiency of the tested DC coupled system.
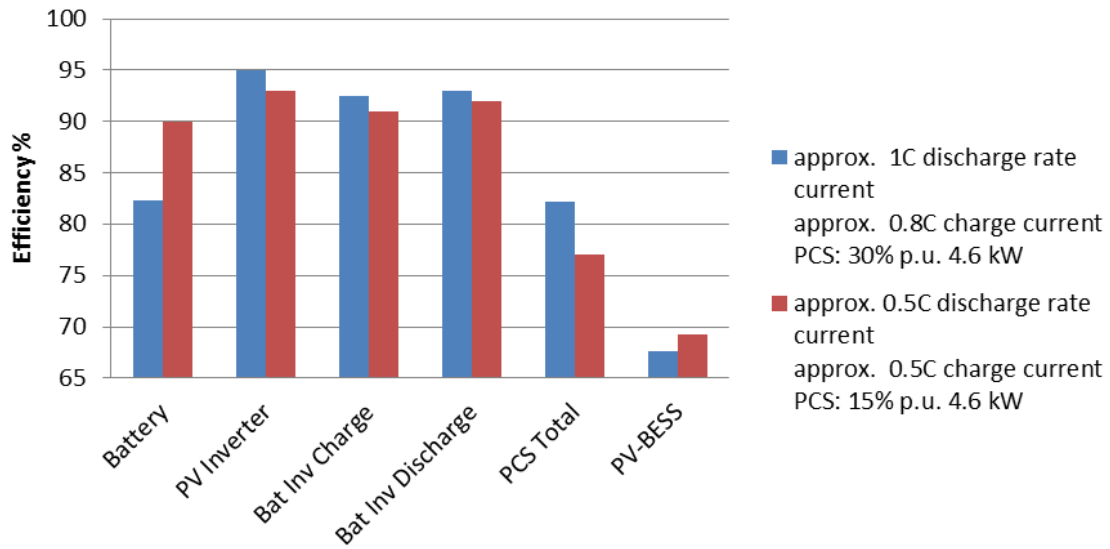
FIGURE 4.18: Results RTE for a AC coupled, lithium based LVBS (MPPT efficiency not considered)

4.4 Performance Evaluation Control System

The test procedure shall determine the speed and accuracy of the PV-BESS to dynamic changes of PV generation or load. Synthetic input profiles are generated as step, ramp or stair-profiles. The analyses can be done in the time domain (See methodology Section **??**) or by evaluating the resulting grid import/self-coverage and export/direct use during a specific test sequence. It requires that the requested charge/discharge power during the sequence is not limited by SOC or maximum battery power limitations. The maximum power for the sequence is defined in the pretest.

- $P_{\mathrm{PV,MPP}} < P_{\mathrm{PVS,MPP(max,charge)}}$
- $P_{\mathrm{Load}} < P_{\mathrm{Load(max.discharge)}}$
- Battery must not be fully charged or discharged

A step response is shown in detail for an AC coupled system in Figure 4.19. The storage system provided operation with a proprietary electricity meter or a D0 compliant smart meter. The test with the D0 smart-meter (orange line) shows oscillations in charge/discharge power. If the proprietary device is used these are not observable. The response time is quite identical

for both tests but the settling time is increased strongly by using the D0 smart-meter. This results in more imported and exported energy into the utility grid.
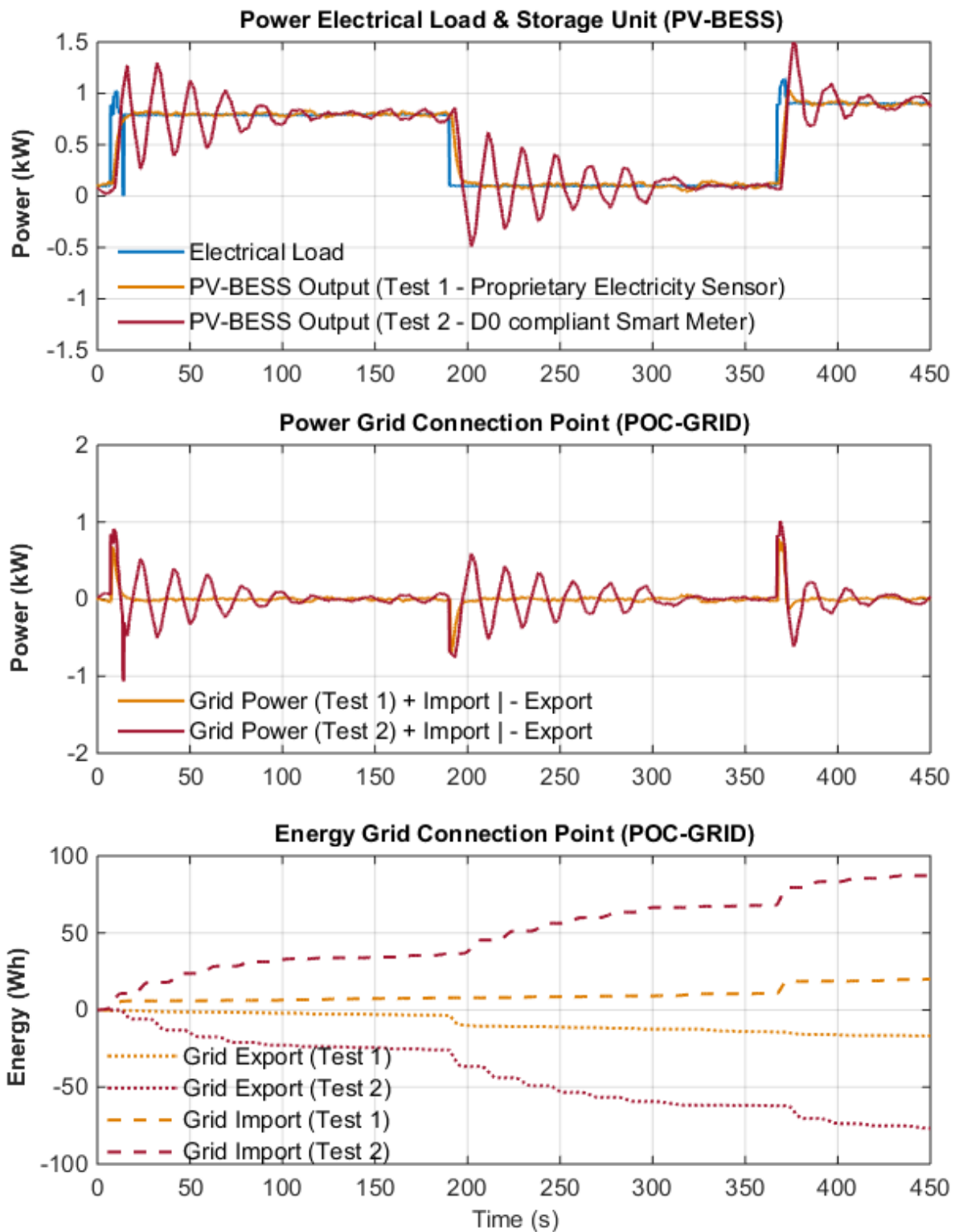
FIGURE 4.19: Step response load for an AC coupled system. Once with the proprietary metering protocol (Test1) and in addition for a D0 smart-meter (Test2) electricity measurement device.

The single load step from 0.1 kW to 0.8 kW is shown in Figure 4.19. The system response is fast for both, the test with the D0 smart-meter and proprietary meter device. The settling time is defined when the PV-BESS output power is kept within 90 an 110% of the load power. For the test with the proprietary device a settling time of six seconds is achieved, the test with the D0 smart meter requires 94 seconds until storage power is within 90 and 110% of load power. The Steady State Error (SSE) for Test 1 is determined by by the oscillations around the set-point in steady state. The maximum deviation of the storage power to the load power for test 1 in steady state is ± 5%. For Test 2 ± 10%.
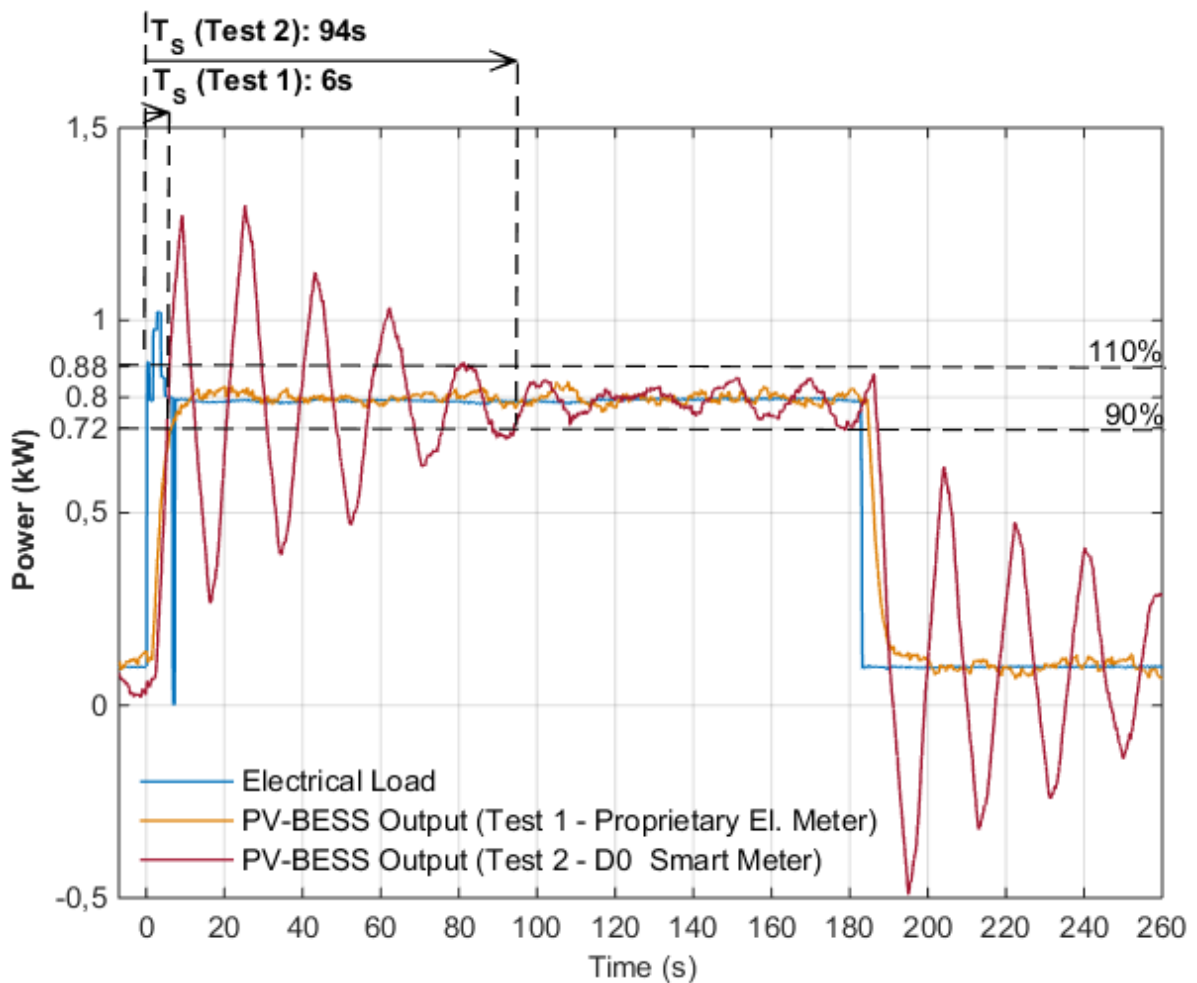
FIGURE 4.20: Step response, comparison proprietary metering protocol and D0 metering device at the same PV-BESS 4.19

.

Figure 4.21 illustrates a sequence with constant PV generation. The load power is controlled that the battery is periodically charged and discharged. The switching period is low at the

beginning of the sequence and decreases at the end of the test. The sequence can be performed in the same way with constant load demand and changing PV irradiation.
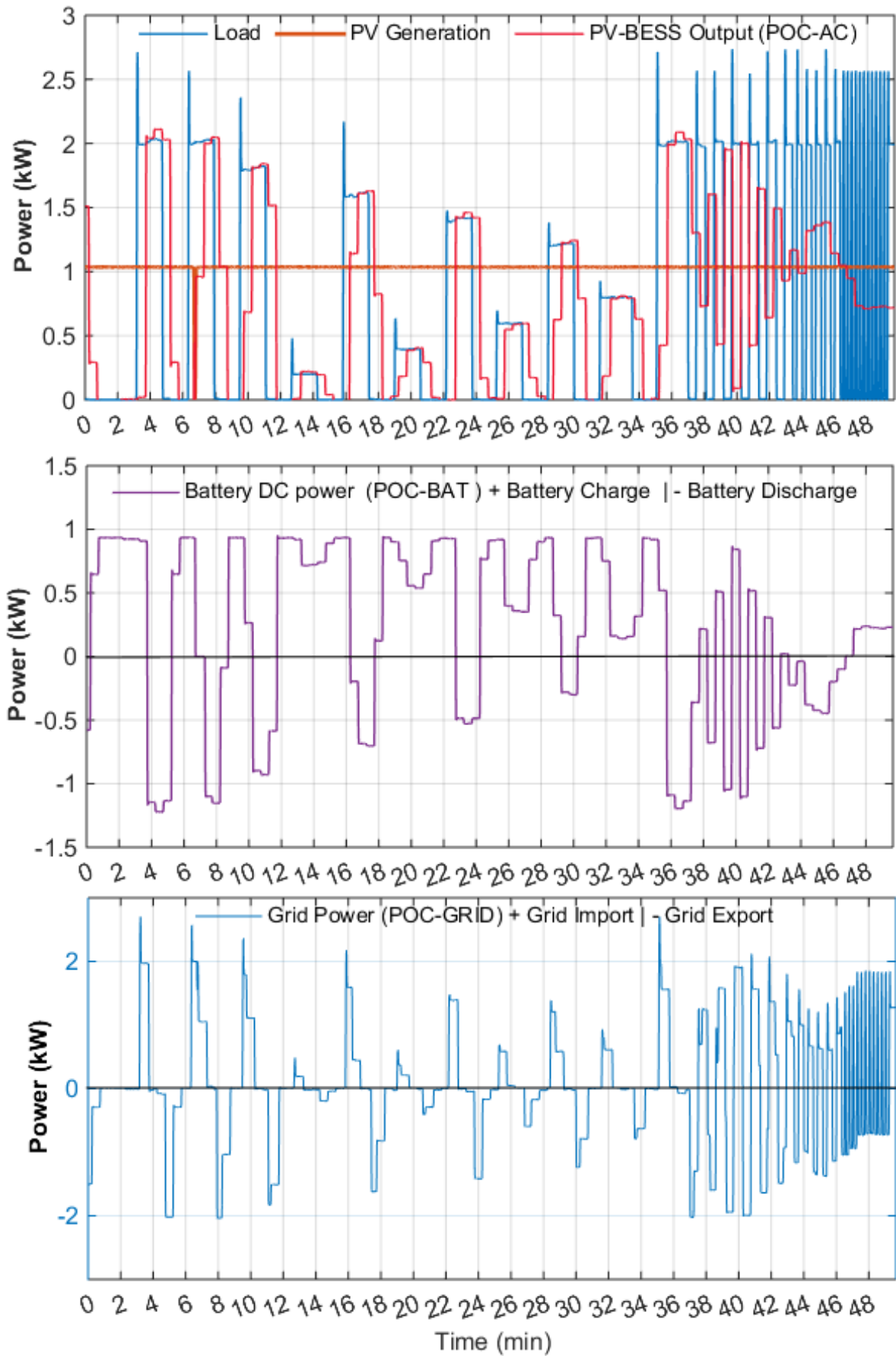
FIGURE 4.21: Step-profile: Emulating surplus and deficit of PV power

The test was performed on a DC hybrid coupled with a D0-smart meter. It takes approximately 5 to 30 seconds until a new set point is reached. The system increases its output power step-wise. At the end of the test, with a 10s switching duty cycle the system does not change it's output power anymore. The battery continuous discharging with constant power.

Figure 4.22 shows an example of a test sequence with dynamically changing input profiles performed for a longer time period. The sequence consists of steps, stair profiles and ramps. The grid exported and imported power result from limited performance of the control system. The performance indicator is given by direct use and self-coverage in Table 4.8 (The calculation of DU (Equation 4.22) and SCV (Equation 4.23) is described in Section 4.6).

TABLE 4.8: Effectiveness of the control system

Energy		(kWh)
$E_{\text{PVS,DC}}$	PV Generation	5.33
E_{Load}	Load	0.51
$E_{\text{Grid,import}}$	Grid Import	4.62
$E_{\text{Grid,export}}$	Grid Export	0.49
Performance Indicator		**(%)**
DU	Direct Use	90.4
SC	Self coverage	89.5
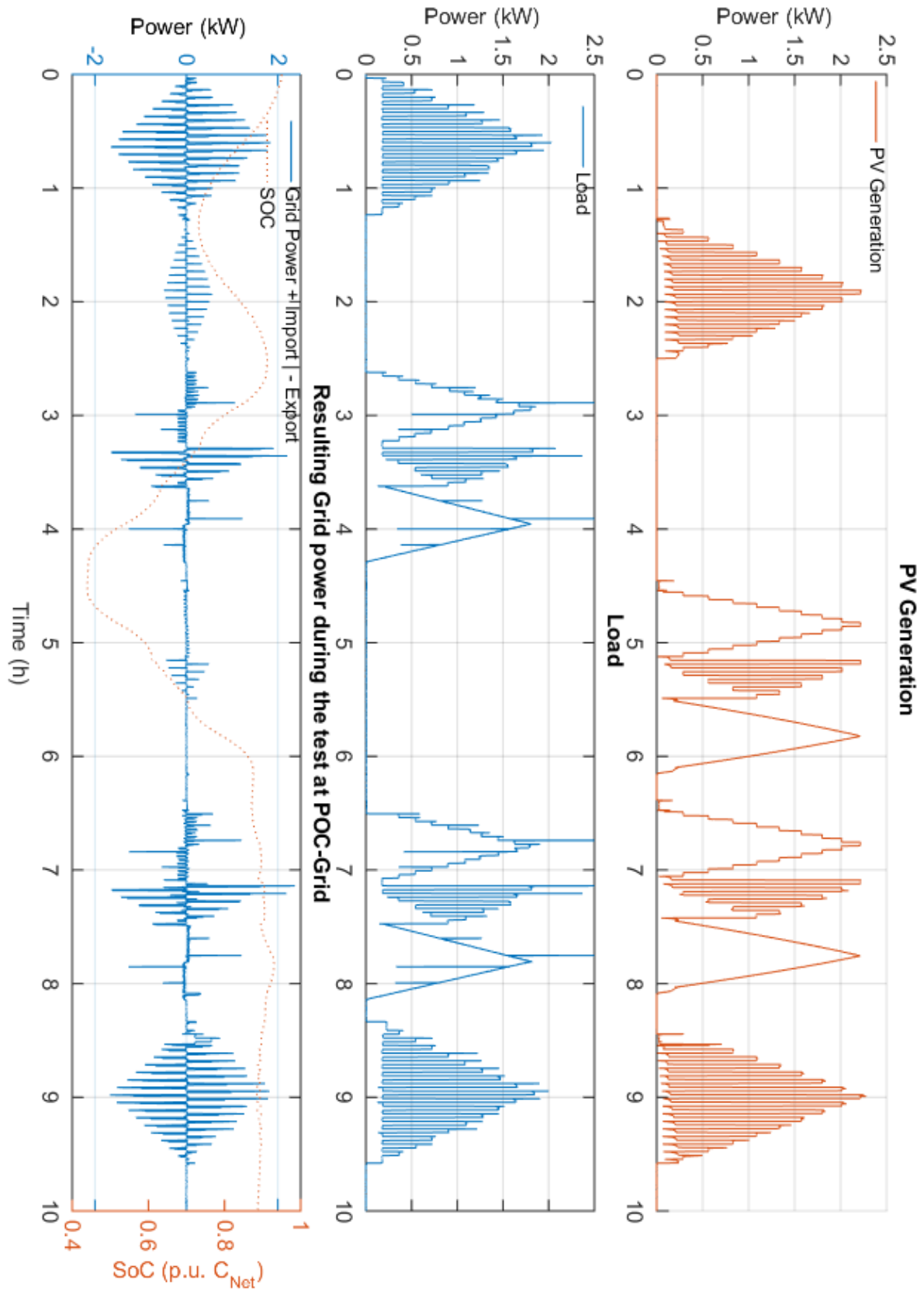
FIGURE 4.22: Control test performed on a DC hybrid coupled system with a D0 smart-meter as input sensor for the EMS

The synthetic test profiles do not give insight about real energy losses in a household. The development of further profiles which emulate the switching behavior of loads in households in a shortened test is anticipated. Nevertheless the described test profiles allow to compare the control system performance of PV-BESSs. A comparison gives the PV-BESS manufacturer insight about deficits and possible optimizations.

4.5 Standby consumption

An approach, adopted from CEC and IEC test procedures for charge controllers, could be applied to measure the standby consumption of the PV-BESS over a specific time period. For instance imported energy form the utility grid and discharged energy from the battery could be measured for 24 hours, when no PV and load power is present. The average power is then calculated for the specific measurement time. The standby consumption may vary, if the system has more than one standby mode (idle, night-mode etc.) In addition the supply (AC or DC) may change as function of the SOC. At a fully charged battery, standby-consumption is probably covered by battery discharge for various PV-BESSs. For a fully discharged battery energy must be drawn from the utility grid. If this is the case for the system under test, it is recommended herein, to perform the test once at a fully charged and once at a fully discharged battery.

The standby consumption of additional devices (external EMS for AC coupled systems, metering device etc.) can be determined according to the standard DIN EN 50564:2011-12. Standby consumption of PV-BESS is not directly tested within this work, but evaluated indirectly during the application related test, described in the next section. Direct evaluation of standby-consumption is content of future developments and seems to be necessary for PV-BESS performance evaluation.

4.6 Application related System Performance

The application related test follows the description in Section 3.6. The test is based on real PV irradiation and demand data at a high sampling rate (1s). The objective is efficiency and effectiveness evaluation during this specific test sequence.

4.6.1 Effectiveness Evaluation

The achieved effectiveness is expressed as degree of direct use and self-coverage and its increase, compared to a PV system without BESS. For the calculation the feed-in and imported energy at the POC-GRID is used. The DU is calculated by total exported and PV generated DC energy according Equation 4.22. DU is increased by feed-in and charging losses. The SC is calculated as the relation between imported power/energy and electricity demand, according Equation 4.23. Standby consumption reduces in principle the degree of self-coverage. For instance additional, imported energy from the grid is necessary at a fully discharged battery for coverage of PV-BESS standby-consumption.

$$\mathrm{DU} = \frac{\sum_{i=1}^{n} (P_{\mathrm{PVS,DC},i} - P_{\mathrm{Grid,export},i}) \cdot \Delta T_i}{\sum_{i=1}^{n} P_{\mathrm{PVS,DC},i}} \cdot 100\% \tag{4.22}$$

$$\mathrm{SC} = \frac{\sum_{i=1}^{n} (P_{\mathrm{Load},i} - P_{\mathrm{Grid,import}i}) \cdot \Delta T_i}{\sum_{i=1}^{n} P_{\mathrm{Load},i} \cdot \Delta T_i} \cdot 100\% \tag{4.23}$$

The measured grid import includes energy which is charged from the utility grid into the battery due to limited performance of the control system. A methodical error is made in the calculation, because this power is not used for coverage of P_{Load}. At the other hand SC is decreased by undesired energy transfer. Theoretically SC can be negative if grid imported energy is used mostly for charging the battery and not for load coverage. The same applies for DU. Grid exported power may include battery discharged power into the grid. More exported power decreases the Direct Use. As grid charge and discharge is undesired for the application of PV-BESS these negative effects ar included in SC and DU.

The application related test is challenged to cover a wide group of users. The achieved annual effectiveness depends on annual demand and PV generation as well es direct matched demand. Analyses of the HTW-Berlin have shown that the annual degree of Self-Coverage varied for 74 observed single family households between 43 and 61 % depending on the user behavior and building equipment. [8] At the other hand the system size itself (PV generator peak power, battery capacity) is a influence factor. A trend is seen that PV-BESS manufactures offer modular expansion of the battery capacity. The system size, considering PV generator and battery size, can be theoretically optimized for one specific household with one individual input profile of demand and PV irradiation. It is obvious that a laboratory test cannot be

applied to all possible system combinations.

An approach could be a portfolio containing different test profiles. The manufacturer declares for which type of residential customer (single family households, amount of persons, etc.) its system is optimized and chooses a certain profile. He/she chooses the appropriate battery size in case of modularity to fit one profile of the portfolio. Such an approach implies that direct comparison of PV-BESS is lost as different profiles were used. At the other hand direct comparison may not be useful as systems are not optimized for exactly one profile. It shall be avoided that the manufacturer develops the system to fit exactly one specific test profile. This can be achieved, if the exact profile for the test is not known and it is only categorized by a generic description of the household (persons, annual demand etc.). As an alternative each category may contain more profiles and one is randomly chosen for the test. Further investigation of load profiles is necessary. Probably a generic synthetic profile with superposed switching behavior of loads provides advantages.

PV irradiation data for instance of central Europe could be chosen. Less dependence between self-coverage of PV-BESS and the specific location was observed by HTW-Berlin for Germany[8]. The PV generator peak power could be sized that the degree of self-coverage is optimized for the used PV and load profile without consideration of a storage system.

The laboratory test must be performed in a relatively short time-period. Compared to one year the annual electricity demand and PV generation vary strongly between summer and winter. The determined effectiveness must not correspond to annual achievable values. Considering the whole lifetime of the PV-BESS, test results are given for BOL. With passing time until EOL battery capacity usually decreases and effectiveness is lowered. An approach for long term effectiveness estimations could be done in a simulation environment, parametrized with data from the laboratory test and battery degradation estimations. Further investigation and long-term validation of simulation models with measurement data from field tests is necessary.

A comparison of achieved effectiveness with simulation based results is theoretically possible. Such an approach is described in Section 3.6, for the evaluation of the control system performance. Some aspects must be considered if this method shall be used. In a real PV-BESS various system states were observed which cannot be analytically modeled with reasonable effort in a generic way. For instance cell-balancing or individual charge procedures. Charge power may be decreased at high SOC levels, discharge power at low SOC levels. Especially

for the evaluation of the control system performance such system states must be considered. It is not content of this thesis to validate the laboratory test with a simulation models and vice versa. This section evaluates effectiveness and efficiency only by use of laboratory measurements.

4.6.2 Efficiency Evaluation

Efficiency is evaluated for the entire System, PCS, battery and single component efficiency (charge controller, PV inverter etc.) under real field operation conditions. The conversion (Section 4.2, Equation 4.3) and overall PCS efficiency (Section 4.2, Equation 4.5) is determinable as instantaneous value and for the entire test period according to Equation 4.3. It is useful to illustrate the instantaneous efficiency in an $\eta(t)/\mathrm{t}$ chart or $\eta(t)/\mathrm{p(t)}$ chart as function of power. The charts allows fast insight at which instant of time or period efficiency is low and possible optimizations could be done. Evaluation of the battery efficiency requires that the test ends with the initial state of charge at the beginning of the sequence (e.g. fully charged or fully discharged battery).

System efficiency evaluation is basically done according the described methodology in Section 3.6, Equation 3.42 and is described by the ratio between AC output and PV input to the PV-BESS during a specific test sequence. Evaluation requires that the test start and end with the same SOC, if not energy differences between start and end of the test are allocated to losses. The given equation is extended herein by the additional input $P_{\mathrm{POC\text{-}AC,import},i}$ (Equation 4.24) to consider eventually occurring energy transfer from the grid into the battery. It is described as the ratio between total output (AC) and total input (DC+AC) the system.

$$\eta_{\mathrm{PV\text{-}BESS}} = \frac{\sum_{i=1}^{n} P_{\mathrm{POC\text{-}AC,export},i} \cdot \Delta T_i}{\sum_{i=1}^{m} P_{\mathrm{PVS,MPP},j} \cdot \Delta T_j + \sum_{i=1}^{n} P_{\mathrm{POC\text{-}AC,import},i} \cdot \Delta T_i} \qquad (4.24)$$

The system efficiency is influenced by the specific energy distribution during the test. It is influenced by the system size, considering PV generation peak power, maximum charge/discharge power and battery capacity. For instance if PV peak power is high and battery capacity very small most energy is directly fed-in to the grid. This implies that the system efficiency is high and corresponds basically to the feed-in or PV inverter efficiency. This approach does not allow comparison of system efficiency between PV-BESS with different sizing. For instance two identical systems are given: One with low battery capacity, one with high battery

capacity. The efficiency of the components is assumed to be identical. The system with lower capacity achieves a lower degree of direct use and self-coverage, but a higher system efficiency because of less charging and discharging the battery. Further investigation is necessary if a normalization/weighting to system size or resulting energy distribution can be done.

4.6.3 Example of Test Results

The applied PV irradiation and load data was used from a four-person household in upper Austria. The test starts with a fully charged battery, with low PV irradiation and a high demand at the first day, moderate and high irradiation for the second and third day. At the end of the test the battery is recharged again with constant power. The test was performed for three days from the month March and September. The results between both months deviate only slightly, therefore the test is described in detail only for the month March. The input profile is illustrated in Figure 4.23.
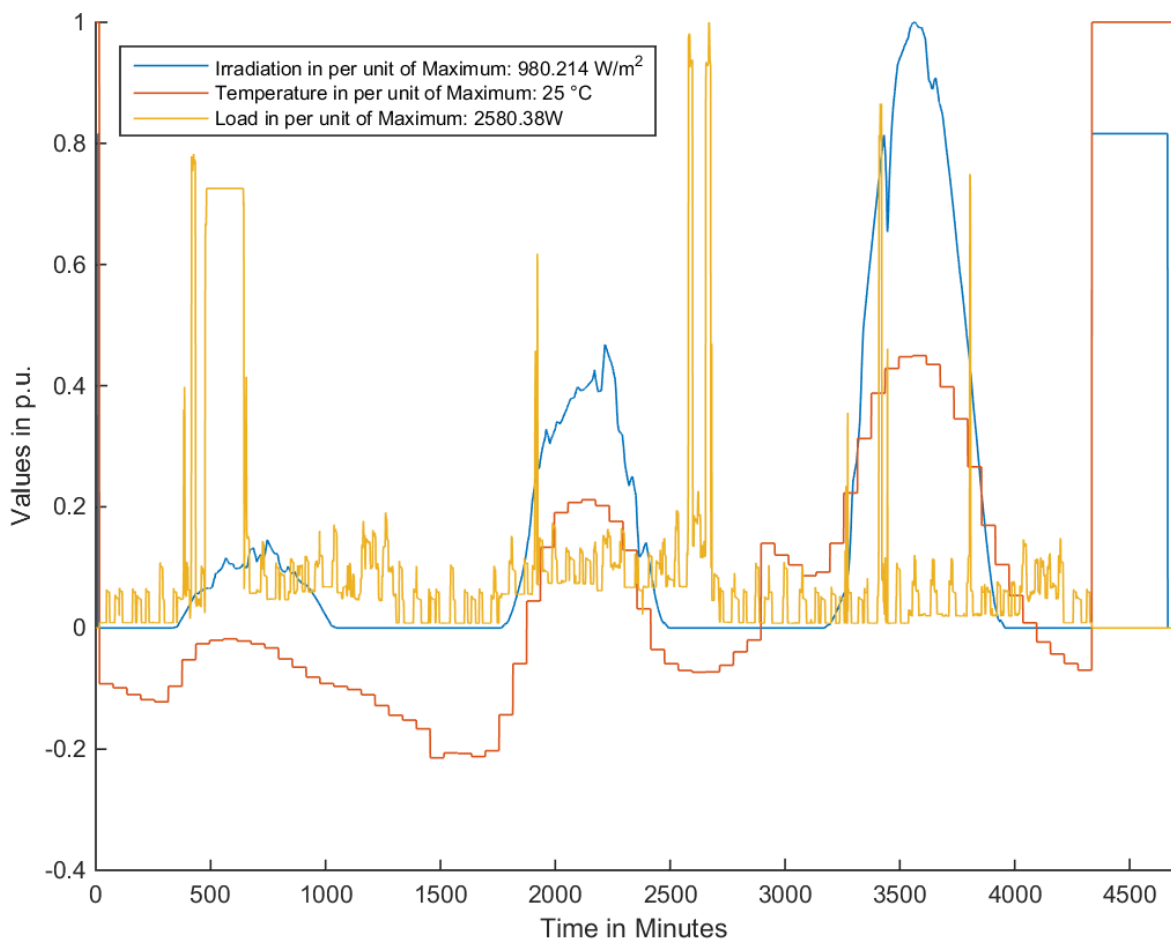

FIGURE 4.23: Example of an input profile for the application related test

AC coupled system

The system under test comprises a single phase PV and battery inverter. Technical data is found in Appendix B. The PV generator is sized to 3.2 kWpeak. The battery is a prototype of a hybrid system using lithium-ion and lead-acid battery modules. The BMS switches automatically between both types, whereas lithium-ion is primary charged and discharged. The aim is to cover short cycles with the lithium battery (high cycle life) and if PV generation is low for longer periods the cheaper lead lead-acid battery with a lower cycle life covers the demand. Table 4.9 shows the battery parameters of each type.

TABLE 4.9: Technical data of the hybrid battery system, used in the application related test.

Type	C_{NOM}	C_{NET}@ $I_{\text{BAT,discharge}}$	$I_{\text{MAX,charge/discharge}}$
Li-Ion	30 Ah/1.5 kWh @51.2V	1.35 kWh @ 28A (0.9C)	28 A
Lead-Acid	170 Ah/8.16 kWh @48V	5.7 kWh @ 50A (0.3C)	28 / 50 A
		7.5 kWh @ 7A (0.04C)	

The test was performed with the proprietary protocol (Test 1) and once with a standard D0 smart-meter (Test 2). Test 2 had a slightly lower electricity demand. This is the case because for Test 1 additional smart-meters were tested at the research test bed during the sequence. The standby-consumption of these devices increases the overall electricity demand. This example was chosen because it shows the influence at efficiency if the input profile of load varies slightly. The concurrency of PV and load power was already illustrated in Section 1.4 in Figure 1.2 for this test profile. It was seen that if no storage is used most of the generated energy is fed into the grid and must be obtained from the grid for demand coverage. This section shows the added value by using a storage system. Test 1 is illustrated in Figure 4.24 and Test 2 in Figure 4.25. Grid exported energy is reduced quite entirely at Day 1 and 2 by charging the battery. At Day 3 that battery is fully charged at about 12:00 for both tests. It is seen that charge power decreases slowly because of the CC/CV charging procedure. Grid import is reduced quite entirely by discharging the battery. At Test 1 the battery is fully discharged (minimum. SOC 5%) at the beginning of the second day (06:00) and energy is imported from the grid, whereas at Test 2 no additional grid import is required. Due to the lower electricity demand the battery is never fully discharged at Test 2. Grid import power was furthermore necessary for both tests when load power exceeded maximum discharge power. For the prototype of the hybrid battery system maximum discharge power depends

on the used battery type (li-ion,lead-acid), which is seen at the second test day between 18:00 and 21:00. The figures comprise instantaneous efficiency of the PCS. Especially at low power discharge during the night efficiency is decreased noticeable for both tests, but more at Test 2. This results from approximately 40 watt less electricity demand and discharge power respectively.
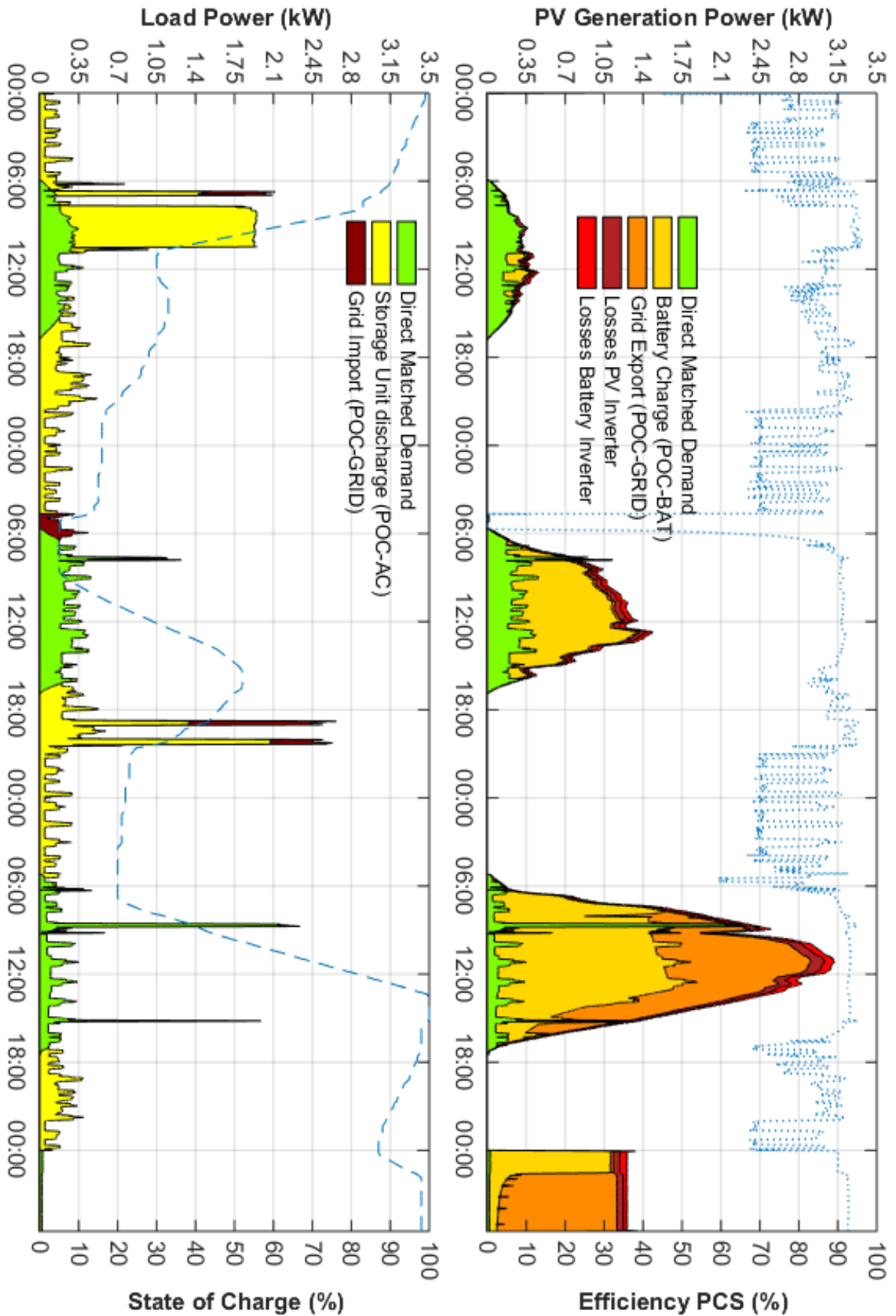
FIGURE 4.24: Three day test sequence, AC coupled system - Test 1. Values are filtered with the 'loess method' for illustration purpose. PV irradiation data from upper Austria, month March (Source:SoDa [18]), load profile from ADRES dataset[19].
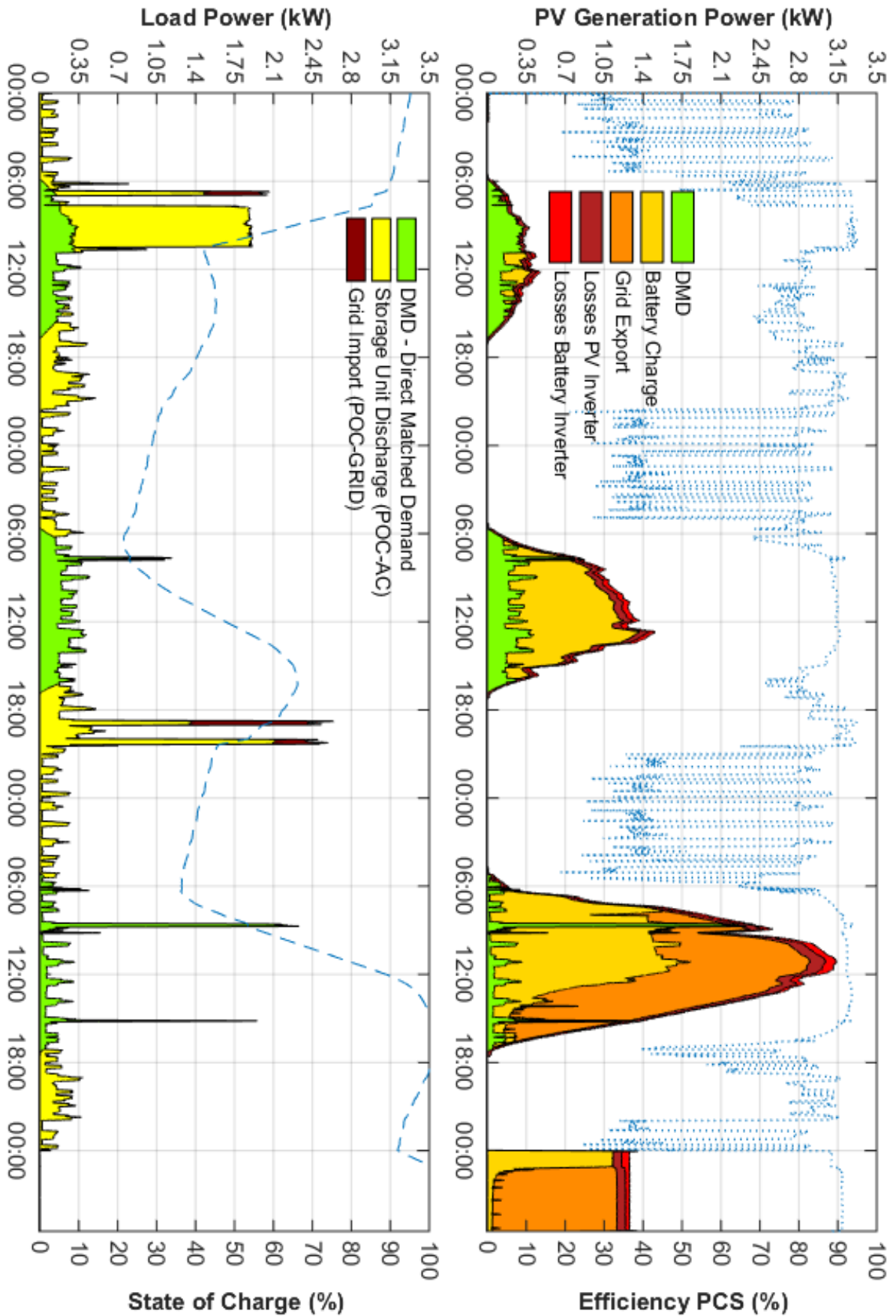
FIGURE 4.25: Three day test sequence, AC coupled system - Test2. Values are filtered with the 'loess method' for illustration purpose. PV irradiation data from upper Austria, month March (Source:SoDa [18]), load profile from ADRES dataset[19].

The relative frequency of power distribution is illustrated for Test 1 in Figure 4.26 and Figure 4.27.
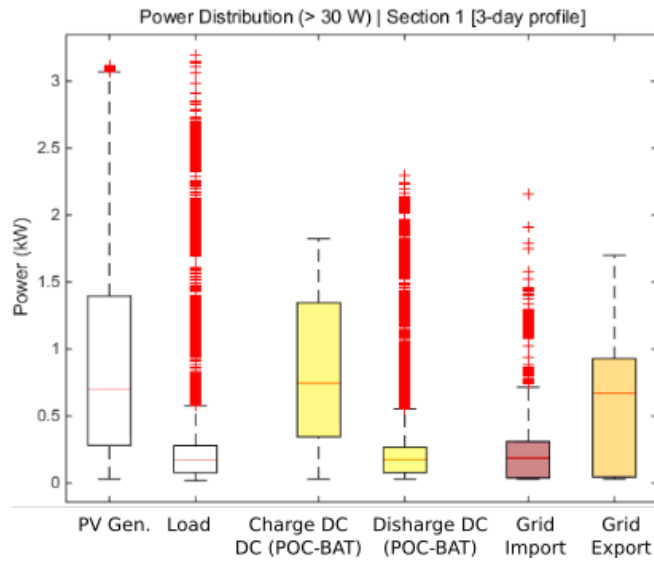
FIGURE 4.26: Power distribution Test 1 (Day 1 to 3)
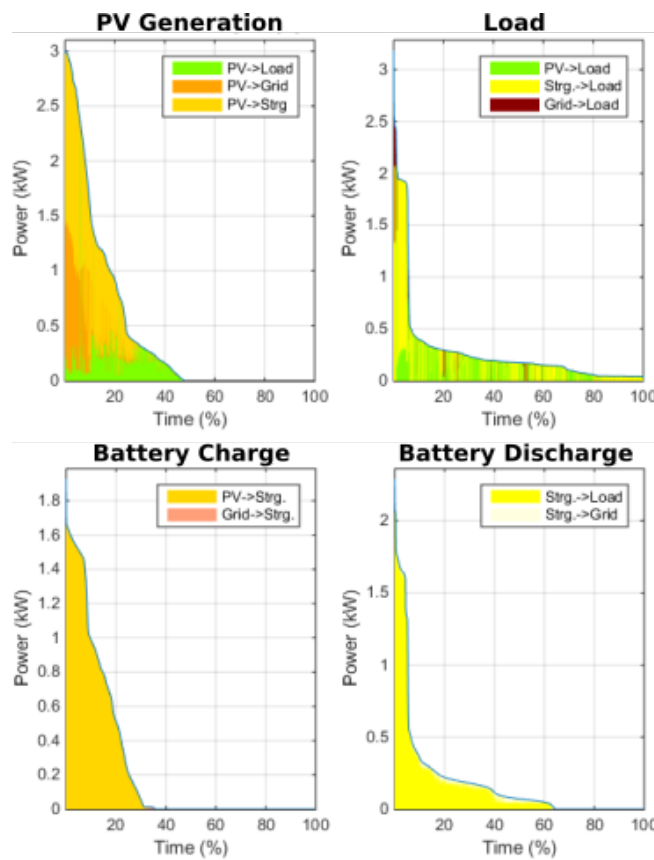
FIGURE 4.27: Power distribution Test 1 (Day 1 to 3). Note: Label Strg. corresponds to battery inverter AC power

Table 4.10 comprises detailed results of component efficiency of Test 1. System efficiency is given only for the entire test time at a fully recharged battery at the end of the test.

TABLE 4.10: Compoment and System efficiency Test 1

	PV inverter	Battery inv. (Charge)	Battery inv. (Discharge)	PCS	System
Day 1	91.1 %	77.6 %	91.0 %	90.7 %	-
Day 2	95.0 %	92.8 %	88.6 %	90.0 %	-
Day 3	95.8 %	93.8 %	83.7 %	81.6 %	-
Day 1 to 3	95.3 %	93 %	89.2 %	90.8 %	-
Day 1 to 3 + recharge	95.3 %	92.7 %	89.2 %	91.1 %	76.2 %

The efficiency is compared with the results of Test 1 in Table 4.11.

TABLE 4.11: Comparison efficiency Test 1 and Test 2 for the entire measurement time including battery recharge at the end of the test

	PV inverter	Battery inv. (Charge)	Battery inv. (Discharge)	PCS	System
Test 1	95.3 %	92.7 %	89.2 %	91.1 %	76.2 %
Test 2	95.5 %	91 %	87.5 %	90.6 %	80.3 %

The round trip efficiency was determined for the battery and storage unit. The average charge current was approx. 13 A, the average discharge current 7 A. As mainly the lead-acid module was charged and discharged the overall battery efficiency is relative low. The RTE of the whole storage unit is 14.1 % lower due to charge/discharge losses of the PCS.

TABLE 4.12: RTE of battery and storage unit

Test	RTE Battery	RTE Battery + charge controller
Test 1	81.6 %	67.5 %
Test 2	81.3 %	65 %

Figure 4.28 and Figure 4.29 shows an efficiency chart, which was generated by instantaneous efficiency values as function of power and battery voltage obtained during the specific sequence of Test 1.
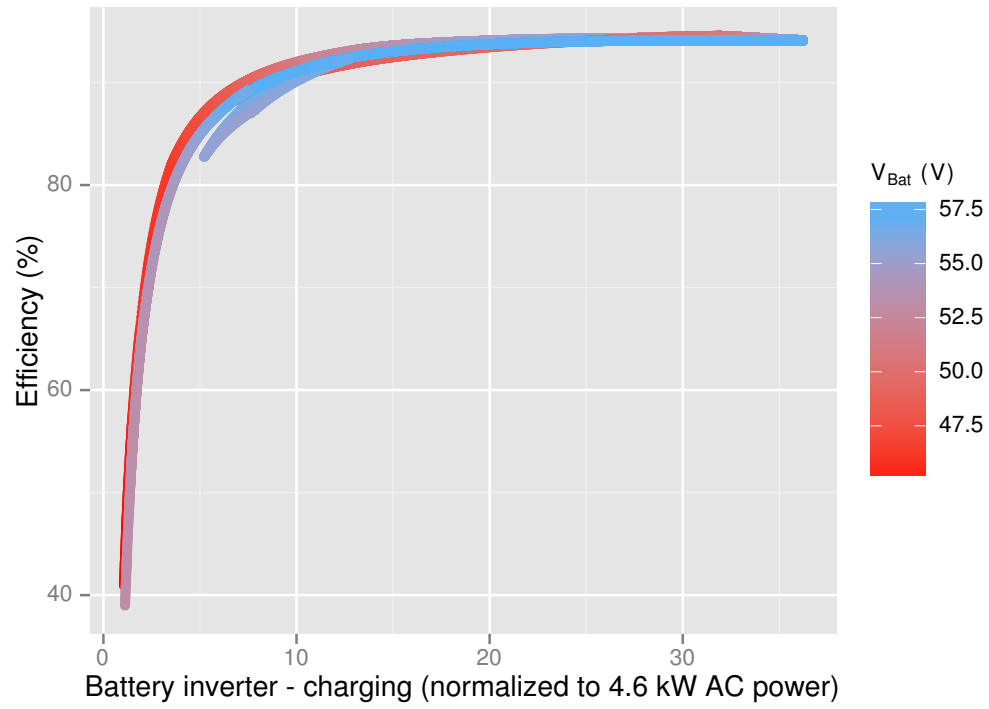
FIGURE 4.28: Battery inverter charge efficiency during the test
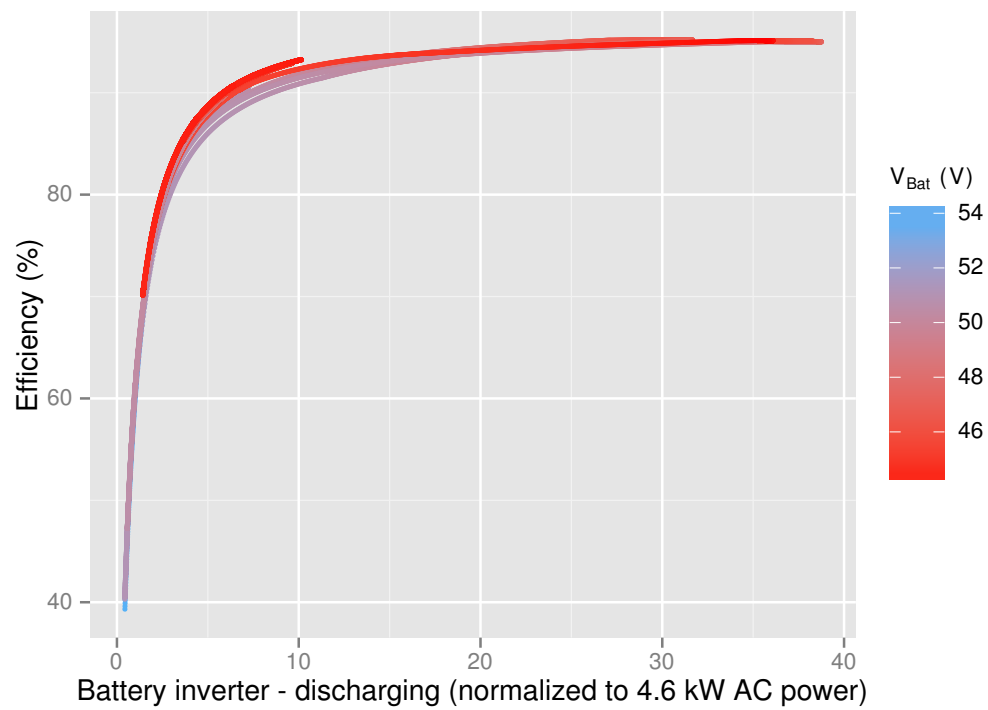
FIGURE 4.29: Battery inverter discharge efficiency during the test

DC coupled system

A DC hybrid coupled LVBS system was tested. The battery capacity was about half of the AC coupled system and a D0 compliant smart-meter is used. Figure 4.30 illustrates the measurement data. The battery is fully discharged within the first 10 hours. Not enough PV generation is present to recharge the battery during the first day. The battery is recharged at the second day but cannot supply the demand during the whole night. At the third day nightly demand is lower and no additional grid import is required.
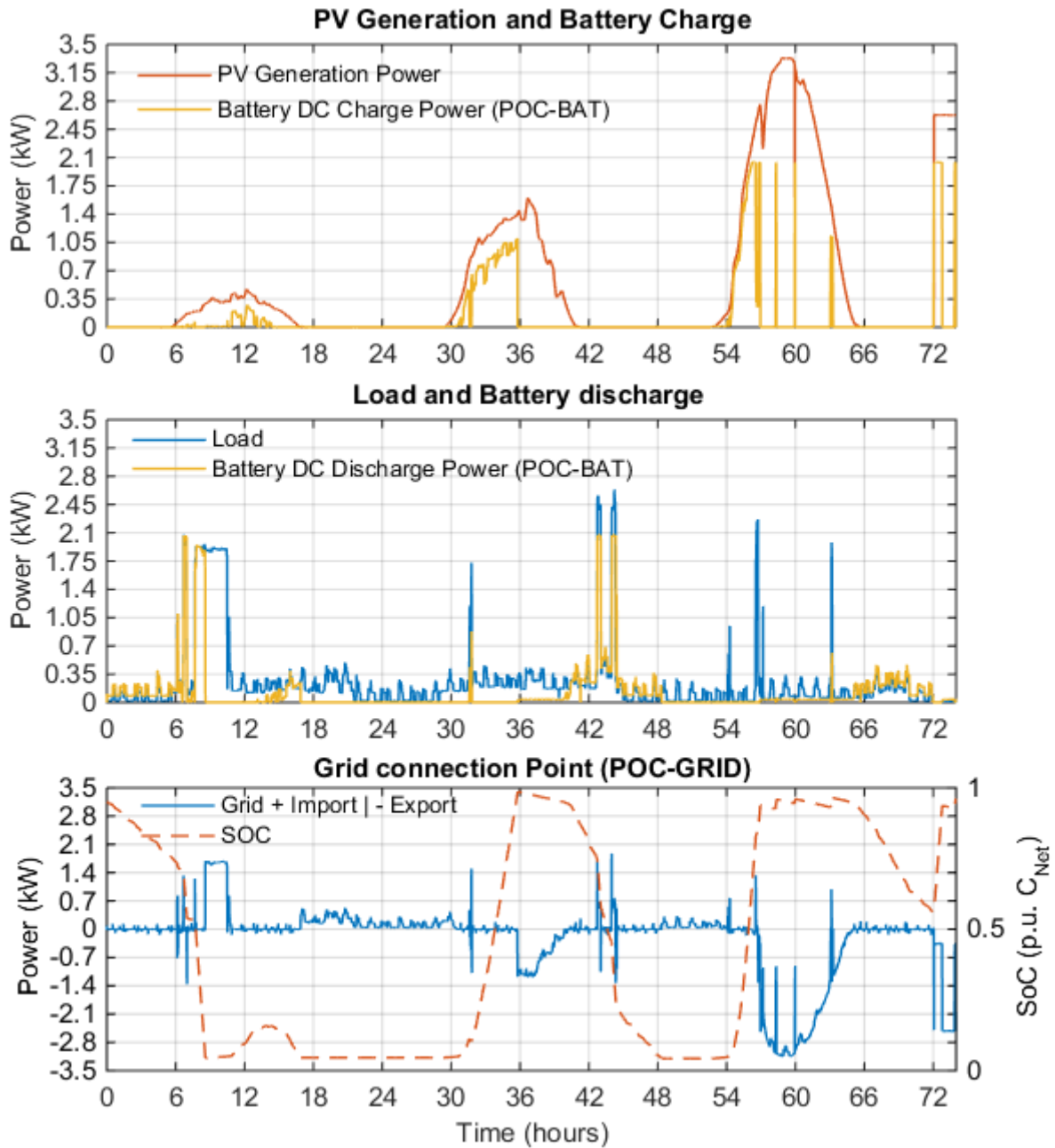
FIGURE 4.30: DC coupled system under test. PV irradiation data from upper Austria, month March (Source:SoDa [18]), load profile from ADRES dataset[19].

The determined efficiency is given in Table 4.13. The efficiency of the Power Conversion system (feed-in, charge/discharge) is determined with 88 to 90% and battery efficiency 97%.

TABLE 4.13: Efficiency DC coupled system (Test 3). Battery BCE = Coulomb Efficiency, BEE = Energy Efficiency)

	PCS	Battery BCE	Battery BEE	System
Day 1 to 3	88.3	/	/	/
Day 1 to 3 + recharge	89.7	99.28	97.4	88.73

4.6.4 Comparison Test Results

Table 4.14 shows the energy distribution for the three tests. A comparison for grid import and export is done with a PV system only without consideration of feed-in losses.

TABLE 4.14: Energy Distribution for Day 1 to 3 of the application related test sequence

Energy	**Test 1 (kWh)** PV /PV-BESS	**Test 2 (kWh)** PV /PV-BESS	**Test 2 (kWh)** PV /PV-BESS
PV Generation	33.6	34.3	35.9
Load	20.5	18.8	18.9
Grid Import	13.4 / 1.4	12.7 / 1.6	12.4 /6.9
Grid Export	26.5 / 7.3	27.7 / 10.3	29.4 /19.9

Table 4.15 shows the degree and increase of Direct Use and Self Coverage, compared to a PV system without storage for the three tests. Test 1 and Test 2 were performed with identical hardware but with a different metering device. Even if the PV generation was slightly higher and demand lower at Test 2 the achieved Self-Coverage is 2 % lower. The DC coupled system had less than half of the battery capacity but has still achieved an increase of 30% compared to a single PV system.

TABLE 4.15: Effectiveness indexes for Day 1 to 3 of the application related test sequence

Description	**Test 1 (%)** PV /PV-BESS	**Test 2 (%)** PV /PV-BESS	**Test 3 (%)** PV /PV-BESS
Direct Use	21 / 78	19 / 70	18 / 45
Self Coverage	35 /93	35 / 91	34 / 63
Increase Direct Use	59	56	29
Increase Self Coverage	57	51	26

Chapter 5

Conclusion and Outlook

This work presents a comprehensive test portfolio for PV battery energy storage systems. It includes evaluation of energy efficiency, control system performance end effectiveness in increasing direct use and self-coverage during an application related test.

One Way Efficiency

Efficiency is evaluated for the main energy conversion paths of the Power Conversion System at full and partial load power.

- PV Feed-In efficiency
- PV Charge efficiency
- Discharge efficiency

PV Feed-In Efficiency

PV Feed-In efficiency relates basically to the widely used European Standard EN-50530 [59] - Overall Efficiency of PV inverters. It considers MPPT, conversion and overall feed-in efficiency at several DC input voltage- and power levels. An automatic test procedure is proposed, in which partial load power and DC input voltage levels are changed iteratively. The test is performed at a fully charged battery. Analyses is done within a defined measurement time at steady state operation. Static efficiency is illustrated in a chart, normalized to rated DC input power. Direct comparison of static feed-in efficiency between a DC and AC coupled system is possible. The European/CEC MPPT efficiency weights the determined feed-in efficiency according an assumed relative frequency of partial load operation of PV

inverters in central Europe or southern regions as California. For a DC coupled PV-BESS the actual output (feed-in) power must not correspond to the weighting factors as energy is used first for charging the battery and not for feed-in. Therefore only MPPT but not conversion and overall European/CEC feed-in efficiency is definable. Further investigation is necessary if an adaption of the weighting factors, related to charge power can be done for DC coupled systems. Dynamic MPPT efficiency shall be evaluated for changing PV input power (ramp-up/down iterations) according EN-50530.

PV Charge / Discharge Efficiency

PV charge and discharge efficiency of the PCS is evaluated for full and partial load charge/discharge power. It is shown that especially for high voltage batteries the span between end of charge voltage and end of discharge voltage is increased and efficiency of the charge controller is a function of battery voltage (SOC and power). Several automatic performable test procedures were presented for determination of full and partial load charge/discharge efficiency as function of the SOC. Further testing is required to obtain knowledge about charge/discharge efficiency at low and high battery voltage, especially in HVB-BESS.

As efficiency is usually given normalized to rated charge/discharge power it does not provide information about average efficiency in the field or specific application. An approach is introducing weighting factors for several power levels. This requires further investigation because system size and concurrency of PV and demand determine the system states considering SOC and power. It implies that a normalization to the PV-BESS system size must be found for evaluation of relative frequency of charge/discharge power during the lifetime of the PV-BESS. A individual simulation approach for each tested system seems obvious. Additionally it is proposed to evaluate discharge efficiency not only at normalized power levels but moreover at constant load power levels. Especially a minimum power level shall be chosen, which represents electrical demand at the evening and during the night.

Charge efficiency is in principle comparable between DC and AC coupled systems. As AC coupled systems allow the use of any PV inverter for provision of charge power it is proposed to use a average efficient state of the art PV inverter for charge efficiency. A tolerance band can be used if the customer uses a lower or higher efficient device.

Round trip efficiency

The PV-BESS round trip efficiency is determined by charge and discharge losses from the PCS and battery during several full cycles with predefined charge and discharge power. In principle only a measurement point at the DC input or provided MPP energy of the PV simulator and energy at the AC output is required. In addition it is recommended to evaluate battery and PCS round trip efficiency by using an additional measurement point at the battery DC terminal. If an AC coupled system is used and no PV inverter is provided by the manufacturer, efficiency shall be evaluated in the same way as described for one way efficiency.

The test starts and ends at a fully charged or fully discharged battery. The battery is estimated to be fully charged if it does not accept more energy after a prescribed charge procedure. It is estimated to be fully discharged if no energy can be withdrawn anymore after a prescribed discharge procedure. It was established that efficiency evaluation and reproducibility is influenced by the quality and tolerance of the integrated SOC estimation. The charge and discharge process is terminated by the BMS and therefore charged and discharged ampere-hours may vary between several cycles. An indicator for misleading SOC estimation is the coulomb efficiency which shall be close to 100% for lithium-ion batteries. During one single cycle coulomb efficiency might be >100% but after some iterations the missing ampere-hours must be compensated with more charge energy. An iteration of single identical performed charge/discharge cycles is necessary to mitigate temporal deviations of the true SOC. In further investigation the deviation of coulomb efficiency between different battery cell-technologies is from interest.

The RTE efficiency is evaluated for more than one discharge or/and charge power level. The power is kept constant during charge and discharge. As alternative one full cycle may consist of two or three steps of constant charge/discharge power. RTE shall be evaluated preferably at application related power levels for PV-BESS. As test time increases progressively with lower charge and discharge power further development of the test procedures must define the required full levels and amount of iterations of identical cycles for maximum system characterization and reproducibility. .

ICT and Control System

Evaluation of control system performance is done in the time domain by analysis of a step response. The settling time is measured after a step of load power or emulated PV irradiation. It is influenced by the moment in time the step is applied. This is the case because grid power is sampled and eventually EMS processing is done at constant time intervals. A system with deficits in the control system was tested, where the EMS samples measurement data only in steps of 30 seconds. For instance if the load step/power is present shortly before the measurement data is sampled and processed the settling time is low. If the load step is applied shortly after the measurement data is sampled the time until the next sample is measured increases the settling time. A mitigation of this effect can be done if iterated load steps are applied and the time between the steps is increased continuously. The accuracy of the system is determined by the Steady State Error after settling time is achieved. Minimum measurement periods and duration of the steps is content of future developments. Additionally to time domain observations, grid imported and exported power is used for performance evaluation of the control system. A combination of step/stair and ramp profiles is used and the sequence is designed with respect to SOC and power limitation. This implies that grid power results only due to limited dynamic of the control system.

The tests with synthetic profiles do not give insight about lost locally usable energy in the application of single family households for long term observations. Nevertheless the control system performance is comparable for different PV-BESS systems. It is demonstrated in the tests that PV-BESS can react fast to changing load and PV irradiation. It is also shown that deficits in the control system can produce strong oscillations, inaccuracies or it takes long until the local electrical demand is covered. The PV-BESS manufacturer shall be able to optimize its control system that a minimum performance is given.

Application Related Test

Efficiency and Effectiveness of the system is evaluated by using high sampled measurement data of PV irradiation and demand of single family households. The test provides operation of the PV-BESS under real field conditions at a variety of system states. The determined efficiency is influenced by the choice of input profiles, system size and power limitations. These aspects are responsible for an individual energy distribution of each specific system

configuration. Therefore efficiency is only conditional comparable between different sized systems.

The evaluated effectiveness (Direct Use and Self-Coverage) does not necessarily give insight about annual achievable values but it allows a comparison between different systems tested with the same input profile. The used profiles shall represent a wide range of users for which the system is sized (amount of persons in the household, high electricity demand due to a heat pump etc.). Further investigation and analysis of PV and load profiles and resulting energy distribution of PV-BESS in single households is required for the design of such test sequences. Further developments may include simulation approaches for long term observation, based on measurement results.

Summary

Detailed technical knowledge about PV-BESS is elaborated. Existing proposals and standards of test methods and procedures were revealed and served as basis for a comprehensive performance evaluation test portfolio.

Efficiency

The portfolio, concerning efficiency evaluation, is briefly described as follows:

- Tests at full and partial load operation
- Conversion, MPP Tracking and battery efficiency
- round trip efficiency tests
- Standby power consumption
- Comparability of products independent of the application and sizing

Effectiveness & Control System

The portfolio, concerning effectiveness evaluation, is briefly described as follows:

- Tests with synthetic generation and demand profiles
- Multi-day tests in an emulated application environment
- Identification of weaknesses in ICT and control system
- Basis for estimation of annual performance

The proposed test procedures can be used for further standardization processes and allow better system characterization and optimization possibilities for the PV-BESS manufacturer. Comparability between different system configurations is not given for each evaluated performance index. This is not seen strictly necessary to meet the customer needs. Moreover the tests shall assure a minimum performance and proper functioning of the PV-BESS and give an indication about the overall quality of the product.

The evaluated charge/discharge efficiency as function of partial load power does not give insight about efficiency in the application but it may serve as basis for introducing a weighted efficiency which represents the power distribution during a PV-BESS lifetime in single family households. In addition the test procedures can be extended from the use case of single family households to the overall residential sector and varying application aims if necessary. The evaluated performance and system characterization in the laboratory tests can be further used for parametrization of simulation models and long-term estimations of effectiveness and most important, profitability of the system.

Bibliography

[1] International Electrotechnical Commission(IEC). IEC 61427-2 (2015-08) Ed. 1.0 - Secondary cells and batteries for renewable energy storage - General requirements and methods of test - Part 2: On-grid applications, 2015. URL `https://www.iec-normen.de/222060/iec-61427-2-2015-08-ed-1-0-zweisprachig.html`.

[2] Chris K. Dyer, Patrick T. Moseley, Zempachi Ogumi, David A. J. Rand, and Bruno Scrosati. *Encyclopedia of Electrochemical Power Sources.* Newnes, May 2013. ISBN 978-0-444-52745-5.

[3] Battery University - BU. Types of Lithium-ion Batteries Battery University, 2015. URL `http://batteryuniversity.com/learn/article/types_of_lithium_ion`.

[4] Fronius International GmbH. Technical Data Fronius Energy Package (Fronius Solar Battery), December 2015. URL `http://www.fronius.com/cps/rde/xchg/SID-3E32C778-8AEB9E74/fronius_international/hs.xsl/83_35483_ENG_HTML.htm`.

[5] M. Martino, C. Citro, K. Rouzbehi, and P. Rodriguez. Efficiency Analysis of Single-Phase Photovoltaic Transformer-less Inverters. *European Association fortheDevelopmentofRenewableEnergies, Environment and Power Quality (EA4EPQ)*, 2012. URL `http://www.researchgate.net/profile/Kumars_Rouzbehi/publication/236953613_Efficiency_Analysis_of_Single-Phase_Photovoltaic_Transformer-less_Inverters/links/0deec52e8f397ccaf5000000.pdf`.

[6] Remus Teodorescu, Marco Liserre, and Pedro Rodríguez. *Grid Converters for Photovoltaic and Wind Power Systems.* John Wiley & Sons, July 2011. ISBN 978-1-119-95720-1.

[7] Niedermayer et. al. Innovatiove Performancetests für PV-Speichersysteme zur Erhöhung der Autarkie und des Eigenverbrauchs, 2015.

[8] Johannes Weniger, Joseph Bergner, Tjarko Tjaden, Volker Quaschning, and Hochschule für Technik und Wirtschaft Berlin, editors. *Dezentrale Solarstromspeicher für die Energiewende*. BWV, Berliner Wissenschafts-Verlag, Berlin, 2015. ISBN 978-3-8305-3548-5.

[9] European Commission. 2020 climate & energy package - European Commission, January 2016. URL `http://ec.europa.eu/clima/policies/strategies/2020/index_en.htm`.

[10] Photovoltaic Austria (Federal Association). Photovoltaic Austria - Daten und Fakten / Graphiken, January 2016. URL `http://www.pvaustria.at/daten-fakten/grafiken/`.

[11] Dr. Harry Wirth. Aktuelle Fakten zur Photovoltaik in Deutschland - Fraunhofer ISE, December 2015.

[12] BDEW Bundesverband der Energie- und Wasserwirtschaft e.V. Strompreisanalyse März 2015, January 2016. URL `https://www.bdew.de/internet.nsf/id/9D1CF269C1282487C1257E22002BC8DD/$file/150409%20BDEW%20zum%20Strompreis%20der%20Haushalte%20Anhang.pdf`.

[13] Jan Kircher, Christopher Siebler, Gunter Bachofer, and Andreas Schelter. Energiewirtschaftlicher Nachmittag, October 2015. URL `https://www.pwc-event.com/inc/ifrShowContentFile.cfm?hash=F8E9C6F3FEFFF6B62995A6C9CA48B920&type=dmsHash`.

[14] Kai-Phillip Kairies, David Haberschusz, Dirk Magnor, Matthias Leuthold, Julia Badeda, and Dirk Uwe Sauer. Wissenschaftliches Mess- und Evaluierungsprogramm Strompeicher - Speicher Monitoring Jahresbericht 2015, 2015.

[15] pv magazine. Produktdatenbank Batteriespeichersysteme für Photovoltaikanlagen, 2014. URL `http://www.pv-magazine.de/marktuebersichten/batteriespeicher/produktdaten-2014/`.

[16] F. Soyck, S. Diekmann, F. Funck, S. Laudahn, B. Engel. Utilization Concept for Residential PV Storage Systems Based on an Innovative Measurement and Control System. pages 2703 – 2708, Hamburg, Germany, 2015. ISBN 3-936338-39-6. doi: 10.4229/EUPVSEC20152015-6DO.8.6.

[17] Kai-Philipp Kairies, Dirk Magnor, and Dirk Uwe Sauer. Scientific Measuring and Evaluation Program for Photovoltaic Battery Systems(WMEP PV-Speicher). *Energy Procedia*, 73:200–207, June 2015. ISSN 18766102. doi: 10.1016/j.egypro.2015.07.672. URL `http://linkinghub.elsevier.com/retrieve/pii/S187661021501440X`.

[18] SoDa Solar Energy Services for Professionals. SoDa - Free time-series of solar radiation data, 2015. URL `http://www.soda-is.com/eng/services/services_radiation_free_eng.php`.

[19] A. Einfall, A. Schuster, C. Leitinger,, D. Tiefgraber, M. Litzlbauer,, S. Ghaemi,, D. Wertz, A. Frohner, C., and Karner. Endbericht: Konzeptentwicklung für ADRES - Autonome Dezentrale Erneuerbare Energie Systeme, August 2012.

[20] M. Stifter and J. Kathan. SunPowerCity - Innovative measures to increase the demand coverage with photovoltaics. pages 1–6, 2010. doi: 10.1109/ISGTEUROPE.2010.5638860.

[21] Rasmus Luthander, Joakim Widén, Daniel Nilsson, and Jenny Palm. Photovoltaic self-consumption in buildings: A review. *Applied Energy*, 142:80–94, March 2015. ISSN 03062619. doi: 10.1016/j.apenergy.2014.12.028. URL `http://linkinghub.elsevier.com/retrieve/pii/S0306261914012859`.

[22] PV-GIS. PVGIS photovoltaic software : free tool to assess the PV output power in europe, africa and asia for electrical stand alone or connected to the grid systems, 2015. URL `http://photovoltaic-software.com/pvgis.php`.

[23] E-Control. Rechnerische Ermittlung Ihr es Strom- und Gasverbrauchs (Prozentverteilung für einen durchschnittlichen Strom-Haushaltkunden), October 2010. URL `http://www.e-control.at/documents/20903/-/-/eb16e36f-c591-4f2b-9895-1eea8a505a4b`.

[24] European Commission. Best practices on Renewable Energy Self-consumption (COMMISSION STAFF WORKING DOCUMENT), July 2015. URL `https://www.parlament.gv.at/PAKT/EU/XXV/EU/07/29/EU_72985/imfname_10565700.pdf`.

[25] Dr. Vladimir Scarpa and Pablo Cortes Lopez,. Matching Circuit Topologies and Power Semiconductors for Energy Storage in Photovoltaic Systems | PowerGuru - Power Electronics Information Portal, September 2014. URL `http://www.powerguru.org`.

[26] Johannes Weniger, Joseph Bergner, Tjarko Tjade, and Volker Quaschning. Economics of residential PV battery systems in the self consumption age. September 2014. URL `https://pvspeicher.htw-berlin.de`.

[27] Johannes Weniger, Tjarko Tjaden, and Volker Quaschning. Sizing of Residential PV Battery Systems. *Energy Procedia*, 46:78–87, 2014. ISSN 1876-6102. doi: 10.1016/j.egypro.2014.01.160. URL `http://www.sciencedirect.com/science/article/pii/S1876610214001763`.

[28] D. Rosewater, J. Johnson, M. Verga, R. Lazzari, C. Messner, R. Bründlinger, J. Kathan, J. Hashimoto, K. Otani. International Development of Energy Storage Interoperability Test Protocols for Photovoltaic Integration. In *OPERATIONS, PERFORMANCE AND RELIABILITY OF PHOTOVOLTAICS (FROM CELLS TO SYSTEMS)*, pages 1538 – 1548, Hamburg. ISBN 3-936338-39-6. doi: 10.4229/EUPVSEC20152015-5DP.1.4. URL `https://www.eupvsec-proceedings.com/proceedings/`.

[29] Tjarko Tjaden, Johannes Weniger, Joseph Bergner, Felix Schnorr, and Volker Quaschning. Impact of the PV Generator's orientation of the energetic assesment of PV-self-consumption systems considering individual residential load profiles. In *29th European Photovoltaic Solar Energy Conference and Exhibition*, 2014. URL `http://www.researchgate.net/profile/Tjarko_Tjaden/publication/267765201_Impact_of_the_PV_Generator's_Orientation_on_the_Energetic_Assessment_of_PV_Self-Consumption_Systems_Considering_Individual_Residential_Load_Profiles/links/545a3d510cf2cf5164843bf9.pdf`.

[30] Carlos Andrés Ramos Paja, Giovanni Petrone, and Andrés Julian Saavedra Montes. Compensación de oscilaciones de voltaje en el enlace DC de sistemas fotovoltaicos conectados a la red. *Revista Facultad de Ingeniería*, (63): 82–92, 2012. URL `http://aprendeenlinea.udea.edu.co/revistas/index.php/ingenieria/article/viewArticle/12488`.

[31] Stefan Spielauer. Diploma Thesis: Evaluation of the Performance of Maximum Power Point Tracking Methods, January 2007.

[32] Mohamed A. Eltawil and Zhengming Zhao. MPPT techniques for photovoltaic applications. *Renewable and Sustainable Energy Reviews*, 25:793–813, September 2013. ISSN

1364-0321. doi: 10.1016/j.rser.2013.05.022. URL `http://www.sciencedirect.com/science/article/pii/S1364032113003250`.

[33] W. Marada and M. Piotrowicz. Efficiency of maximum power point tracking in photovoltaic system under variable solar irradiance. *Bulletin of the Polish Academy of Sciences Technical Sciences*, 62(4), January 2014. ISSN 2300-1917. doi: 10.2478/bpasts-2014-0077. URL `http://www.degruyter.com/view/j/bpasts.2014.62.issue-4/bpasts-2014-0077/bpasts-2014-0077.xml`.

[34] Shaowu Li, Amine Attou, Yongchao Yang, and Dongshan Geng. A maximum power point tracking control strategy with variable weather parameters for photovoltaic systems with DC bus. *Renewable Energy*, 74:478–488, February 2015. ISSN 0960-1481. doi: 10.1016/j.renene.2014.08.056. URL `http://www.sciencedirect.com/science/article/pii/S0960148114005266`.

[35] Se-Jin Kim and Young-Cheol Lim. A Single-Phase Embedded Z-Source DC-AC Inverter. *The Scientific World Journal*, 2014, 2014. ISSN 2356-6140. doi: 10.1155/2014/539297. URL `http://www.ncbi.nlm.nih.gov/pmc/articles/PMC4124760/`.

[36] Michael A. Roscher and Dirk Uwe Sauer. Dynamic electric behavior and open-circuit-voltage modeling of LiFePO4-based lithium ion secondary batteries. *Journal of Power Sources*, 196(1):331–336, January 2011. ISSN 03787753. doi: 10.1016/j.jpowsour.2010.06.098. URL `http://linkinghub.elsevier.com/retrieve/pii/S0378775310010852`.

[37] Battery University - BU. BU-105 Battery Definitions and what they mean, September 2015. URL `http://batteryuniversity.com/learn/article/battery_definitions`.

[38] M. Einhorn, F.V. Conte, C. Kral, and J. Fleig. Comparison, Selection, and Parameterization of Electrical Battery Models for Automotive Applications. *IEEE Transactions on Power Electronics*, 28(3):1429 –1437, March 2013. ISSN 0885-8993. doi: 10.1109/TPEL.2012.2210564. 00024.

[39] Erabhoina Hari Mohan, Varma Siddhartha, and ;International advanced research centre for powdered metallurgy and new material (ARCI), Balapur, Hyderabad-500005, India. Urea and sucrose assisted combustion synthesis of LiFePO4/C nano-powder for lithium-ion battery cathode application. *AIMS Materials Science*, 1(4):191–201, 2014. ISSN 2372-0468. doi: 10.3934/matersci.2014.4.191. URL `http://www.aimspress.com/article/10.3934/matersci.2014.4.191`.

[40] A. Abdollahi, X. Han, G. V. Avvari, N. Raghunathan, B. Balasingam, K. R. Pattipati, and Y. Bar-Shalom. Optimal battery charging, Part I: Minimizing time-to-charge, energy loss, and temperature rise for OCV-resistance battery model. *Journal of Power Sources*, February 2015. ISSN 0378-7753. doi: 10.1016/j.jpowsour.2015.02.075. URL `http://www.sciencedirect.com/science/article/pii/S0378775315003092`.

[41] Shuo Zhang, Chengning Zhang, Rui Xiong, and Wei Zhou. Study on the Optimal Charging Strategy for Lithium-Ion Batteries Used in Electric Vehicles. *Energies*, 7 (10):6783–6797, October 2014. ISSN 1996-1073. doi: 10.3390/en7106783. URL `http://www.mdpi.com/1996-1073/7/10/6783/`.

[42] Y. S. Wong, W. G. Hurley, and W. H. Wölfle. Charge regimes for valve-regulated lead-acid batteries: Performance overview inclusive of temperature compensation. *Journal of Power Sources*, 183(2):783–791, September 2008. ISSN 0378-7753. doi: 10.1016/j.jpowsour.2008.05.069. URL `http://www.sciencedirect.com/science/article/pii/S0378775308011117`.

[43] Mayr Johann. Diplomarbeit: Modellierung und Simulation einer PhotovoltaikErzeugungseinheit mit Energiespeicher und Netzkopplung, 2013.

[44] IEC. International Electrotechnical Vocabulary IEC-60050 or IEV (Electropedia: The World's Online Electrotechnical Vocabulary), 2015. URL `http://www.electropedia.org/iev/iev.nsf/display?openform&ievref=617-04-01`.

[45] IRENA International Renewable Energy Agency. IRENA Battery Storage Report 2015 - Battery Storage for Renewables: Market Status and Technology Outlook, January 2015. URL `http://www.irena.org/documentdownloads/publications/irena_battery_storage_report_2015.pdf`.

[46] Armin U. Schmiegel and Andreas Kleine. Optimized Operation Strategies for PV Storages Systems Yield Limitations, Optimized Battery Configuration and the Benefit of a Perfect Forecast. *Energy Procedia*, 46:104–113, 2014. ISSN 1876-6102. doi: 10.1016/j.egypro.2014.01.163. URL `http://www.sciencedirect.com/science/article/pii/S1876610214001799`.

[47] Jiahao Li and Michael A. Danzer. Optimal charge control strategies for stationary photovoltaic battery systems. *Journal of Power Sources*, 258:365–373, July 2014. ISSN

0378-7753. doi: 10.1016/j.jpowsour.2014.02.066. URL `http://www.sciencedirect.com/science/article/pii/S0378775314002596`.

[48] IEC. IEC 62053-31:1998 Electricity metering equipment (a.c.) - Particular requirements - Pulse output devices for electromechanical and electronic meters (two wires only), 1998. URL `https://www.vde-verlag.de/normen/207848-iec/iec-62053-31-1998.html`.

[49] IEC. IEC 62056-21:2002 Electricity metering - Data exchange for meter reading, tariff and load control - Part 21: Direct local data exchange, 2002. URL `https://webstore.iec.ch/publication/6398&preview=1`.

[50] Takuro Sato, Daniel M. Kammen, Bin Duan, Martin Macuha, Zhenyu Zhou, Jun Wu, Muhammad Tariq, and Solomon Abebe Asfaw. *Smart Grid Standards: Specifications, Requirements, and Technologies*. John Wiley & Sons, February 2015. ISBN 978-1-118-65379-1.

[51] Mathias Uslar, Michael Specht, Christian Dänekas, Jörn Trefke, Sebastian Rohjans, José M. González, Christine Rosinger, and Robert Bleiker. *Standardization in Smart Grids: Introduction to IT-Related Methodologies, Architectures and Standards*. Springer Science & Business Media, December 2012. ISBN 978-3-642-34916-4.

[52] Oliver Müller and Christian Schäfer. Fallstudie - Smart Metering - Revolution der Messtechnik in der Energiebranche?, September 2009. URL `http://winfwiki.wi-fom.de/index.php/Smart_Metering_-_Revolution_der_Messtechnik_in_der_Energiebranche%3F`.

[53] Stefan Feuerhahn, Michael Zillgith, Christof Wittw, and Christian Wietfeld. DLMS/-COSEM, SML and IEC 61850 for Smart Metering Applications, July 2011. URL `http://www.openmuc.org/fileadmin/user_upload/papers/smartgridcomm2011-final.pdf`. 00019.

[54] VDE. VDE-AR-N 4400 Anwendungsregel:2011-09 Messwesen Strom (Metering Code), September 2009. URL `https://www.vde-verlag.de/normen/0400052/vde-ar-n-4400-anwendungsregel-2011-09.html`.

[55] Summer R. Ferreira, David M. Rose, David A. Schoenwald, Kathy Bray, David Conover, Michael Kintner-Meyer, and Vilayanur Viswanathan. Protocol for Uniformly Measuring and Expressing the Performance of Energy Storage Systems. tecnical SAND2013-7084, Sandia National Laboratories, Albuquerque, New Mexico 87185 and Livermore,

California 94550, August 2013. URL `http://www.sandia.gov/ess/publications/SAND2013-7084.pdf`. Sandia National Laboratories (first 2 authors) Pacific Northwest National Laboratory.

[56] David LUBKEMAN, Paul LEUFKENS, and Alex FELDMAN. Battery Energy Storage Testing for Grid Standard Compliance and Application Performance. In *Proceedings of the 21st International Conference on Electricity Distribution*, 2011. URL `http://www.cired.net/publications/cired2011/part1/papers/CIRED2011_0674_final.pdf`.

[57] Nicolas Martin, Elisabeth Lemaire, Evangelos Rikos, George Messinis, and Paul Crolla. Criteria and procedures for performance testing - Grid connected storage. Technical report, DERri - Distributed Energy Resources Research Infrastructures, 2013.

[58] Fabian Niedermayer, Jan v. Appen, Martin Braun, Armin Schmiegel, Nico Kreutzer, Martin Rothert, and Andreas Reischl. Innovative Performancetests für PV-Speichersysteme zur Erhöhung der Autarkie und des Eigenverbrauchs. page 12, Bad Staffelstein, Germany, May 2015. bibtex: Niedermayer2015.

[59] CENELEC Members. European Standard EN 50530 : 2010 - Overall Efficiency of PV Inverters, April 2010.

[60] International Electrotechnical Commission. IEC-61683 Photovoltaic systems - Power conditioners - Procedure for measuring efficiency, November 1999. 00000.

[61] Jubaer Ahmed and Zainal Salam. An improved perturb and observe (P&O) maximum power point tracking (MPPT) algorithm for higher efficiency. *Applied Energy*, 150:97–108, July 2015. ISSN 0306-2619. doi: 10.1016/j.apenergy.2015.04.006. URL `http://www.sciencedirect.com/science/article/pii/S0306261915004456`. bibtex: ahmed_improved_2015.

[62] DI Jürgen Wolfahrt. Optimum Efficiency and Flexible Use - High Frequency Transformer with Transformer Switchover, April 2012. URL `https://www.fronius.com/cps/rde/xbcr/SID-4725BB5C-2C0F62DA/fronius_international/SE_TA_High_Frequency_Transformer_With_Transformer_Switchover_EN_320487_snapshot.pdf`.

[63] Peter Friedrichs, Tsunenobu Kimoto, Lothar Ley, and Gerhard Pensl. *Silicon Carbide: Volume 2: Power Devices and Sensors*. John Wiley & Sons, April 2011. ISBN 978-3-527-62908-4. bibtex: friedrichs_silicon_2011.

[64] Michael Frisch (Vincotech Gmbh) and Temesi Ernö (Vincotech Kft.). High Efficient Topologies for Next Generation Solar Inverter, July 2008. URL `http://www.bodospower.com/restricted/downloads/bp_2008_08.pdf`. bibtex: michaelfrischvincotechgmbh_high_2008.

[65] Johann W. Kolar and Johann Miniböck. High- performance rectifier system with 99.2% efficiency, March 2012. URL `https://www.pes.ee.ethz.ch/uploads/tx_ethpublications/HighPerformanceRectifierSystem_ElektronikPraxis_English_1_.pdf`. bibtex: johannw.kolar_high_2012.

[66] International Electrotechnical Commission. IEC 62509:2010 - Battery charge controllers for photovoltaic systems Performance and functioning, October 2010.

[67] Suzanne Foster Porter, Brian Maloney, Paul Bendt, Haresh Kamath, Tom Geist, Jordan Smith, Loïc Gaillac,, and José Salazar. Energy Efficiency Battery Charger System Test Procedure (Version 2.2), November 2008. URL `http://www.etcc-ca.com/sites/default/files/OLD/images/stories/etcc_report_industrial_battery_chargers_final_v5.pdf`.

[68] Electronic Code of Federal Regulations. Appendix Y to Subpart B of Part 430Uniform Test Method for Measuring the Energy Consumption of Battery Chargers, May 2011. URL `http://www.energy.ca.gov/appliances/battery_chargers/documents/reference/10CFR430_Sub_B_Apnd_Y.pdf`.

[69] U.S. Department of Energy. Energy Conservation Program: Test Procedures for External Power Supplies, October 2014. URL `http://energy.gov/sites/prod/files/2014/10/f18/externalpowersupplies_tp_nopr.pdf`.

[70] SMA Technologie AG. Techical Datasheet: SUNNY ISLAND 3.0m / 4.4m - The custom-fit solution for on-grid and off-grid, December 2015. URL `http://files.sma.de/dl/17632/SI30M-44M-DEN1445-V11web.pdf`.

[71] Bob York. Lead-Acid Batteries, May 2012. URL `http://my.ece.ucsb.edu/York/Bobsclass/194/LecNotes/Lect%20-%20Batteries.pdf`.

[72] Yuejiu Zheng, Minggao Ouyang, Languang Lu, Jianqiu Li, Zhendong Zhang, and Xiangjun Li. Study on the correlation between state of charge and coulombic efficiency for commercial lithium ion batteries. *Journal of Power Sources*, 289:81–90, September 2015. ISSN 0378-7753. doi: 10.1016/j.jpowsour.2015.04.167. URL `http://www.sciencedirect.com/science/article/pii/S0378775315008356`.

[73] Ronald Dell and David Anthony James Rand. *Understanding Batteries.* Royal Society of Chemistry, January 2001. ISBN 978-0-85404-605-8.

[74] Grzegorz Piatowicz, Andrea Marongiu, Julia Drillkens, Philipp Sinhuber, and Dirk Uwe Sauer. A critical overview of definitions and determination techniques of the internal resistance using lithium-ion, lead-acid, nickel metal-hydride batteries and electrochemical double-layer capacitors as examples. *Journal of Power Sources*, 296:365–376, November 2015. ISSN 0378-7753. doi: 10.1016/j.jpowsour.2015.07.073. URL `http://www.sciencedirect.com/science/article/pii/S0378775315301245`. bibtex: pilatowicz__critical__2015.

[75] Battery University - BU. Elevating Self-discharge - Battery University, January 2016. URL `http://batteryuniversity.com/learn/article/elevating_self_discharge`.

[76] International Electrotechnical Commission (IEC). IEC 61427-2 (2013) Secondary Cells and Batteries for Renewable Energy Storage - General requirements and methods of test - Part 2: On-grid applications, 2013.

[77] Aitor Makibar and Luis Narvante. Characterisation and Efficiency Test of a Li-Ion energy Storage System for PV Systems. pages 1652 – 1658, Hamburg, 2015. ISBN 3-936338-39-6. doi: 10.4229/EUPVSEC20152015-5BO.9.5.

[78] Battery University - BU. Battery Testing, Test Methods and Procedures, 2015. URL `http://www.mpoweruk.com/testing.htm`.

[79] OVE/Austrian Standards Institute. ÖVE/ÖNORM | EN 50564 Electrical and electronic household and office equipment Measurement of low power onsumption (Edition 2012-01-01), January 2012.

[80] Fabian Niedermayer. Test Procedures for Grid-Connected Residential PV-Battery Systems, June 2013. URL `http://www.iwes.fraunhofer.de/de/publikationen/uebersicht/2013/`

test-procedures-for-grid-connected-residential-pv-battery-system/_jcr_
content/pressrelease/linklistPar/download/file.res/130612_Intersolar_FN.
pdf. Fraunhofer IWES & Uni Kassel SMA BayWa r.e Solutronicc Bosch Power Tec.

[81] Heinrich Häberlin. Wirkungsgradevon Photovoltaik-Wechselrichtern ('Totaler Wirkungs-
grad' und 'Dynamischer Wirkungsgrad'), February 2005. URL `www.pv-test-ch`.

[82] Qi Zhang and Ralph E. White. Calendar life study of Li-ion pouch cells. *Journal
of Power Sources*, 173(2):990–997, November 2007. ISSN 0378-7753. doi: 10.1016/j.
jpowsour.2007.08.044. URL `http://www.sciencedirect.com/science/article/pii/
S0378775307015911`.

[83] Jens Groot. *State-of-Health Estimation of Li-ion Batteries: Cycle Life Test Methods*.
Licentiate Thesis at the Graduate School in Energy and Environment, Chalmers Uni-
versity of Technology, Göteborg, Sweden, 2012. URL `http://komar.bitcheese.net/
files/JensGroot.pdf`.

[84] MIT Electric Vehicle Team. A Guide to Understanding Battery Specifications, 2008.
URL `http://web.mit.edu/evt/summary_battery_specifications.pdf`.

[85] Roberto Franada and Sonia Leva. Energy comparison of MPPT techniques for PV
Systems, June 2008. URL `http://www.wseas.us/e-library/transactions/power/
2008/27-545.pdf`.

[86] Ökosolar PV GmbH, Zeltweg. Datasheet Ökosolar Power Storage, February 2015. URL
`http://www.oekosolar.com/produkte/batteriespeicher-power-storage/index.
php`.

[87] sia energy GmbH & Co. KG, 88239 Wangen. Datasheet PROline Sonnenspeicher, July
2015. URL `http://www.sia-energy.de/download/datenblatt_PROline.pdf`.

[88] SMA Technologie AG. Datenblatt SB 3600se-10 / SB 5000se-10: SUNNY BOY 3600
/ 5000 SMART ENERGY - Die einfache Kombination aus PV-Wechselrichter und Spe-
icher, October 2014. URL `http://files.sma.de/dl/21567/SB5000SE-DDE1441W.pdf`.

[89] Samsung SDI. ENERGY STORAGE SYSTEM for Homes, Introducing the
Samsung SDI All-in-One The Smart Battery Storage Solution, September 2015.
URL `http://www.samsungsdi.com/download?pathGbn=ESS_DOWN_PATH&fn=B26_AIO_
for_enduser(EN)_UK082015_V4.pdf`.

[90] Fronius GmbH, Wels. Technische Daten Fronius Energy Package, January 2015. URL `https://www.fronius.com/cps/rde/xbcr/SID-C1B2DCF8-E58B040F/fronius_deutschland/SE_DOC_DBL_Fronius_Symo_Hybrid_DE_1__386730_snapshot.pdf`.

[91] Website: Photovoltaik Shop / TST Arge Solarstrom 84337 Schönau, Germany. Nedap NES PR50sb-BS/S24 POWER ROUTER 5 kW mit Batterie Manager - TST Photovoltaik Online Shop, January 2016. URL `http://www.photovoltaik-shop.com/nedap-nes-pr50sb-bs-s24-power-router-5-kw-mit-batterie-manager.html`.

[92] STUDER INNOTEC SA, 1950 Sion, Switzerland. Technische Daten Xtender Serie - 667 ko., August 2013. URL `http://www.studer-innotec.com/upload/folders/410.pdf`.

[93] Herzog Felix (Varta). Daten und Fakten - Varta Familiy, September 2015. URL `https://www.varta-storage.com/fileadmin/media/files/downloads/150824_technisches_Datenblatt_family.pdf`.

Appendix A

Glossary

Terminology and Nomenclature

Absorbed Glas Mat

Lead-acid battery type, where the acid is absorbed by a fiberglass mat. Therefore the battery is spill proof.

AC coupled system

PV-BESS where the battery is connected over a bidirectional inverter to the AC link.

AC link

Point of Connection (POC-AC) of electrical loads, PV-BESS and utility grid.

AC/AC converter

An AC/AC converter converts an AC waveform to another AC waveform. It allows transformation of voltage and frequency.

AC/DC converter

Electronic circuit used for converting the voltage and current of an AC power source in DC power.

Ampere-hour Method (Coulomb-counting)

SOC is estimated by measured charged and discharged battery current.

Auxiliary heating

Heating by use of electric elements.

Battery Capacity

The battery capacity is defined as electrical charge, a cell or battery can deliver under specified discharge conditions. The SI unit for electric charge, or quantity of electricity, is the coulomb (1 C = $1A \cdot s$) but in practice, capacity is usually expressed in ampere hours (Ah) [1].

Battery inverter

Charge Controller which allows battery DC charge and discharge from and to the AC link.

Battery Management System

Electronic system used for such as by protection of the battery from operating outside the safe operating area, it calculates the SOC and monitors the state of individual cells and keeps them at the same charge state (cell-balancing)

Battery Module

A battery module is a standardized and interchangeable assembly of cells connected in series or/and parallel [76].

Beta Parameter Based MPPT method

MPPT Tracking method, achieving high efficiency

C-rate

The capacity of a rechargeable battery is commonly rated at 1C, meaning that a 1,000mAh battery should provide a current of 1,000mA for one hour. The same battery discharging at 0.5C would provide 500mA for two hours, and at 2C, the 1,000mAh battery would deliver 2,000mA for 30 minutes. 1C is also known as a one-hour discharge; a 0.5C or C_2 is a two-hour, and a 2C is a half-hour discharge.

Calendar Life

The calendar life, or service life is the expected lifetime, expressed in calendar years. Thereby cell degradation is evaluated at minimal usage. [82] The calendar life is often tested by storing cells in controlled temperature and at a fixed charge level . At certain time intervals the cell performance is measured and the battery calendar life expressed as the time the battery can be stored until the performance drops below a predefined level. [83]

Cell Balancing

Equalization of single cell voltage if multiple battery cells are connected in series

Charge Controller

Device used for battery current and voltage regulation.

Closed Circuit Voltage

The voltage between the battery terminals with load applied. The terminal voltage varies with SOC and discharge/charge current. [84] Charging the battery raises the voltage and discharging lowers it. The voltage behavior under a load and charge is governed by the current flow and the internal battery resistance. [37]

Closed-Loop Feedback Control System

Control system designed to achieve and maintain a desired set point of the output by comparing the output variable with a reference variable

Coulomb Efficiency

Battery efficiency defined as ratio between discharged and charged ampere-hours.

Crystalline Silicon Solar Cell

PV cells, based on crystalline forms of silicon. These can be mono- or multicrystalline

Cycle life

The cycle life, is expressed as number of cycles a battery can perform until a certain capacity loss is observed. It is influenced by average SOC, respective DOD and charge/discharge current. Depending on the chemistry it can be recommended to fully charge the battery or not, in order to increase the cycle life. In pv-battery applications the maximum current and DOD is often limited for an extended cycle life.

DC coupled system

PV-BESS where the battery is connected over a bidirectional charge controller to the PV generator or DC link of a PV inverter.

DC generator coupled system

PV-BESS where the battery is connected over a bidirectional charge controller to the PV generator output and input of a standard PV inverter.

DC hybrid coupled system

PV-BESS where the battery is connected over a bidirectional charge controller to the DC link of a PV inverter

DC input

DC input of a PV inverter. May consist of several inputs for PV strings.

DC link

Point of Connection in a DC hybrid coupled system of DC input stage, charge controller and inverter DC/AC stage.

DC/AC converter

Electronic circuit (rectifier) used for converting the voltage and current of a DC power source in AC power.

DC/DC converter

Electronic circuit used for converting the voltage of a DC power source to a higher or lower DC voltage level and it allows inversion of the voltage sign.

Depth of Discharge

Amount of charge removed from the battery at the given state, related to the total amount of charge, which can be stored in a battery, and is usually expressed as a percentage [2]. The maximum DOD is given by the manufacturer as ratio between net and nominal capacity.

Direct Matched Demand

Direct matched electricity demand from local PV generation

Direct Use

Ratio of the directly used PV energy (electrical loads, battery charge, losses) to the overall PV generation, considering the concurrency between demand and generation.

E-Rate

Similar to the C-rate to normalize battery discharge power to the battery capacity, expressed in kWh.

EIA-485

A standard for configuration of communication links, defining electrical characteristics of transmitters and receivers

Electrical Demand

Demand of electrical appliances. In the context of this thesis electrical demand of single family household.

End Of Charge Voltage

Upper limit of the voltage range in which the battery is operable and performs according to specifications [1](other terms: final charge voltage)

End of Discharge Voltage

Lower limit of the voltage range in which the battery is operable and performs according to specification. [1](other terms: cut-off voltage)

End of Life

The EOL is often determied by a capacity loss of 20 % related to BOL. Therefore the SOH can be taken as indicator. Figure 2.9 (IV-VI) illustrates that it is therefore necessary to make a clear statement, which value at BOL is taken as reference. Sometimes the EOL is not strictly defined for a capacity loss of 80%, furthermore more parameters can be taken as multidimensional array into account. [2]

Energy Content

Stored energy in a battery as product of ampere-hours and Open Circuit Voltage.

Energy Management System

Energy Management System used for an optimized energy distribution in a PV-BESS. In order to satisfy the specific application aims several charge/discharge strategies and Demand Side Management (DSM) may be used

Feed-In Tarrif

A feed-in tariff (FIT) is an energy supply policy that promotes the rapid deployment of renewable energy resources. A FIT offers a guarantee of payments to renewable energy developers for the electricity they produce. plural

Flooded Lead-Acid battery

The electrodes are immersed in an excess of liquid electrolyte of sulfur acid. In general, the gas, produced during charge, does not recombine to liquid. The gas is vented into the atmosphere. In order to compensate the loss of the electrolyte, a filling up of water is required at regular maintenance intervals. [2] plural

Full Charge/Discharge Cycle

A cycle in which the bettery is charged from fully discharged state to fully charged state followed by a further discharge to fully discharged state.   plural

Full Sized Battery

Battery system composed of battery modules, BMS and BSS.

HF transformer

High frequency transformer, usually up to 25kHz in PV inverters for isolation purpose

Information and Communications Technology System

High level control system and provided communication methods for interaction between single components.

Internal Battery Resistance

Resistance within a battery, which is responsible for higher battery voltage during charging and lower battery voltage during discharging. It varies for the specific battery chemistry and SOC. Battery Energy Efficiency decreases with higher internal resistance.

Lead-Acid battery

Secondary battery with an aqueous electrolyte based on dilute sulphuric acid, a positive electrode of lead dioxide and a negative electrode of lead. Novel types of lead acid batteries incorporate various amounts of carbon or carbon structures, but the active materials are still lead, lead dioxide and sulphuric acid [44] plural

LF transformer

Low frequency transformer, 50/60Hz grid frequency

Lithium-Ion battery

A lithium-ion battery contains a non-aqueous electrolyte and a negative electrode of lithium or containing lithium [44]. plural

Maximum Power Point

The amount of electrical power generated by a photovoltaic system depends on solar irradiance (solar energy per unit area of the solar panels surface) and other conditions such as temperature and cloud cover. The current and voltage at which a solar module generates the maximum power is known as the maximum power point. It is the product of the MPP voltage(U_{MPP}) and MPP current(I_{MPP}). [85]

Maximum Power Point Tracking

Maximum power point tracking (MPPT) modifies the electrical operating point of a solar energy system to ensure it generates the maximum amount of power. This involves finding the current or voltage of the solar panel at which maximum power can be generated. [85]

Modbus RTU

Serial communication protocol, used for communication to a device with a remote terminal unit (RTU)

Modbus TCP/IP

Serial communication protocol, based on TCP/IP

Net Capacity

Usable capacity of a battery at specified discharge current and temperature, expressed in ampere-hours or kilo-watthours. The net capacity is reduced to nominal capacity by discharge limitations given by the PV-BESS.

Nominal Battery Voltage

The nominal voltage is sometimes associated to the mid point between fully charged- and discharged battery, based on a specified discharge current. The nominal cell voltage differs between cell chemistries and is usually declared by the battery cell manufacturer.

Nominal Capacity

Usable capacity of a battery at specified discharge current and temperature, expressed in ampere-hours or kilo-watthours. Nominal capacity does not concern to discharge limitations of the PV-BESS. Nominal capacity is usually declared by the battery cell manufacturer.

Open Circuit Voltage

The voltage between the battery terminals with no load applied. Chemistry and the number of cells connected in series provide the OCV [37]. The open circuit voltage depends on the battery state of charge, and is increasing with it. [84] Charging and discharging agitates the battery and full voltage stabilization takes up to 24 hours (OCV relaxation) [37].

Operational Fully Charged

Fully charge battery in the application of PV-BESS. The battery is usually fully charged when it terminates the charge process and does not accept further charge after an appropriate time of battery voltage relaxation.

Perturb and Observe

Commonly used MPPT method, due to easy implementation. This methods monitors the output power after perturbing the input voltage. The perturbation of the voltage is continued if power is increased. If power is decreased the perturbation is performed in the other direction.

Point of Connection

One common connection point several electrical devices are connected

Point of Connection between residential customer and the utility grid

Point of Connection between residential customer and the utility grid

PV Battery Energy Storage System

Grid tied, PV Battery Energy Storage System plural

PV generation

Generation of DC energy from solar irradiance by a PV cells / PV generator.

PV generator

It generates electrical power depending on solar irraddiance and temperature of PV cells assembled to PV modules.

PV inverter

Device which converts variable DC input current and voltage of a PV generator into grid synchronized AC power.

PV irradiation

Global and diffuse solar exposure of a PV module

PV module

A PV module , sometimes called a panel, is a grouping of PV cells

PV system

PV system including PV generator, PV inverter and wiring.

Round Trip Efficiency

The ratio of energy put in (kWh), to the energy retrieved from storage (kWh).

Sealed Lead-Acid battery

describe procedure

Self-Coverage

Ratio between Direct Matched Demand to total electricity demand.

Smart Meter

Electricity / Energy meter which allows extended possibilities for data read out

State of Charge

Ratio between battery capacity and ampere-hours stored in the battery.

State of Health

Indicator for the battery condition over lifetime. State of Health is described as ratio between actual available capacity and capacity at Beginning of Life.

Storage Unit

Storage unit (Battery + charge controller)

Thin Film Solar Cell

PV cell composed of one or more thin layers of photovoltaic material on a substrate (glass, plastic, etc.

Total Coverage

Ratio between total generation and total demand

Utility Grid / Public Grid

Public electricity grid, in which generated energy from suppliers is delivered to consumers

Valve-Regulated Lead-Acid battery

Sealed Lead-Acid battery type containing a valve to release pressure produced by overcharging.

Voltage Efficiency

Battery efficiency determined by the ratio of discharge and charge voltage.

Zero Voltage Switching

Switching method for DC/DC converters, with the aim of increased efficiency

Appendix B

AC coupled system under test - Application related test

B.1 PV inverter

TABLE B.1: Mitsubishi PV-PNS-06ATL-GER, technical data

Description	Value	Unit
Input Parameter		
Input range DC (MPPT)	160-650	V
Min. input voltage DC	150	V
Max. input voltage DC	700	V
Number of strings	3	
Number of MPP-Tracker	1	
Max. input current DC	18	A
Max. input current DC per string	6	A
Output Parameter		
Rated AC power	4.6	kW
Max AC power	5	kW
Max AC current	21.7	A
Rated AC voltage	230	V
Efficiency according to the datasheet		
Max. eff. at max. voltage	96.2	%
European weighted efficiency	95.4	%
Power consumption at night	0.5	W

B.2 Battery Inverter

TABLE B.2: Battery-inverter, SMA-Sunny Island 6.0 | general specification

Description	Value	Unit
On-Grid specifications		
Rated grid voltage	230	V
Rated grid frequency	50	Hz
AC voltage range	172.5 to 264.5	V
AC frequency range	40 to 70	Hz
Maximum AC curent (on grid)	20	A
Maximum AC input current	50	A
Maximum AC power (on grid)	4.6	kVA
Maximum AC input power	11.5	kW
Battery (DC) specifications		
Rated input voltage	48	V
DC voltage range	41 to 63	V
Rated DC charging current	90	A
Rated DC discharging current	103	A
Maximum charging current	110	
Battery Type	FLA, VRLA (100 Ah to 10.000 Ah) Li-Ion (CanBus avlb.) 50 Ah to 10.000 Ah)	
Charge control	IUoU charge procedure with automatic full charge and equalization charge for LeadAcid	
Efficiency according to the datasheet		
Max. efficiency	96	%
No load consumption	26	W
Standby	7	W

B.3   Battery

TABLE B.3: Battery stack - Manufacturer-Data

Description	Values			Unit
Cells configuration				
	Module 1	**Module 2**	**Stack**	
Technology	LiFePO4	Lead Acid	-	
Cell Type	Vison V-LFP10S	VRLA		
Nominal cell voltage	3.2	12	-	V
Nominal cell capacity	10 @1C	170 @C_{10}	-	Ah
Cells configuration	16 ‖ 16 ‖ 16	4	-	-
BMS	TI XY	-	N/A	
Firmware BMS	-	-	-	
Module configuration				
SOC range	10 to 100	30 to 100	-	%
Energy	1.5	6.18	7.68	kWh
Capacity	30	-	200	Ah
Useable Energy	-	-	-	kWh
Useable Capacity	-	-	N/A	Ah
Rated DC Voltage	51.2	48	N/A	V
Rated / max charge current	20 / -	28 / -	-	A
Rated / discharge current	20 / -	50 / -	-	A
Rated / max charge power	20 / -	28 / -	-	A
Rated / max discharge power	20 / -	50 / -	-	A

Appendix C

Source of pictures PV-BESS overview

The sources of the used pictures of PV-BESS in Figure 1.10 are listed below:

- Ökosolar PV GmbH: Oekosolar Power Storage [86]
- Sia energy: Sia ProLine [87]
- SMA: Sunny Boy Smart Energy (1-ph) [88]
- Samsung SDI: Samsung-ESS [89]
- Fronius GmbH: Fronius Symo Hybrid [90]
- NEDAP: NEDAP Power Router [91]
- SMA: Sunny Island [88]
- Studer Innotex SA: Studer X-tender [92]
- Varta: Varta Enigon [93]